NATIONAL ADVISORY COMMITTEE FOR AERONAUTICS

TECHNICAL NOTE 2661

A SUMMARY OF DIAGONAL TENSION

PART I - METHODS OF ANALYSIS

By Paul Kuhn, James P. Peterson,
and L. Ross Levin

Langley Aeronautical Laboratory
Langley Field, Va.

Washington
May 1952

A SUMMARY OF DIAGONAL TENSION

PART I - METHOD OF ANALYSIS

PLANE-WEB SYSTEMS

1. Theory of the "Shear-Resistant" Beam
2. Theory of Pure Diagonal Tension
3. Engineering Theory of Incomplete Diagonal Tension
4. Formulas and Graphs for Strength Analysis of Flat-Web Beams
5. Structural Efficiency of Plane-Web Systems
6. Design Procedure
7. Numerical Examples

CURVED-WEB SYSTEMS

8. Theory of Pure Diagonal Tension
9. Engineering Theory of Incomplete Diagonal Tension
10. Formulas and Graphs for Strength Analysis of Curved-Web Systems
11. Combined Loading
12. General Applications
13. Numerical Examples

CONTENTS

	Page
SUMMARY	1
INTRODUCTION	1
FREQUENTLY USED SYMBOLS	2
PLANE-WEB SYSTEMS	5
1. Theory of the "Shear-Resistant" Beam	5
2. Theory of Pure Diagonal Tension	6
2.1. Basic concepts	7
2.2. Theory of primary stresses	7
2.3. Secondary stresses	11
2.4. Behavior of uprights	12
2.5. Shear deformation of diagonal-tension web	14
3. Engineering Theory of Incomplete Diagonal Tension	15
3.1. General considerations	16
3.2. Basic stress theory	17
3.3. Remarks on accuracy of basic stress theory	22
3.4. Comparison with analytical theories	23
3.5. Amplification of theory of upright stresses	25
3.6. Calculation of web buckling stress	26
3.7. Failure of the web	27
3.8. Upright failure by column action	31
3.9. Upright failure by forced crippling	32
3.10. Interaction between column and forced-crippling failure	33
3.11. Web attachments	34
3.12. Remarks on reliability of strength formulas	36
3.13. Yielding	38
4. Formulas and Graphs for Strength Analysis of Flat-Web Beams	41
4.1. Effective area of upright	41
4.2. Critical shear stress	42
4.3. Nominal web shear stress	43
4.4. Diagonal-tension factor	43
4.5. Stresses in uprights	43
4.6. Angle of diagonal tension	44
4.7. Maximum web stress	44
4.8. Allowable web stresses	45
4.9. Effective column length of uprights	46
4.10. Allowable stresses for double uprights	46
4.11. Allowable stresses for single uprights	47
4.12. Web-to-flange rivets	48

Page

4.13. Upright-to-flange rivets 48
4.14. Upright-to-web rivets 49
4.15. Effective shear modulus 50
4.16. Secondary stresses in flanges 50

5. Structural Efficiency of Plane-Web Systems 51

6. Design Procedure 55

7. Numerical Examples 56
Example 1. Thin-web beam 56
Example 2. Thick-web beam 60

CURVED-WEB SYSTEMS 63

8. Theory of Pure Diagonal Tension 63

9. Engineering Theory of Incomplete Diagonal Tension 68
9.1. Calculation of web buckling stress 68
9.2. Basic stress theory 68
9.3. Accuracy of basic stress theory 71
9.4. Secondary stresses 71
9.5. Failure of the web 72
9.6. General instability 73
9.7. Strength of stringers 73
9.8. Strength of rings 74
9.9. Web attachments 75
9.10. Repeated buckling 76

10. Formulas and Graphs for Strength Analysis of Curved-Web Systems 78
10.1. Critical shear stress 78
10.2. Nominal shear stress 78
10.3. Diagonal-tension factor 78
10.4. Stresses, strains, and angle of diagonal tension 79
10.5. Bending moments in stringers 79
10.6. Bending moment in floating ring 80
10.7. Strength of web 80
10.8. Strength check, stringers and rings 80
10.9. Riveting 81

11. Combined Loading 82

12. General Applications 86

	Page
13. Numerical Examples	86
Example 1. Pure torsion	86
Example 2. Combined loading	91
Example 3. Angle of twist	95
APPENDIX - PORTAL-FRAME EFFECT	97
REFERENCES	99
FIGURES	102

NATIONAL ADVISORY COMMITTEE FOR AERONAUTICS

TECHNICAL NOTE 2661

A SUMMARY OF DIAGONAL TENSION

PART I - METHODS OF ANALYSIS

By Paul Kuhn, James P. Peterson,
and L. Ross Levin

SUMMARY

Previously published methods for stress and strength analysis of plane and curved shear webs working in diagonal tension are presented as a unified method. The treatment is sufficiently comprehensive and detailed to make the paper self-contained. Part I discusses the theory and methods for calculating the stresses and shear deflections of web systems as well as the strengths of the web, the stiffeners, and the riveting. Part II, published separately, presents the experimental evidence.

INTRODUCTION

The development of diagonal-tension webs is one of the most outstanding examples of departures of aeronautical design from the beaten paths of structural engineering. Standard structural practice had been to assume that the load-bearing capacity of a shear web was exhausted when the web buckled; stiffeners were employed to raise the buckling stress unless the web was very thick. Wagner demonstrated (reference 1) that a thin web with transverse stiffeners does not "fail" when it buckles; it merely forms diagonal folds and functions as a series of tension diagonals, while the stiffeners act as compression posts. The web-stiffener system thus functions like a truss and is capable of carrying loads many times greater than those producing buckling of the web.

For a number of years, it was customary to consider webs either as "shear-resistant" webs, in which no buckling takes place before failure, or else as diagonal-tension webs obeying the laws of "pure" diagonal tension. As a matter of fact, the state of pure diagonal tension is an ideal one that is only approached asymptotically. Truly shear-resistant webs are possible but rare in aeronautical practice. Practically, all webs fall into the intermediate region of "incomplete diagonal tension." An engineering theory of incomplete diagonal tension is presented herein which may be regarded as a method for interpolating between the two

limiting cases of pure-diagonal-tension and "shear-resistant" webs, the limiting cases being included. A single unified method of design thus replaces the two separate methods formerly used. Plane webs as well as curved webs are considered.

All the formulas and graphs necessary for practical use are collected in two sections, one dealing with plane webs and one with curved webs. However, competent design work, and especially refinement of designs, requires not only familiarity with the routine application of formulas but also an understanding of the basis on which the methods rest, their reliability, and their accuracy. The method of diagonal-tension analysis presented herein is a compound of simple theory and empiricism. Both constituents are discussed to the extent deemed useful in aiding the reader to develop an adequate understanding. The detailed presentation of the experimental evidence, however, is made separately in Part II (reference 2); a study of this evidence is not considered necessary for engineers interested only in application of the methods.

FREQUENTLY USED SYMBOLS

A	cross-sectional area, square inches
E	Young's modulus, ksi
G	shear modulus, ksi
G_e	effective shear modulus (includes effects of diagonal tension and of plasticity), ksi
H	force in beam flange due to horizontal component of diagonal tension, kips
I	moment of inertia, inches^4
J	torsion constant, inches^4
L	length of beam, inches
L_e	effective column length of upright, inches
M	bending moment, inch-kips
P	force, kips
P_U	internal force in upright, kips

Q	static moment about neutral axis of parts of cross section as specified by subscript or in text, inches^3
R	total shear strength (in single shear) of all upright-to-web rivets in one upright, kips
R''	shear force on rivets per inch run, kips per inch
R_R	value of R required by formula (40)
R_d, R_h	restraint coefficients for shear buckling of web (see equation (32))
S	transverse shear force, kips
T	torque, inch-kips
d	spacing of uprights, inches
d_c	clear upright spacing, measured as shown in figure 12(a)
e	distance from median plane of web to centroid of (single) upright, inches
h	depth of beam, inches
h_c	clear depth of web, measured as shown in figure 12(a)
h_e	effective depth of beam measured between centroids of flanges, inches
h_R	depth of beam measured between centroids of web-to-flange rivet patterns, inches
h_U	length of upright measured between centroids of upright-to-flange rivet patterns, inches
k	diagonal-tension factor
k_{ss}	theoretical buckling coefficient for plates with simply supported edges
q	shear flow (shear force per inch), kips per inch
t	thickness, inches (when used without subscript, signifies thickness of web)
α	angle between neutral axis of beams and direction of diagonal tension, degrees

δ	deflection of beam, inches
ϵ	normal strain
μ	Poisson's ratio
ρ	centroidal radius of gyration of cross section of upright about axis parallel to web, inches (no sheet should be included)
σ	normal stress, ksi
σ_o	"basic allowable" stress for forced crippling of uprights defined by formulas (37), ksi
τ	shear stress, ksi
τ^*_{all}	"basic allowable" value of web shear stress given by figure 19, ksi
ωd	flange flexibility factor, defined by expression (19a)

Subscripts:

DT	diagonal tension
IDT	incomplete diagonal tension
PDT	pure diagonal tension
F	flange
S	shear
U	upright
W	web
all	allowable
av	average
cr	critical
cy	compressive yield
e	effective

max.	maximum
ult	ultimate

Symbols Used Only for Curved-Web Systems

R	radius of curvature, inches
Z	curvature parameter, defined in figure 30
d	spacing of rings, inches
h	length of arc between stringers, inches

Subscripts:

RG	ring
ST	stringer

PLANE-WEB SYSTEMS

1. Theory of the "Shear-Resistant" Beam

Typical cross sections of built-up beams are shown in figure 1. When the web is sufficiently thick to resist buckling up to the failing load (without or with the aid of stiffeners), the beam is called "shear-buckling resistant" or, for the sake of brevity, "shear resistant." Web stiffeners, if employed, are usually arranged normal to the longitudinal axis of the beam and have then no direct influence on the stress distribution.

If the web-to-flange connections are adequately stiff, the stresses in built-up beams follow fairly well the formulas of the engineering theory of bending

$$\sigma = \frac{Mz}{I} \tag{1}$$

$$q = \frac{SQ}{I} \tag{2}$$

with the understanding that the shear flow in outstanding legs of flange angles and similar sections is computed by taking sections such as A-A in figure 1(a). As is well-known, the distribution of the shear flow over the depth of the web follows a parabolic law. Usually, the difference between the highest shear flow in the web (along the neutral axis) and the lowest value (along the rivet line) is rather small, and the design of the web may be based on the average shear flow

$$q_{av} = \frac{SQ_F}{I}\left(1 + \frac{2Q_W}{3Q_F}\right) \tag{3}$$

where Q_F is the static moment about the neutral axis of the flange area and Q_W, the static moment of the web material above the neutral axis. When the depth of the flange is small compared with the depth of the beam (fig. 1(c)) and the bending stresses in the web are neglected, the formulas are simplified to the so-called "plate-girder formulas"

$$\sigma_F = \frac{M}{h_e A_F} \tag{4}$$

$$q = \frac{S}{h_e} \tag{5}$$

which imply the idealized structure shown on the right in figure 1(c).

When the proportions of the cross section are extreme, as in figures 1(a) and 1(b), formulas (1) and (2) should be used, because the use of formulas (3) to (5) may result in large errors. In such cases, the web-to-flange connection, particularly if riveted, is often overloaded and yields at low loads. The beam then no longer acts as an integral unit, the two flanges tend to act as individual beams restrained by the web, and the calculation of the stresses becomes very difficult and inaccurate.

2. Theory of Pure Diagonal Tension

The theory of pure diagonal tension was developed by Wagner in reference 1. The following presentation is confined to those results that are considered to be of practical usefulness, and the method of presentation of some items is changed considerably. Mathematical complexities have been omitted, and an empirical formula is introduced for one important item where Wagner's theory appears to be unconservative.

2.1. Basic concepts.- A diagonal-tension beam is defined as a built-up beam similar in construction to a plate girder but with a web so thin that it buckles into diagonal folds at a load well below the design load (fig. 2). A pure-diagonal-tension beam is the theoretical limiting case in which the buckling of the web takes place at an infinitesimally small load. Although practical structures are not likely to approach this limiting condition closely, the theory of pure diagonal tension is of importance because it forms the basis of the engineering theory of diagonal tension presented in section 3.

The action of a diagonal-tension web may be explained with the aid of the simple structure shown in figure 3(a), consisting of a parallelogram frame of stiff bars, hinged at the corners and braced internally by two slender diagonals of equal size. As long as the applied load P is very small, the two diagonals will carry equal and opposite stresses. At a certain value of P, the compression diagonal will buckle (fig. 3(b)) and thus lose its ability to take additional large increments of stress. Consequently, if P is increased further by large amounts, the additional diagonal bracing force must be furnished mostly by the tension diagonal; at very high applied loads, the stress in the tension diagonal will be so large that the stress in the compression diagonal is negligible by comparison.

An analogous change in the state of stress will occur in a similar frame in which the internal bracing consists of a thin sheet (fig. 3(c)). At low values of the applied load, the sheet is (practically) in a state of pure shear, which is statically equivalent to equal tensile and compressive stresses at 45° to the frame axes, as indicated on the inset sketch. At a certain critical value of the load P, the sheet buckles, and as the load P is increased beyond the critical value, the tensile stresses become rapidly predominant over the compressive stresses (fig. 3(d)). The buckles develop a regular pattern of diagonal folds, inclined at an angle α and following the lines of the diagonal tensile stress. When the tensile stress is so large that the compressive stress can be neglected entirely by comparison, the sheet is said to be in the state of fully developed or "pure" diagonal tension.

2.2. Theory of primary stresses.- A girder with a web in pure diagonal tension is shown in figure 4(a). To define this condition physically, assume that the web is cut into a series of ribbons or strips of unit width, measured horizontally. Each one of these strips is inclined at the angle α to the horizontal axis and is under a uniform tensile stress σ.

The free-body diagram of figure 4(b) shows the internal forces in the strips intercepted by the section A-A combined into their resultant D. Since all strips have the same stress, the resultant is located at mid-height. The horizontal component H_D (= S cot α) of D is balanced

by compressive forces H in the two flanges. The two forces H must be equal, D being at mid-height, therefore

$$H = -\frac{S}{2}\cot\alpha \tag{6}$$

The total flange force is thus

$$F = \pm\frac{M}{h} + H = \pm\frac{M}{h} - \frac{S}{2}\cot\alpha \tag{7}$$

In the free-body diagram of figure 4(c), each strip is cut at right angles, giving the stress-carrying face a width of $\sin\alpha$; the force on each strip is therefore $\sigma t \sin\alpha$. The number of strips intercepted by section A-A is equal to $h \cot\alpha$; the total force D on all strips is therefore

$$D = \sigma t \sin\alpha \times h \cot\alpha = \sigma h t \cos\alpha$$

But from statics

$$D = \frac{S}{\sin\alpha}$$

Therefore

$$\frac{S}{\sin\alpha} = \sigma h t \cos\alpha$$

or

$$\sigma = \frac{S}{ht \sin\alpha \cos\alpha} = \frac{2S}{ht \sin 2\alpha} \tag{8}$$

The upright is under compression, counteracting the tendency of the diagonal tension to pull the flanges together (fig. 4(d)). The force P_U acting on each upright consists of the vertical components of the forces acting in all the strips appertaining to each upright, that is, in d

strips (since the strips have unit width horizontally). But as just found, the vertical component of $h \cot \alpha$ strips is equal to S; therefore

$$P_U : S : : d : h \cot \alpha$$

or

$$P_U = -S \frac{d}{h} \tan \alpha \tag{9}$$

If each strip is connected to the flange by one rivet, the force on this rivet is equal to the force $\sigma t \sin \alpha$ in the strip. Since the strips are of unit width horizontally, this is the rivet force per inch run, designated by R''. Substitution of the value of σ from formula (8) gives

$$R'' = \frac{S}{h \cos \alpha} \tag{10}$$

The angle α is usually somewhat less than 45°; consequently, a slightly conservative value for most cases is

$$R'' \approx 1.414 \frac{S}{h} \tag{10a}$$

All stresses or forces are now known in terms of the load P, the dimensions h and d of the beam, and the angle α. To complete the solution, the angle α must be found; the principle of least work may be used to find it.

The internal work in one bay of the beam is given by the expression

$$W = \frac{\sigma^2}{2E} dht + \frac{\sigma_U{}^2}{2E} A_{U_e} h + \frac{\sigma_F{}^2}{2E} A_F d$$

(The subscript e on A_U is necessary only for single uprights and will be explained in connection with formula (22). For double uprights it is unnecessary.) By substituting into this expression the stress values in terms of S that follow from formulas (8), (9), and (6), which are

$$\sigma = \frac{2S}{ht \sin 2\alpha} = \frac{2\tau}{\sin 2\alpha} \tag{11}$$

$$\sigma_U = - \frac{Sd}{hA_{U_e}} \tan \alpha = - \frac{\tau dt}{A_{U_e}} \tan \alpha \tag{12}$$

$$\sigma_F = - \frac{S}{2A_F} \cot \alpha = - \frac{\tau ht}{2A_F} \cot \alpha \tag{13}$$

differentiating to obtain the minimum, and omitting the constant factor S^2/E, there results

$$\frac{dW}{d\alpha} = - \frac{8d}{ht} \frac{\cos 2\alpha}{\sin^3 2\alpha} + \frac{d^2}{hA_{U_e}} \frac{\sin \alpha}{\cos^3 \alpha} - \frac{d}{2A_F} \frac{\cos \alpha}{\sin^3 \alpha}$$

Substituting into this expression the values for the stresses given by equations (11), (12), and (13) and equating to zero results in the relation

$$-\sigma \frac{4 \cos 2\alpha}{\sin^2 2\alpha} - \frac{\sigma_U}{\cos^2 \alpha} + \frac{\sigma_F}{\sin^2 \alpha} = 0$$

from which

$$\tan^2 \alpha = \frac{\sigma - \sigma_F}{\sigma - \sigma_U} \tag{14}$$

If σ, σ_F, and σ_U are expressed in terms of S and α, trigonometric equations for α are obtained; the most convenient one is

$$\tan^4 \alpha = \frac{1 + \frac{ht}{2A_F}}{1 + \frac{dt}{A_{U_e}}} \tag{15}$$

After the angle α has been computed by formula (15), the stresses can be computed by formulas (11) to (13). In plane webs, the angle α generally does not deviate more than a few degrees from an average value of 40°.

2.3. Secondary stresses.- Formulas (11), (12), and (13) define the primary stresses caused directly by the diagonal tension. There are also secondary stresses which should be taken into account when necessary. The vertical components of the web stresses σ acting on the flanges cause bending of the flanges between uprights as shown in figure 5(a). The flange may be considered as a continuous beam supported by the uprights; the total bending load in one bay is equal to P_U and, if it is assumed to be uniformly distributed, the primary maximum bending moment occurs at the upright and is

$$M_{max} = \frac{Sd^2 \tan \alpha}{12h} \tag{16}$$

In the middle of the bay there is a secondary maximum moment half as large.

If the bending stiffness of the flanges is small, the deflections of the flanges indicated in figure 5(a) are sufficient to relieve the diagonal-tension stress in those diagonal strips that are attached to the flange near the middle of the bay. The diagonals attached near the uprights must make up for this deficiency in stress and thus carry higher stresses than computed on the assumption that all diagonals are equally loaded. In figure 5(b), this changed distribution of web stress is indicated schematically by showing tension diagonals beginning only near the uprights. The redistribution of the web tension stresses also causes a reduction in the secondary flange bending moments. On the basis of simplifying assumptions, these effects have been evaluated by Wagner (reference 1) and may be expressed by the following formulas:

$$\sigma_{max} = (1 + C_2)\frac{2S}{ht \sin 2\alpha} \tag{17}$$

$$M_{max} = C_3 \frac{Sd^2 \tan \alpha}{12h} \tag{18}$$

Graphs for the factors C_2 and C_3 will be given under section 4, where all graphs are collected for convenience of application. The factors are functions of the flange-flexibility parameter ωd, which is defined by

$$\omega d = d \sin \alpha \sqrt[4]{\left(\frac{1}{I_T} + \frac{1}{I_C}\right)\frac{t}{4h}} \tag{19}$$

where the subscripts T and C denote tension and compression flange, respectively. For practical purposes it is sufficiently accurate to use the following simplified form of this formula, in which the angle α is assumed to be slightly less than 45°, and the sum of the reciprocals is replaced by four times the reciprocal of the sum

$$\omega d \approx 0.7d \sqrt[4]{\frac{t}{h(I_T + I_C)}} \tag{19a}$$

In reference 1, Wagner gave a second value of ωd, 1.25 times as large as the value given by equation (19a), based on a different derivation, and recommended that the second value be used because it is more conservative. Previous papers have usually quoted this more conservative value of ωd, but it appears to be more conservative than necessary; it was based on the assumption that $d \gg h$, a condition which is now avoided in actual designs.

2.4. Behavior of uprights.- The uprights in a diagonal-tension beam may be double (on both sides of the web) or single; both types are always fastened to the web. The buckling strength of the uprights cannot be computed immediately by ordinary column formulas because the web restrains the uprights against buckling. As soon as an upright begins to buckle out of the plane of the web, the tension diagonals crossing the upright become kinked at the upright, and the tensile forces in the diagonals develop components normal to the web tending to force the upright back into the plane of the web, as indicated by the auxiliary sketch in figure 6(a). The restoring force exerted by the diagonal-tension band upon the upright is evidently proportional to the deflection (out of the plane of the web) of the upright at the point where the diagonal crosses it. The upright is therefore subjected to a distributed transverse restoring load that is proportional to the deflection; the problem of finding the buckling load of such a compression member is well-known, and methods of solution may be found in reference 3, for instance. Wagner has given the results of calculations for double uprights with clamped or pinned ends in the form of curves (fig. 6(b)), showing the ratio P_U/P_{U_E} as a function of the ratio d/h, where P_U is the buckling load of the upright and P_{U_E} the Euler load, that is, the buckling load that the same upright would carry if it were a pin-ended column not fastened to the web.

The assumption of clamped ends would be justified only if the ends of the uprights were fastened rigidly to the flanges and if, in addition, the flanges had infinite torsional stiffness. Usually, beam flanges have a rather low torsional stiffness and thus do not justify the assumption of clamped ends for the uprights. Tests of beams with very thin webs have furthermore shown that even Wagner's curve for pin-ended double

uprights as shown in figure 6(b) is entirely too optimistic for low values of d/h. The straight line marked "Experiment" in figure 6(b) (from reference 4) is slightly conservative for the average of the tests available, but several test points fall so close to it that only a large number of new tests could justify a higher curve (see Part II (reference 2)). In order to make this experimental curve applicable to uprights not in the Euler range, it may be expressed as a formula for reduced or effective column length of the upright in the form

$$L_e = \frac{h}{\sqrt{4 - 2(d/h)}} \tag{20}$$

which is valid for $d < 1.5h$; for $d > 1.5h$, of course, $L_e = h$. In practice, d is seldom chosen larger than h in order to keep the flange-flexibility factor ω_d low.

Single uprights are, in effect, eccentrically loaded columns. As long as the load is infinitesimal, the eccentricity e is evidently the distance from the plane of the web to the centroid of the upright. If the uprights are very closely spaced, the web between uprights must deflect (on the average) in the same manner as the uprights. Under this condition, the eccentricity is equal to the initial value e all along the upright and does not change with increase in load. The upright is therefore designed by the formulas used for an eccentrically loaded compression member with negligible deflection; the bending moment in the upright is eP_U, and the stress in the fibers adjacent to the web is

$$\sigma_U = \frac{P_U}{A_U}\left(1 + \frac{e^2}{\rho^2}\right) = \frac{P_U}{A_{U_e}} \tag{21}$$

where ρ is the radius of gyration of the cross section and A_{U_e} is the effective cross-sectional area, which is evidently defined by the expression

$$A_{U_e} = \frac{A_U}{1 + \frac{e^2}{\rho^2}} \tag{22}$$

Approximate values of the ratio A_{U_e}/A_U are shown in figure 7 for typical single uprights. It should be noted that the web sheet contributes no "effective width" to the upright area under the condition of pure diagonal tension considered here. Formula (22) would also apply to a double upright

not symmetrical about the web. In most cases, however, double uprights are symmetrical; in this case, $e = 0$, and thus $A_{U_e} = A_U$.

If the uprights were extremely widely spaced, the major portion of the web would remain in its original plane (on the average, i.e., averaging out the buckles). Consequently, the compressive load acting on the uprights would remain in the original plane, and the upright would act as an eccentrically loaded column under vertical loads, except for the modification introduced by the elastic transverse support furnished by the web. However, barring freak cases, extremely wide spacing of the uprights would result in the nonuniform distribution of diagonal tension shown in figure 5(b). In this configuration, the direction of the compressive load (as seen in a plane transverse to the plane of the web) is determined essentially by the configuration of the web in the vicinity of the upright-to-flange joint; conditions are therefore again similar to those in the case of the closely spaced uprights. On the basis of this consideration, formulas (21) and (22) are being used for all single uprights regardless of spacing, and the available experimental evidence indicates that this practice is acceptable at the present stage of refinement of the theory.

2.5. Shear deformation of diagonal-tension web.- The shear deformation of a web working in pure diagonal tension is larger than it would be if the web were working in true shear (a condition that could be realized by artificially preventing the buckling). The effective (secant) shear modulus G_{PDT} of a web in pure diagonal tension can be obtained by a simple strain-energy calculation as follows: Consider one bay of the web system and denote by γ the shear deformation of the bay. The external work performed during loading is

$$W_1 = \frac{1}{2} S\gamma d = \frac{1}{2} S \frac{S}{htG_{PDT}} d$$

The internal strain energy stored is

$$W_2 = \frac{\sigma^2}{2E} dth + \frac{\sigma_U^2}{2E} A_{U_e} h + \frac{\sigma_F^2}{E} A_F d$$

Now σ, σ_U, and σ_F can be expressed as functions of S by formulas (11) to (13); after transposing terms and canceling, there results the formula

$$\frac{E}{G_{PDT}} = \frac{4}{\sin^2 2\alpha} + \frac{dt}{A_{U_e}} \tan^2\alpha + \frac{ht}{2A_F} \cot^2\alpha \tag{23a}$$

which may be transformed with the aid of equation (15) into

$$\frac{E}{G_{PDT}} = 2\left(2 + \frac{dt}{A_{U_e}} \sin^2\alpha + \frac{ht}{2A_F} \cos^2\alpha\right) \tag{23b}$$

or

$$\frac{E}{G_{PDT}} = 2\left(2 - \frac{\sigma_F}{\sigma} - \frac{\sigma_U}{\sigma}\right) \tag{23c}$$

In beams of the type considered here, the flanges are usually so heavy that the term containing the flange area is negligible. Equation (23a) can then be simplified to

$$\frac{E}{G_{PDT}} = \frac{2}{\sin^2\alpha} \tag{23d}$$

When the uprights as well as the flanges are very heavy, the angle α becomes equal to 45°, and

$$G_{PDT} = \frac{E}{4} \tag{23e}$$

3. Engineering Theory of Incomplete Diagonal Tension

The two preceding sections presented "analytical" theories of the shear-resistant beam and of the beam in pure diagonal tension. An engineering or "working" theory will now be developed that connects these two analytical theories. It may be considered as a method of interpolating between the two analytical theories, guided by an empirical law of development of the diagonal tension. The purpose of this section is to present the engineering theory, to explain physical considerations and certain details, to describe (where it seemed advisable) how empirical data were obtained, and to indicate the accuracy of the method. The section thus forms the basis for section 4, which gives in concise form all the information needed for actual analysis. This division of subject

material between two sections entails some disadvantages for a first reading; however, the advantage of having section 4 in the form of a "ready reference" section for practical application, unencumbered by background material, is felt to outweigh the disadvantage.

3.1. General considerations.- When a gradually increasing load is applied to a beam with a plane web, stiffened by uprights and free from large imperfections, the following observations may be made: At low loads, the beam behaves in accordance with the theory of the shear-resistant beam; the web remains plane and there are no stresses in the uprights. At a certain critical load, the web begins to buckle; these buckles are almost imperceptible, and very careful measurements are necessary to define the pattern. As the load is increased more and more, the buckles become deeper and more distinct and the buckle pattern changes slowly to approach more and more the pattern of parallel folds characteristic of well-developed diagonal tension (fig. 2). The process of buckle formation and development is accompanied by the appearance and development of axial stresses in the uprights.

It is clear, then, that the theory of the shear-resistant beam can be verified directly by stress measurements at sufficiently low loads; it is furthermore possible (although rare) that a beam may remain in the shear-resistant regime until web fracture or some other failure takes place. The state of pure diagonal tension, however, is a theoretical limiting case; a physical beam may approach this limit fairly closely, but it can never reach the limit, because some failure will take place before the limit is reached. A direct experimental verification of the theory of pure diagonal tension is thus impossible. Fortunately the theory is so simple (as long as the effect of flexibility of the flanges may be neglected) that experimental verification is unnecessary.

Physical intuition suggests, and measurements have confirmed, that the state of pure diagonal tension is approached fairly closely when the applied load is several hundred times the buckling load. Beam webs that fail at loads several hundred times the buckling load are encountered in practice, but they are the exception rather than the rule. For the great majority of webs, the ratio of failing load to buckling load is much less, and the theory of pure diagonal tension gives poorer and poorer approximations as this ratio decreases.

In order to improve the accuracy of the stress prediction, it is necessary to recognize that most practical webs work in incomplete diagonal tension, or in a state of stress intermediate between true shear and pure diagonal tension. The first suggestion for such an improvement was made by Wagner (reference 5) for curved webs and was adopted by others for the design of plane webs. The suggestion as applied to the braced frame of figures 3(a) and 3(b) may be stated as follows: As the load P increases from zero, both diagonals work initially. At a certain

load P_{cr}, the compression diagonal will buckle, the load in the diagonal being D_{cr}. For any further increase in the load P, the load D in the compression diagonal is assumed to remain constant and equal to D_{cr}. Applied to the sheet-braced frame of figures 3(c) and 3(d), the assumption may be phrased as follows: If the applied shear stress τ is larger than τ_{cr}, only the excess $(\tau - \tau_{cr})$ above the critical shear is assumed to produce diagonal-tension effects.

Let τ_{DT} denote that portion of the applied shear stress τ which is carried by diagonal-tension action. The mathematical formulation of the assumption then becomes

$$\tau_{DT} = \tau - \tau_{cr} = \tau\left(1 - \frac{\tau_{cr}}{\tau}\right) \tag{24}$$

The "applied shear stress" $\tau(=S/ht)$ is evidently a nominal stress, that is to say, it does not exist physically as a shear stress.

3.2. Basic stress theory.- The use of formula (24) improves the prediction of the upright stresses, but the improvement is of significant magnitude only for a narrow range of proportions. An improved theory was therefore sought, with the following desired characteristics:

(1) The theory should cover the entire range of beam proportions, from the shear-resistant to the pure-diagonal-tension beam

(2) The theory should be as simple as possible, because each airplane contains hundreds of elements that must be designed by considerations of diagonal-tension action

A theory of this type has been developed in a series of steps (references 4 and 6 to 9). This section presents that portion of the theory which deals with the calculation of the primary stress conditions.

The applied nominal shear stress τ is split into two parts: a shear stress τ_S carried by true shear action of the web, and a portion τ_{DT} carried by diagonal-tension action. Thus

$$\tau = \tau_S + \tau_{DT}$$

or

$$\tau_{DT} = k\tau \qquad ; \qquad \tau_S = (1 - k)\tau \tag{25}$$

where k is called the "diagonal-tension factor." It may be noted that formula (24) is a special case of this general formulation, with the factor k defined by

$$k = 1 - \frac{\tau_{cr}}{\tau} \tag{26}$$

by virtue of the assumption made. In the improved theory, the factor k is still considered to be a function of the "loading ratio" τ/τ_{cr} but was determined empirically from a series of beam tests. The empirical expression (reference 4) is

$$k = \tanh\left(0.5 \log_{10} \frac{\tau}{\tau_{cr}}\right) \qquad \left(\tau \gtrsim \tau_{cr}\right) \tag{27}$$

For $\frac{\tau}{\tau_{cr}} < 2$, expression (27) is approximated closely by the expression

$$k = 0.434\left(\rho + \frac{1}{3}\rho^3\right) \tag{27a}$$

where

$$\rho = \frac{\tau - \tau_{cr}}{\tau + \tau_{cr}}$$

For $\tau \leqq \tau_{cr}$, the factor k is zero and the web is working in true shear. As the loading ratio τ/τ_{cr} approaches infinity, the factor k approaches unity, which denotes the condition of pure diagonal tension.

Figure 8 shows the state of stress in the web for the limiting cases ($k = 0$ and $k = 1.0$) and for the general intermediate case. Superposition of the two stress systems in the general case gives for the stress σ_1 along the direction α and the stress σ_2 perpendicular to this direction, respectively,

$$\sigma_1 = \frac{2k\tau}{\sin 2\alpha} + \tau(1 - k)\sin 2\alpha \tag{28a}$$

$$\sigma_2 = -\tau(1 - k)\sin 2\alpha \qquad (28b)$$

(For these equations, and for all equations of this section, it is assumed that the flanges are not sufficiently flexible to produce significant nonuniformity of stress.)

The value of k given by expression (27) is less than that given by (26) except for the limiting cases $\left(\frac{\tau}{\tau_{cr}} = 1.0 \text{ and } \frac{\tau}{\tau_{cr}} \longrightarrow \infty\right)$. This fact implies that the true shear stress in the sheet must develop values larger than τ_{cr}, contrary to the assumption on which expression (24) is based. At first glance, the assumption that the diagonal compressive stress does not increase beyond the critical value appears plausible, particularly if one bears in mind the picture of the braced frame in figure 3(b). However, it is well-known that deeply corrugated sheet can carry very high shear stresses before collapsing. In the light of this fact, it does not seem reasonable to assume that the hardly perceptible buckles which form in a web loaded just beyond the critical stress deprive the sheet immediately of all ability to carry any further increase in diagonal compressive stress and consequently any increase in true shear stress.

If the sheet is thus assumed to be able to carry diagonal compressive stress, it is consistent to assume that it can also carry compressive stresses parallel to the uprights or to the flanges; in other words, some effective width of sheet should be assumed to cooperate with the uprights and the flanges. Trial calculations for the upright stresses developed in test beams gave satisfactory agreement when the effective width working with the upright was assumed to be given by the expression

$$\frac{d_e}{d} = 0.5(1 - k) \qquad (29)$$

The effective width of 0.5d immediately after buckling may be thought of as produced by the sinusoidal distribution of stresses indicated in figure 9. The assumption of linear decrease with k was made as the simplest expedient possible.

With the assumptions made so far, the formula for the stress in an upright is obtained by modifying formula (12), which is valid for pure diagonal tension, to read

$$\sigma_U = -\frac{k\tau \tan \alpha}{\frac{A_{U_e}}{dt} + 0.5(1 - k)} \qquad (30a)$$

Similarly, formula (13) for the flange stress produced by the diagonal tension becomes

$$\sigma_F = - \frac{k\tau \cot \alpha}{\frac{2A_F}{ht} + 0.5(1 - k)} \tag{30b}$$

Formula (14) for the angle α may be written in the modified form

$$\tan^2\alpha = \frac{\epsilon - \epsilon_F}{\epsilon - \epsilon_U} \tag{30c}$$

This form is more general than formula (14), because it is applicable when web, flanges, and uprights are made of materials having different Young's moduli. The strains appearing in formula (30c) are defined by

$$\epsilon_F = \frac{\sigma_F}{E} \quad ; \quad \epsilon_U = \frac{\sigma_U}{E} \quad ; \quad \epsilon = \frac{1}{E}(\sigma_1 - \mu\sigma_2)$$

with the stresses σ_1 and σ_2 defined by equations (28a) and (28b); therefore,

$$\epsilon = \frac{\tau}{E}\left[\frac{2k}{\sin 2\alpha} + (1 - k)(1 + \mu)\sin 2\alpha\right] \tag{30d}$$

For practical purposes, $\sin 2\alpha$ may be taken as unity, because the angle α lies between 45° and 38° for almost all reasonably well designed webs. Expression (30d) then becomes

$$\epsilon \approx \frac{\tau}{E}\left[1 + \mu + k(1 - \mu)\right] \tag{30e}$$

All charts and graphs for plane diagonal tension shown in this paper were calculated by use of this approximation. (For curved webs, the approximation is too inaccurate because the angle α assumes much lower values.)

It might be noted that the buckle pattern immediately after buckling is not a pattern of parallel folds; this pattern is only approached asymtotically. Consequently, the term "angle of folds" has, strictly speaking, no meaning for incomplete diagonal tension, but it is sometimes used for the sake of brevity instead of the more correct term "angle of diagonal tension."

The stress component $\tau(1 - k) \sin 2\alpha$ in formula (28a) arises from the true shear existing in the web. This component affects the diagonal web strain ϵ and thus the angle α. The state of diagonal tension produced by the component kS of the applied shear load is therefore not a state of "pure" diagonal tension. It is a state of "controlled" diagonal tension in which the angle α is affected by the simultaneous presence of a true shear stress in the web. In order to bring out this distinction where necessary, the following set of symbols is used:

DT "controlled" diagonal-tension component of the total stress system when $0 < k < 1.0$

IDT (for incomplete diagonal tension) total stress system when $0 < k < 1.0$

PDT (for pure diagonal tension) stress system when $k = 1.0$

The "coupling" between diagonal tension and shear in the IDT case makes it impossible to calculate the angle α directly, as in the PDT case. Equations (30) must be solved by successive approximations. A value of α is assumed, and equations (30a), (30b), and (30d) are evaluated. From the resulting stresses, the strains are computed and inserted into equation (30c). If the angle computed from (30c) does not agree with the assumed angle, a new computation cycle is made with a changed value of α. With a little experience, three cycles are usually sufficient. For most practical problems, the necessity of going through this procedure has been eliminated by the preparation of a chart (section 4) which gives the answer directly for beams with flanges sufficiently heavy to make ϵ_F negligible compared with ϵ.

In keeping with the separation of the total stress system in a web into a shear part and a diagonal-tension part (expressions (25)), the shear deformation of a web may be separated into corresponding parts

$$\gamma_{IDT} = \gamma_S + \gamma_{DT}$$

With $\gamma = \frac{\tau}{G}$ and $\tau = 1$, this relation becomes

$$\frac{1}{G_{IDT}} = \frac{1 - k}{G} + \frac{k}{G_{DT}} \qquad (31a)$$

where G_{DT} is evaluated by using formula (23a) in the modified form appropriate to the DT case

$$\frac{E}{G_{DT}} = \frac{4}{\sin^2 2\alpha} + \frac{\tan^2\alpha}{\frac{AU_e}{dt} + 0.5(1 - k)} + \frac{\cot^2\alpha}{\frac{2A_F}{ht} + 0.5(1 - k)} \qquad (31b)$$

In most beams, the flange area is sufficiently large to permit neglecting the last term in formula (31b). With this simplification, the ratio G_{IDT}/G becomes a function of the two parameters AU_e/dt and k (or τ/τ_{cr}) and can therefore be given on a simple graph (section 4).

In some rare cases, it may be desirable to estimate the shear deformation up to the failing load of the beam. For some materials, it will then be necessary to multiply G_{IDT} by a plasticity correction factor. A graph showing this factor for 24S-T3 sheet is given in section 4. The graph represents an average curve derived from a series of tests on square panels, stiffened by varying amounts to produce different degrees of diagonal tension.

3.3. Remarks on accuracy of basic stress theory.- In the strength design of webs, reasonably accurate results may be achieved with the aid of empirical data without benefit of a theory of diagonal tension. The uprights, however, cannot be designed with any degree of reliability without benefit of such a theory. The appraisal of a theory therefore should concern itself primarily with the accuracy of predicting the upright stresses.

The engineering theory given in section 3.2 contains two main elements strongly affecting the upright stresses that require verification: expression (27) for the diagonal-tension factor k and expression (29) for the effective width of sheet. It has not been considered important to date to attempt separate verification of these two items; special test specimens with construction features not representative of actual beams would be required, and the elaborate instrumentation necessary would preclude the possibility of making checks over a wide range of proportions. The method actually chosen was to measure the upright stresses in a series of beams. Such measurements constitute only a check on the accuracy with which expressions (27) and (29), used in conjunction, predict the upright stresses, but this type of check is considered reasonably satisfactory except perhaps for thick webs.

The direct evidence used originally to establish the empirical relation (27) and to chose simultaneously the assumption (29) was obtained

by analyzing the upright stresses measured on 32 beams tested by the NACA. (See Part II (reference 2).) The criterion used for fixing the relations was that no unconservative (low) predictions of upright stress should result for any one test beam as long as the load was below about 2/3 of the ultimate. It was possible to fulfill this criterion without being unduly conservative on the average (see Part II for details). On the average, the predictions were about 10-percent conservative (for loads below 2/3 of the ultimate). In 20 percent of the cases, the predictions were about 20-percent conservative. In more than half of the cases where the prediction was 20-percent or more conservative, the upright stress was quite low at 2/3 load (about 7 ksi); the estimated probable accuracy of the upright stress under this condition was about 10 percent.

At high loads, predicted values of the upright stresses were considerably lower than the observed values for some beams. Analysis of the data - more particularly those obtained later on thick-web beams - tended to indicate that the predictions would be low when the shear stress in the web exceeded the yield value. The explanation is probably that yielding of the web has a double effect: It causes the effective width of sheet cooperating with the uprights to decrease more rapidly and it causes the diagonal tension to develop more rapidly than in the elastic range. No method of correcting for these effects of yielding has been developed as yet.

Errors in predicted upright stresses do not entail errors of the same magnitude in the predicted failing loads of beams. The first reason for this fact is that the upright stresses increase at a higher rate than the load. The second - usually more important - reason is that any overestimate of the upright stress resulting from an error in k will be accompanied by an overestimate of the allowable stress, because the allowable upright stresses depend on k. For instance, for the two beams used as numerical examples in section 7, an overestimate of the upright stress by 10 percent is accompanied by an overestimate of the allowable stress by 7 percent, and thus by only a 3-percent overestimate of the failing load of the entire beam. As a result, errors in the predicted upright stresses appear to be overshadowed by the uncertainties existing at present in the prediction of the allowable stresses; until these uncertainties are reduced, corrections for the errors mentioned in the preceding paragraph may be of small value. It is also pertinent to observe that the measurements of upright stresses at high loads are not reliable in some cases.

3.4. Comparison with analytical theories.- Any analytical theory of incomplete diagonal tension is unavoidably complex, and attempts to develop such a theory have been made only fairly recently. Koiter has developed approximate solutions (reference 10) for a beam in which the uprights are not connected to the web; they act thus purely as compression

posts and do not influence the buckling of the web. Comparative calculations made by Koiter for several values of A_U/dt give upright stresses somewhat over 20 percent in excess of those given by the engineering theory when $\frac{\tau}{\tau_{cr}} = 8$; for $\frac{\tau}{\tau_{cr}} = 100$, the excess is of the order of 5 percent. The excess stresses may be explained qualitatively by the fact that the web does not furnish any contribution to the effective area of the upright if the upright is not connected to the web, as assumed by Koiter; the discrepancy obviously decreases continuously as the ratio τ/τ_{cr} increases. In view of the simplifying assumption of disconnected uprights made in the theory, the agreement may be considered as satisfactory. The effective shear modulus calculated by Koiter is somewhat lower than that calculated by the engineering theory, as would be expected. For the limiting case of infinitely stiff uprights, the differences are 9 and 5 percent for τ/τ_{cr} equal to 8 and 100, respectively. For uprights of practical sizes (A_U/dt of 0.67 and 0.18), the differences are at most 3 percent.

A physically more realistic theory was developed by Denke (reference 11), who assumed a buckle pattern consistent with the fact that the uprights are connected to the web. Calculations made by Denke (reference 12) for a series of 28 NACA test beams show in almost all cases somewhat lower upright stresses than predicted by the engineering theory. This implies rather close average agreement with the test results because the engineering theory is conservative on the average (having been adjusted to avoid unconservative predictions in any one beam). The predictions by Denke's theory were slightly unconservative in some cases; significantly unconservative predictions (about 30 percent) were made for two beams with very low stiffening ratios A_U/dt, a fact that may be of importance in the application of the theory to thick-web beams.

Koiter's theory was intended to apply primarily at large loading ratios but was considered by him to be reasonably applicable at loading ratios down to unity. Denke's theory was set up from the beginning to cover the entire range of loading ratios from unity to infinity. Such a wide scope of the theories could be obtained only by rather severe simplifying assumptions. A different line of attack was chosen by Levy (references 13 and 14), who used a more exact theory at the expense of being restricted to low loading ratios. A comparison of upright loads calculated by Levy's theory and calculated by the engineering theory is shown in figure 10. Upright loads rather than stresses are shown to permit including the limiting case of infinite upright area. The loads shown are based on the maximum stress, which occurs in the middle of the upright. The maximum stress will be discussed in the next section; its use in figure 10 does not affect the comparison and permitted direct use of Levy's data without conversion. For the case $\left(\frac{A_U}{dt} = 0.25; \frac{d}{h} = 0.4\right)$,

the two theories agree closely. For the other two cases, the engineering theory gives somewhat unconservative (low) stresses as compared with Levy's theory. Test results, on the other hand, have indicated so far that the engineering theory tends to give somewhat conservative values for the upright stresses, but the number of reliable tests is small for low values of the ratio τ/τ_{cr} (about 2), where the percentage differences are largest. It is an open question, therefore, which theory is closer to the truth.

3.5. Amplification of theory of upright stresses.- Under the condition of pure diagonal tension (and constant shear load along the length of the beam), the upright stress σ_U is constant along the length of the upright. However, it had long been noted in tests that this stress actually has a maximum value $\sigma_{U_{max}}$ at the middle of the upright and decreases towards the ends, a fact referred to as "gusset effect" (reference 7). The stress σ_U given by the engineering theory is the average taken along the length of the upright. (This is the manner in which the experimental data used to established expression (27) for k were evaluated.)

Section 3.9 discusses the observation that most upright failures in practical beams can be ascribed to a local-crippling type of failure. It seems reasonable to assume that the maximum stress $\sigma_{U_{max}}$ is a better index for such a type of failure than the average value σ_U. This assumption is supported by the observation that all attempts to base an empirical formula for the allowable value (causing failure) of the upright stress showed much larger scatter when σ_U was used as index than when $\sigma_{U_{max}}$ was used.

The variability of σ_U, or the ratio $\sigma_{U_{max}}/\sigma_U$, is largest just after buckling of the web and decreases as the diagonal tension develops. The accuracy and the scope of the available experimental data are not adequate to establish the ratio $\sigma_{U_{max}}/\sigma_U$ empirically. On the other hand, the stress conditions just beyond buckling are reasonably amenable to a theory of the type developed by Levy (references 13 and 14). The calculations given in these two references cover two configurations $\left(\frac{d}{h} = 0.4 \text{ and } 1.0\right)$. For lack of better information, the ratio $\sigma_{U_{max}}/\sigma_U$ is assumed to vary linearly with the ratio d/h; with this assumption, the two calculated sets of values fix the relation. The calculations cover the range of τ/τ_{cr} up to about 6 or 8 and thus provide only a narrow range of variation of the factor k; under these conditions, it is not considered

justified to make a more elaborate assumption than that of linear variation of $\sigma_{U_{max}}/\sigma_U$ with k.

The resulting graph (section 4) thus rests on a limited set of data and should be considered as tentative. Such experimental evidence as exists from beam tests tends to indicate that the ratio obtained from the graph is probably somewhat less reliable than the basic stress theory itself.

3.6. Calculation of web buckling stress.- Theoretical formulas for the critical shear stress τ_{cr} are available for plates with all edges simply supported, all edges clamped, or one pair of edges simply supported and the other pair clamped. With an accuracy sufficient for all practical purposes, a formula covering all these cases can be written in the form

$$\tau_{cr,elastic} = k_{ss}E\left(\frac{t}{d}\right)^2\left[R_h + \frac{1}{2}\left(R_d - R_h\right)\left(\frac{d}{h}\right)^3\right] \qquad (32)$$

where k_{ss} is the theoretical buckling coefficient for a plate with simply supported edges having a width d and a length h (where $h > d$). The coefficients R_h and R_d are coefficients of edge restraint, taken as $R = 1$ for simply supported edges and $R = 1.62$ for clamped edges; the subscripts denote the edge to which the coefficient applies. Formula (32) represents all available theoretical results (references 3 and 15 to 17) with a maximum error believed to be less than 4 percent; a more precise evaluation of this error is not possible at present because some of the published solutions for plates with mixed edge conditions are known to be somewhat in error because of an erroneous choice of buckle pattern (reference 18), but the correct values have not yet been computed.

In actual beam webs, the edge supports are furnished by the flanges and the uprights; the panel edges are thus neither simply supported nor clamped, and the actual edge conditions may or may not lie between these two conditions. Some available theories consider the effect of bending stiffness of the uprights, but they still give results differing over 100 percent from test results over a considerable portion of the practical range of proportions. (The most important reason for the weakness of the theory is probably the one discussed in section 3.9.) For the time being, calculations of τ_{cr} for diagonal-tension analysis are therefore based on formula (32), supplemented by empirical restraint coefficients which are functions of the ratio t_U/t (section 4). It is probable, however, that theoretical coefficients based on an adequate

theory should eventually replace the empirical coefficients, particularly for beams designed to fail at low ratios of τ/τ_{cr} (say less than 4).

When the uprights are much thinner than the web, the coefficient R_h becomes very low. In such a case, the critical stress calculated by formula (32) may be less than that calculated with complete disregard of the presence of the uprights. The latter value should then be used, because low values of the empirical restraint coefficients (less than about 0.5) are not covered by tests and thus are unreliable, and because formula (32) obviously gives meaningless results when R_h approaches zero.

Formula (32) is valid only as long as the calculated critical stress is below the limit of proportionality for the material used. Beyond this limit, corrections based on the theory of plastic buckling must be applied; the theories presented in references 19 and 20 have been used to compute the correction curves given in section 4 for bare and clad webs, respectively.

3.7. Failure of the web.- As is well-known, the engineering beam theory is not entirely capable of predicting the failure of beams, even of simple cross sections; it must be supplemented by empirically determined moduli of rupture. In an analogous manner, the engineering theory of incomplete diagonal tension must be supplemented by empirical failure moduli. This section deals with the failure of webs. Since a modulus of rupture is a fictitious stress, the method of computing the stress must also be specified and constitutes an integral part of the definition of the modulus.

The stress in a web may be expressed either as a nominal shear stress or as a nominal diagonal-tension stress; the first alternative is used here. The peak nominal stress in a sheet panel may then be defined by the formula

$$\tau'_{max} = \tau\left(1 + k^2C_1\right)\left(1 + kC_2\right) \tag{33a}$$

In this expression, C_1 is a correction factor to allow for the fact that the angle α of the diagonal tension differs from 45°; by formula (11), for $k = 1$

$$C_1 = \frac{1}{\sin 2\alpha} - 1$$

The factor C_2 is the stress-concentration factor arising from flexibility of the flanges and introduced in equation (17). (Both factors are given graphically in section 4.) The effect of factor C_2 is assumed to vary linearly with k in expression (33a) for lack of better data. The effect of factor C_1 is assumed to vary with the square of k on the basis of test results on curved diagonal-tension webs, in which the angle α varies over a wider range than in plane webs. In the plane webs under consideration here, the angle is usually near 40°, and the factor C_1 is unimportant.

In curved webs, the determination of the angle α (and thus the determination of C_1) is somewhat tedious. Consequently, a slightly different procedure for calculating the web strength is used that may also be applied to plane webs, with results differing at most by 2 to 3 percent from those obtained by the first procedure. (This error is less than the scatter found in tests of nominally identical webs.) In the second procedure, the peak web stress is written as nominal shear stress in the form

$$\tau_{max} = \tau\left(1 + kC_2\right) \qquad (33b)$$

that is to say, the angle factor C_1 is omitted. On the other hand, the allowable stress is now no longer considered as a property of the material alone but is considered to be a function of the angle α_{PDT}, the angle that the folds would assume if the web were in a state of pure diagonal tension.

In order to determine the allowable stresses, a series of 97 tests was made on long webs of 24S-T3 and Alclad 75S-T6 aluminum alloy (reference 21). The external loads were applied as equal and opposite axial forces to the flanges; the loading was thus essentially a pure shear loading. The diagonal-tension factor k at failure was varied chiefly by using different h/t ratios of the webs. The rivet factor $\left(1 - \frac{\text{Diameter}}{\text{Pitch}}\right)$ was varied from about 0.6 to about 0.9; 0.6 is about the lowest value likely to be encountered in practice, 0.9 marks roughly the region where rivet failure or sheet bearing failure becomes critical. The uprights were heavy but were not connected to the web except for the lowest values of k and were not connected to the flanges in order to eliminate "Vierendeel frame" action. In most tests, bolts were used instead of rivets, with the nuts drawn up "just snug" because friction between the sheet and the flange is a very important, but highly variable, factor. The sheet was protected from direct contact with the bolt heads by heavy washers. Some tests were made with the nuts tight, and older

tests with riveted panels were used to estimate the increase in strength obtained by friction effects.

Almost all tests fell within a scatter band of ±10 percent from the average for a given value of k. The scatter may be attributed to differences in friction, material properties, and workmanship, the first factor probably being the largest one. About 85 percent of the tests fell within ±5 percent of the average and, at low values of k, more than 90 percent fell within the ±5-percent band. The curves of "basic allowable" stress given in section 4 (denoted by τ^*_{all} and shown in fig. 19) represent the line 10 percent below the average of the scatter band; they are furthermore corrected as noted to specified material properties (defined by the ultimate tensile strengths) which lie well below the typical values.

Because of the large sizes of the flanges and uprights used in the tests, the angle factor C_1 was zero ($\alpha = \alpha_{PDT} = 45^\circ$) and the stress-concentration factor C_2 was also zero. The tests thus established the basic allowable values of τ'_{max}, or of τ_{max} for $\alpha_{PDT} = 45^\circ$ (shown as the top curves in figs. 19(a) and 19(b) of section 4). Detailed test results are given in Part II.

The curves for values of α_{PDT} other than 45° were calculated as follows: By formula (11), the tensile stresses vary inversely with $\sin 2\alpha_{PDT}$; the values of τ^*_{all} for $k = 1.0$ were therefore calculated by multiplying the experimental value obtained for 45° by $\sin 2\alpha$. In webs working in true shear, the allowable stress is evidently not influenced by the sizes of the flanges and the uprights; therefore, all curves of τ^*_{all} must have as common end point at $k = 0$ the experimental value of allowable true shear stress. For any given value of α_{PDT}, the two end points of the curve were thus established. The connecting curve was drawn on the assumption that the difference between the curve in question and the experimental curve for 45° varied linearly with the factor k.

The curves for angles well below 45° are needed mostly for curved webs rather than plane webs, and such experimental confirmation as exists for low angles was obtained on curved webs.

The name "basic" was given to those curves because they serve as a basis for a system of computation. They determine directly the allowable stresses for the attachment conditions that existed in the main tests (bolts with heads protected by washers, nuts just snug). For other conditions (rivets, web sandwiched between flange angles, etc.), the basic allowable values are modified as specified in section 4 on the basis of auxiliary tests.

It should be noted that all shear stresses are based on the gross section, not on the net section between rivet holes. This simple procedure is possible because the tests disclosed an interesting fact: When the ratio of rivet pitch to diameter was varied (for a fixed value of the diagonal-tension factor k), it was found that not the failing stress on the net section, but the failing stress on the gross section was a constant within the scatter limits mentioned previously. This somewhat surprising result indicates that the stress-concentration factor varies with the rivet factor in such a manner as to just offset the change in net section. Qualitatively, the change in stress-concentration factor agrees with that found in straight tension tests: As the net section decreases (for constant gross section), the stress distribution becomes more uniform, and the ultimate stress based on the net section approaches the ultimate found in standard tensile specimens without holes. The quantitative result that the change in stress concentration just offsets the change in net area should, of course, be regarded as a peculiarity of the specific materials tested.

In the relatively thin sheets used in these tests, the diagonal-tension folds are quite deep, and sharp local buckles form in the vicinity of the bolt heads. If the bolt heads bear directly on the sheet, these local buckles cause additional stresses around the bolts that lower the allowable shear stress. In a number of comparative tests (reference 22 and other data), the decrease was found to be about 10 percent. Rivet heads are larger than the corresponding bolt heads and thus presumably give about the same conditions as bolt heads protected by washers. The difference cannot be shown directly by tests because rivets have the additional feature of setting up friction, which can be fairly well eliminated when bolts are used by leaving the nuts loose. Use of the "basic allowable" curves when the attachment is by means of rivets would therefore imply the assumption that the rivets have lost their clamping pressure in service but that there are no additional local stresses under the rivet heads even if no washers are used. Tests on riveted panels and beams (using no washers) showed generally strengths at least 10 percent higher than those developed with just-snug bolts with washers.

Because the buckles in thicker sheet are less severe, one might believe that the thicker sheet would have higher failing stresses; however, a few beam tests on sheet up to 0.2 inch thick do not support this belief. All these tests, however, did fall in the center of the scatter band or higher, so that somewhat higher allowables might be permissible in thicker sheets.

When single uprights are used, the simplest construction results if the web is riveted to the outside of the flange angle, because the uprights then require no joggling. Preliminary results indicate that such an unsymmetrical arrangement of the web results in lower web failing

stresses if the web is thick. With webs having $\frac{h}{t} = 60$ and offset by 2.4 times their thickness from the center line of the flanges, the web failing stress was reduced by about 10 percent. On webs with $\frac{h}{t} = 120$ and more, no detrimental effect was noted.

Adjacent to an upright which introduces a heavy load into a web, the web stress is not uniformly distributed over the depth of the web. If the entire shear load is introduced at one station (as in a tip-loaded cantilever, for instance), the efficiency of the web may be as low as 60 percent, and efficiencies higher than 80 percent are very difficult to achieve. The factor of stress concentration (reciprocal of the web efficiency) cannot be estimated with any degree of accuracy at present; even the location of the point of maximum stress (top or bottom flange) cannot always be predicted, because it depends on the degree to which the diagonal tension is developed. Under these circumstances, the only safe procedure is to reinforce the web by a doubler plate in the first bay.

If the load introduced at the tip does not constitute the entire shear load applied to the beam, or if the point of load application is not the tip (for example, fuselage reaction in wing spar continuous through fuselage), the conditions are less severe, but some allowance for stress concentration must be made. Also, contrary to elementary theory, a heavy local load will produce some shear stresses in the web outboard of the station of load application. The integral of the shear stresses taken over the depth of the beam is, of course, zero in order to fulfill the requirements of statics.

3.8. Upright failure by column action.- As discussed in section 2.4, the web acts as a restraining medium that modifies the effective column length. Because tests have indicated that the theoretical formulas for the restraint action are too optimistic, an empirical formula for pure diagonal tension has been introduced (formula (20)), and section 4 gives a modification of this formula appropriate for incomplete diagonal tension.

Column failure by true elastic instability is possible only in (symmetrical) double uprights. A single upright is an eccentrically loaded compression member. A theory for single uprights is difficult to formulate because the eccentricity of the load is a function of the deformations of the upright and of the web, which are very complex; the failing stress of the upright is thus a function of the web properties as well as of the upright properties. It is evidently advisable that the stress σ_U in a single upright (formula (21)) be limited to the column yield stress for the upright material.

In four tests of beams with very slender single uprights, a two-half-wave type of failure has been observed. The wave form was clearly visible at low loads and, at two-thirds of the ultimate load, the deformations were indisputably excessive on three beams. As a tentative method of avoiding this situation, it is suggested that the average stress over the cross section of the upright be limited to the allowable column stress for a slenderness ratio $h_U/2\rho$. This rule is conservative (in general) as far as ultimate strength is concerned, but the sacrifice appears to be necessary in order to achieve reasonably small deformations at limit load.

3.9. Upright failure by forced crippling.- Almost all failures on uprights (double or single) of open section may be explained as being caused by forced crippling. The deformation picture may be described as follows: Let the angle section shown in figure 11 represent a portion of the upright. The shear buckle forming in the web forces the free edge A-A of the attached leg to take on a wave form. The amplitude of this wave is a maximum at the free edge and zero along the heel B-B of the angle. If the deformations are large, then a similar wave appears along the free edge C-C of the outstanding leg, but the amplitude is very much smaller, because this edge is under tension, the upright being under eccentric bending. If the stiffener were of Z-section, the line C-C would also remain straight, and only an extremely small wave amplitude would be noticed along the free edge of the free leg.

(The deformation picture just described probably indicates the main reason why the existing theories of the buckling of stiffened webs often give very poor results. They assume that the stiffener bends with the sheet without deformation of the cross section. This assumption might yield an acceptable result if the stiffener were welded to the web along the heel line B-B. Actually, it is riveted to the web along a line between the free edge A-A and the heel line B-B. Thus, the bending stiffness that comes into play is more nearly that of the attached leg alone, rather than that of the entire stiffener.)

The physical action of a strip along the edge A-A of the upright is analogous to that of a beam-column. The strip is under the compressive stress σ_U created by the diagonal tension, and under a lateral pressure exerted by the web buckle. The problem is thus not one of elastic instability, as is true of the problems normally called local crippling. Large deformations can and do occur while the compressive stress in the upright is negligible.

No theoretical attention has been given to the problem of forced crippling, although the possibility that forced crippling acts as a "trigger mechanism" for failure had been suggested by several experimenters. It must be admitted that a theoretical analysis would be very

difficult because a large-deflection theory of plates would be required (at least if the analysis is carried to the ultimate load, as it should in order to be practically useful). An empirical formula has therefore been developed that fits single or double uprights with a change in coefficient (section 4). A rather large collection of data was available to establish this formula because almost all upright failures encountered could be ascribed to forced crippling. The cross sections included angles and Z-sections, both with and without lips, and J-sections.

The probability of failure by forced crippling evidently depends on the "relative sturdiness" of upright and web; a sturdy upright will not be deformed severely by a thin web. The empirical formula developed assumes that the relative sturdiness can be measured by the ratio of thickness of upright to thickness of web. Such a single-parameter description of the complex phenomenon of forced local crippling can obviously be no more than a first approximation and therefore cannot give very high accuracy. The test results show a scatter band of ±20 percent. The constants recommended for design are based on the lower edge of the scatter band.

No information is available on forced crippling of closed-section uprights; it is doubtful whether closed uprights with flat sides offer material advantages over open sections.

Upright sections are not infrequently chosen by the criterion that the moment of inertia should be a maximum for a given area. This one-sided emphasis is quite misleading; a greater moment of inertia for a given area means a thinner section, which has less local bending stiffness and is thus more susceptible to forced crippling. In order to demonstrate this fact, two beams (about 70 in. deep) were built, having the same web thickness, upright spacing, and upright area, but differing in moment of inertia of the (single) uprights. The moment of inertia was doubled on the second beam, but this beam carried only 75 percent of the load carried by the first beam; the first beam failed by web rupture, the second, by forced crippling of the uprights. (See Part II.)

3.10. Interaction between column and forced-crippling failure.- It should be realized that column failure and forced-crippling failure are not, in reality, two completely independent types of failure; forced deformation of the cross sections will affect the column behavior of the upright. A certain amount of interaction effect is included automatically in the formulas for the allowable stresses because they are empirical. It is possible, however, that for very different proportions, or for different loading conditions than those that existed in the tests, some direct allowance for interaction may be necessary. For instance, the uprights were, in all but a very few tests, subjected only to the compressive loads arising out of the diagonal-tension action of the webs; they were not subjected to externally applied compressive loads. In

cases where the compressive stress due to externally applied loads is of the same order of magnitude as that caused by the diagonal-tension action, the problem of interaction between forced crippling and column buckling may become serious. It might be mentioned that a forced-crippling problem also exists when externally applied compression is the only force acting, that is to say, the skin buckles of a stiffened compression panel generally reduce the failing stress of the attached stiffener below that of the free stiffener.

3.11. Web attachments.- The web-to-flange rivets or bolts carry a load per inch run R'' equal to S/h for a shear-resistant beam ($k = 0$) and $1.414S/h$ for a beam in pure diagonal tension ($k = 1$, see formula (10a)). Linear interpolation between these two values gives for incomplete diagonal tension

$$R'' = \frac{S}{h_R}(1 + 0.414k) \tag{34}$$

The depth h_R used in formula (34) is the distance between the rivet lines in the top and bottom flanges if the rivet lines are single, or the distance between the centroids of rivet patterns in the most general case of multiple rivet lines. There is a wide-spread custom of using the effective depth h_e instead of h_R, a practice that has been found to give definitely unconservative results on some test beams; in many cases, of course, the unconservatism is sufficiently small to be covered by the hidden factors of safety usually existing in rivet design.

Literal interpretation of the basic concept of incomplete diagonal tension would require that the rivet load be considered as made up of two components: a force $(1 - k)S/h$ acting horizontally, caused by the shear component of the load, and a force $kS/h \cos \alpha$ (according to formula (10)) acting at the angle α. The two forces should be added vectorially. The resulting formula for R'' is more complicated than formula (34) and gives somewhat lower values (except, of course, at $k = 0$ and $k = 1$). This formula might be considered more rational than formula (34), but this purported greater rationality is spurious because the factor k expresses average stress conditions in the panel, and the conditions along the riveted edge are not average. Experimentally, the "more rational" formula has been found to be somewhat unconservative (see Part II) and is therefore not given here.

The upright-to-flange rivets simply carry the upright load into the flange and require no special comments.

The upright-to-web rivets must be investigated for several conditions that justify some comments.

In double uprights, the rivets must have sufficient shear strength to permit the upright to develop its potential column strength. In civil-engineering practice, where built-up columns are frequent, various rules are used to determine the required shear strength, and they lead to widely different results. Tests were therefore made on several series of double-angle columns (reference 23); the formula derived from these tests (given in section 4.14) is essentially based on one of the methods used in civil engineering, in which the shear strength is computed as though the member were loaded not as a column, but as a beam (by a distributed transverse load).

A riveted-up section evidently cannot achieve the same strength as an (otherwise identical) monolithic section. For the purpose of obtaining the formula just mentioned, the required shear strength has been defined arbitrarily as the shear strength that will permit the riveted-up section to develop 98 percent of the strength of the monolithic section. To be entirely consistent, then, the usual column allowable stress should be reduced by 2 percent; however, this small reduction may be omitted because the formula for effective column length is somewhat conservative. If the rivet strength provided in an actual case is much less than that given by the formula, the allowable column stress must be reduced. This situation should not arise in new designs, but it did arise in a number of the test beams designed before the formula was developed. A reduction factor derived from the tests is given in section 4.

With single uprights, the shear buckles in the web tend to lift the sheet off the upright; with double uprights, the web buckles tend to split the two upright sections apart. These actions produce tensile forces in the rivets, and an empirical criterion for tensile strength is therefore given in section 4. It should be noted that tensile failure of a rivet is equivalent to tensile failure of the rivet shank only when the head is relatively high. With low rivet heads, the tensile failure is caused by shearing the head off axially; with flush rivets, tensile failure may be caused by the rivet pulling through the sheet. Because flush rivets have a low tensile strength, the problem usually demands most attention on the outside skin; it is therefore discussed somewhat more fully in the section 9.9, which deals with the attachment of curved webs.

The criterion for the required tensile strength of rivets is based on rather scanty direct evidence (Part II). However, out of 135 beams tested by manufacturers, the great majority satisfied the criterion (which is one reason why the available direct evidence is scanty). One large company is using a shear criterion which gives practically the same results as the tensile criterion does for rivets where shank failure determines the tensile strength. It is believed, therefore, that the criterion is not unduly severe, although it may be conservative.

3.12. Remarks on reliability of strength formulas.- In sections 3.7 to 3.11, the various types of failures have been discussed in a general fashion. In section 4, specific formulas recommended for use in design are presented. The formulas are derived from test plots forming scatter bands and are consistently based on the lower edges of the scatter bands; they are thus intended to give a very high degree of assurance that any given beam under consideration will carry the design load. Because the scatter bands are fairly wide, this high degree of assurance of safety is necessarily obtained at the expense of considerable conservatism for most beams.

The following remarks are based on the analysis of 64 beams tested by the NACA, 135 beams tested by five manufacturers, and about 140 NACA tests made to establish the strength of webs under nearly pure shear loading. The remarks are rather general; a more detailed discussion is given in Part II.

The degree to which the formulas fulfill the intended purpose of safe design may be characterized by the following statement: It is estimated that predictions unconservative by more than 2 percent should occur in less than 5 percent of all cases, and predictions unconservative by more than 5 percent should occur only with negligible frequency. Excluded are local regions where large loads are introduced and beams with very flexible flanges ($\omega d > 2.5$).

The scatter exhibited in web-rupture tests may be ascribed to the variations of three factors:

(1) Material properties

(2) Local stress conditions around rivets or bolts

(3) Friction between sheet and flange

In the NACA tests on webs under pure shear loading, the material properties were fairly uniform, and individual corrections were made. The webs were attached by bolts, with the nuts carefully adjusted to be just snug; the friction between the sheet and the flange was therefore small. Nevertheless, the width of the scatter band was about ±10 percent, which must be attributed mostly to variations in item (2). In beam tests, then, the failing strengths of webs may be expected to average 10 percent higher than the recommended allowable values adjusted to actual material properties, and occasional values 20 percent higher than the allowables may be found. An additional increase above the allowable may be realized from the portal-frame effect (see appendix).

It may be remarked that the procedure of correcting for actual material properties is not very accurate. This correction is commonly

based on the tensile strength developed by a coupon of standard shape. Such a single tensile coupon neither evaluates possible anisotropy, nor does it evaluate compressive properties; these factors should be evaluated because shear is equivalent to tension and compression at $\pm 45^{\circ}$ to the axis. Furthermore, the standard tensile test does not evaluate the static notch sensitivity of the material. Fragmentary test evidence indicates that an increase in tensile strength brought about by a deviation from the specified heat treatment may be more than overbalanced by an increase of the static notch sensitivity. The standard tensile test therefore does not appear to be a very reliable index for correcting the strength of a web that fails at rivet holes, although its use is probably preferable to making no correction.

Plots of upright stresses causing failure by forced crippling show a width of scatter band of ±20 percent. Thus, the average of a sufficiently large number of tests of different designs may be expected to be $\frac{1}{0.8} = 1.25$ times higher than the recommended allowable values, and occasional uprights may develop 1.5 times the allowable value. For uprights failing by column action, the data available are insufficient to establish a width of scatter band. Taken at face value, however, they appear to indicate about the same width of band as for failure by forced crippling. The width of the scatter bands for upright failure is probably caused largely by inadequacy of the empirical formulas, and only to a very minor extent by variation of material properties. Consequently, higher allowable stresses would seem acceptable if they are verified for any given case by a specific test.

It should be remarked that upright failure at a load 1.5 times the design load is, of course, possible only if the web also develops 1.5 times the design load. In a well-designed beam, such a contingency should not arise because the scatter band for web strength is much narrower. Many of the test beams under discussion here, however, were deliberately built with overstrength webs in order to obtain data on upright failure.

A discussion of the accuracy of strength predictions would be incomplete without some mention of pitfalls in test technique.

If ordinary hydraulic jacks are used to apply the load, and the load is measured by measuring the oil pressure, calibration tests must be made to check for friction in the jack. (Values up to 40 percent have been measured.)

If the beam tested is a cantilever, the slope of the beam axis at the tip may be quite large in the last stages of the test. The force applied to the jack is then inclined, and the horizontal thrust component may greatly increase the friction in the jack. This component

also falsifies the bending moment in the beam and should be eliminated by using rollers. Rollers should also be used when the beam is tested as a "simple beam" on two supports; a beam bolted to two supports cannot be considered as a "simple beam" when the deflections are large.

When individual beams are being tested, it is almost always necessary to provide supports against lateral failure. Care is necessary to reduce the friction against these supports. Thick-web beams roll over with considerable force and thus produce considerable friction against fixed side supports. Wooden guides are objectionable because there is danger that the beam flange may dig into the supports and hang up.

3.13. Yielding.- According to the official design rules, the stress in a structural member should not exceed the yield stress when the structure is subjected to the design yield load. For members subjected to axial stress, such as spar caps, the application of the rule is clear and simple. The stress can be calculated or measured, if necessary; stress peaks due to bolt holes or similar discontinuities are so localized that they are neglected by common tacit consent. The allowable yield stress either constitutes a part of the official materials specifications, or it may be measured by a well-defined and readily applicable procedure. For shear webs, however, the situation is much less clear. Except in the rare case of a truly shear-resistant web, the stress system is complicated, and the allowable yield stress is not covered by the specifications. The suggested procedure which follows is an attempt to formulate a simple procedure consistent in its main features with that used for axially stressed members.

The nominal web stress given by formula (33a) is used to define the stress existing in the web. (Formula (33b) could be used just as well; the reason for using (33a) in this discussion is given subsequently.)

In the basic case of a pure-diagonal-tension web having factors C_1 and C_2 equal to unity, the nominal web shear stress is equal to one-half of the tensile stress (formula (11), with $\alpha = 45^\circ$). Consequently, the allowable yield value of the nominal web shear stress is one-half of the specification tensile yield stress of the web material. For a web working in pure shear, the procedure for establishing an allowable yield value is somewhat arbitrary, because the standard materials specifications do not specify a shear yield stress. However, typical values of shear yield stress are often supplied by the materials manufacturer. While these values are not obtained on sheet material and are thus open to some question, they are probably acceptable for the purpose on hand. The typical shear yield stress may be converted into an allowable value by multiplication with the ratio of specification tensile yield to typical tensile yield stress. With the allowable values of the nominal web shear stress established in this manner for $k = 1.0$ (pure diagonal tension)

and $k = 0$ (pure shear), their magnitudes for intermediate values of k can be estimated by using the curves for the allowable ultimates as guides; this procedure is evidently approximate but should be sufficiently accurate. A curve established in this manner is given in section 4 for 24S-T3 material.

A brief investigation shows that the criterion for yielding of the web overrides the ultimate strength criterion for 24S-T3 alloy only under a special combination of factors (ultimate allowable based on tight rivets, ratio of design yield to design ultimate load 0.74 according to Navy Specifications). For 75S-T6 alloy, the curve of allowable yield stress lies above the "basic allowable" ultimate stress and therefore cannot override the ultimate strength criterion.

The procedure outlined here agrees fairly well with the average of a number of experimental yield loads determined by several methods in manufacturer's tests, but there is a large scatter for the thinner webs ($t < 0.06$ in.). Most of the scatter can be explained by the fact that the methods used depend on judgment rather than on measurement. A method of this nature may give reasonably consistent results if applied by one skilled individual, or by a small group of individuals working in close cooperation within one organization. The same method used by a different organization, however, may give widely differing results. (Most of the thick-web data analyzed were obtained within one organization and were reasonably consistent.)

The reason for defining the web stress by formula (33a) rather than by formula (33b) is that only one curve is needed to define the allowable stress. The use of formula (33b) would require that a family of curves of allowable yield stress be constructed, in the same manner as the curves of allowable ultimate stress (see section 3.7).

In practice, "detectable permanent set" has not infrequently been used in place of the yield criterion. This practice would correspond to using the proportional limit, rather than the yield stress, if sensitive means of detection are employed and consequently seems inconsistent with the design practice for such members as spar caps. Individual companies may use such conservative rules as a matter of design policy. Conservative yield allowables imply some weight penalty but decrease the possibility of unanticipated yielding due to local stress concentrations not taken into account in the stress analysis. In very thin webs, for instance, yielding may occur because of compression in the unsupported region under a joggled upright if the joggle is long; stress concentrations also occur in the web corners at uprights through which large local loads are introduced into the web.

The general criterion that "there shall be no permanent set" is empty until it is supplemented by a specification as to what quantity

shall be measured in order to determine whether a permanent change has taken place. In order to make the result independent of the measuring instrument used, the description "detectable set" should be replaced by a quantitative definition. In order to arrive at a decision as to what quantity should be measured, and how much permanent change should be permitted, it will be necessary to consider why permanent set is not desired. The answer to this question may be given by aerodynamic or functional rather than purely structural considerations. These considerations indicate that a host of problems arises as soon as an attempt is made to refine the methods for designing against permanent set.

4. Formulas and Graphs for Strength Analysis of Flat-Web Beams

No attempt should be made to use the following formulas until section 3 has been carefully read.

4.1. Effective area of upright

(a) Double (symmetrical) uprights:

$$A_{U_e} = A_U$$

(no sheet included in A_U)

(b) Single uprights:

$$A_{U_e} = \frac{A_U}{1 + \left(\frac{e}{\rho}\right)^2}$$

(no sheet included in A_U)

e distance from median plane of web to centroid of cross section

ρ radius of gyration of cross section (pertaining to moment of inertia about centroidal axis parallel to web)

An estimate of the ratio A_{U_e}/A_U may be made with the aid of figure 7.

(c) Indefinite-width uprights: When the outstanding leg of an upright is very wide (for example, when a bulkhead between spars is flanged over and riveted to the spar webs), consider A_{U_e} as consisting of the attached leg plus an area $12t_U^2$ (i.e., effective width of outstanding leg is $12t_U$).

(d) Uprights with legs of unequal thickness: Use the thickness of the leg attached to the web to determine the ratio t_U/t (required for formula (36) or (37), section 4.10 or 4.11).

4.2. Critical shear stress

In the elastic range, the critical shear stress is given by formula (32), which takes the alternative forms

$$\tau_{cr,elastic} = k_{ss}E\left(\frac{t}{d_c}\right)^2\left[R_h + \frac{1}{2}\left(R_d - R_h\right)\left(\frac{d_c}{h_c}\right)^3\right] \qquad \left(d_c < h_c\right)$$

$$\tau_{cr,elastic} = k_{ss}E\left(\frac{t}{h_c}\right)^2\left[R_d + \frac{1}{2}\left(R_h - R_d\right)\left(\frac{h_c}{d_c}\right)^3\right] \qquad \left(d_c > h_c\right)$$

k_{ss} from figure 12(a)

(If $d_c > h_c$, read abscissa of fig. 12(a) as d_c/h_c.)

d_c, h_c "clear" dimensions (see fig. 12(a))

R_d, R_h restraint coefficients from figure 12(b). (Subscript h refers to edges along uprights; subscript d to edges along flanges.)

With $\tau_{cr,elastic}$ known, find τ_{cr} from figure 12(c).

Note 1: When attached legs of double uprights are crowned so as to touch web only along rivet line, use d instead of d_c.

Note 2: If τ_{cr} calculated by the first formula is less than τ_{cr} calculated with the presence of uprights disregarded, use the latter value.

4.3. Nominal web shear stress

The nominal web shear stress is calculated by the formula

$$\tau = \frac{S_W}{h_e t}$$

where

S_W web shear force (external shear minus vertical component of flange forces)

For unusual proportions, use formula (3). When calculating I and Q_W for use with this formula, multiply web thickness by (estimated) diagonal-tension factor k.

4.4. Diagonal-tension factor

The diagonal-tension factor k is obtained from figure 13, with $\frac{td}{Rh} = 0$.

When $\frac{I}{\tau_{cr}} < 2$, use formula (27a).

4.5. Stresses in uprights

The ratio σ_U/τ can be found from figure 14 if the beam flanges are reasonably heavy. If not, use procedure described near end of section 3.2.

The stress σ_U is the average taken along the length of the upright. (For a double upright, σ_U is uniform over the cross section; for a single upright, σ_U is the stress in the median plane of the web along the upright-to-web rivet line.)

The maximum value of σ_U occurs at midheight; the ratio $\sigma_{U_{max}}/\sigma_U$ is given by figure 15.

4.6. Angle of diagonal tension

The angle α of the diagonal tension is found with the aid of figure 16(a), if it is desired, by using the ratio σ_U/τ obtained previously (section 4.5). The recommended procedure for finding the allowable web stress requires use of the angle α_{PDT}, which is found by equation (15); a graphical solution based on this equation is given in figure 16(b).

4.7. Maximum web stress

The maximum (nominal) web stress is calculated by either expression (33a) or (33b); these expressions are, respectively,

$$\tau'_{max} = \tau\left(1 + k^2C_1\right)\left(1 + kC_2\right)$$

and

$$\tau_{max} = \tau\left(1 + kC_2\right)$$

The factor C_1 is taken from figure 17, the angle α obtained from figure 16(a) being used. The factor C_2 is taken from figure 18.

4.8. Allowable web stresses

(For failure in web-to-flange attachment line.)

Figure 19 gives "basic allowable" values (denoted by τ^*_{all}) for τ_{max} that are used as follows for different types of connections:

(a) Bolts just snug, heavy washers under bolt heads, or web plate sandwiched between flange angles: Use basic allowables.

(b) Bolts just snug, bolt heads bearing directly on sheet: Reduce basic allowables 10 percent.

(c) Rivets assumed to be tight: Increase basic allowables 10 percent.

(d) Rivets assumed to be loosened in service: Use basic allowables.

If the nominal web shear stress is expressed as τ_{max} (section 4.7), the allowable value is taken from the curve with the appropriate value of α_{PDT}. If the nominal web shear stress is expressed as τ'_{max} (section 4.7), the allowable value is taken from the top curve labeled $\alpha_{PDT} = 45^\circ$.

Rivets are assumed to be not of any countersunk type.

Note 1: The allowable web stresses defined by figure 19 are valid only if the standard allowable bearing stresses (on sheet or rivets) are not exceeded.

Note 2: For webs unsymmetrically arranged with respect to flanges and with $\frac{h}{t} < 100$, the allowable web stress should be reduced. (See section 3.7.)

Note 3: At points where local loads are introduced into the web, the allowable web stress should be reduced. (See section 3.7, last two paragraphs.)

4.9. Effective column length of uprights

The effective column length L_e of an upright is given by the empirical formula

$$\left.\begin{aligned} L_e &= \frac{h_U}{\sqrt{1 + k^2\left(3 - 2\frac{d}{h_U}\right)}} \qquad (d < 1.5h) \\ L_e &= h_U \qquad\qquad\qquad\qquad (d > 1.5h) \end{aligned}\right\} \tag{35}$$

where

h_U length of upright, measured between centroids of upright-to-flange rivet patterns

4.10. Allowable stresses for double uprights

(Webs and uprights made of the same aluminum alloy; open-section uprights riveted to web.)

(a) To avoid forced-crippling failure, the maximum upright stress $\sigma_{U_{max}}$ should not exceed the allowable value σ_o defined by the empirical formulas

$$\sigma_o = 21k^{2/3}\left(t_U/t\right)^{1/3} \text{ ksi} \qquad (24S\text{-}T3 \text{ alloy}) \tag{36a}$$

$$\sigma_o = 26k^{2/3}\left(t_U/t\right)^{1/3} \text{ ksi} \qquad (75S\text{-}T6 \text{ alloy}) \tag{36b}$$

Nomographs for these formulas are given in figure 20. If σ_o exceeds the proportional limit, multiply it by a plasticity correction factor η, which can be taken as

$$\eta = \frac{E_{sec}}{E}$$

with the moduli determined from the compression stress-strain curve of the upright material.

(b) To avoid column failure, the stress σ_U should not exceed the column allowable taken from the standard column curve for solid sections with the slenderness ratio L_e/ρ as argument. (The curve for solid sections is considered adequate because the forced-crippling criterion considers local failure.)

4.11. Allowable stresses for single uprights

(Webs and uprights made of the same aluminum alloy; open-section uprights riveted to web.)

(a) To avoid forced-crippling failure, the maximum upright stress $\sigma_{U_{max}}$ should not exceed the allowable value σ_o defined by the empirical formulas

$$\sigma_o = 26k^{2/3}\left(t_U/t\right)^{1/3} \text{ ksi} \qquad \text{(24S-T3 alloy)} \qquad (37a)$$

$$\sigma_o = 32.5k^{2/3}\left(t_U/t\right)^{1/3} \text{ ksi} \qquad \text{(75S-T6 alloy)} \qquad (37b)$$

Nomographs for these formulas are given in figure 20. If σ_o exceeds the proportional limit, apply the plasticity reduction factor as for double uprights.

(b) To avoid column failure or excessive deformation, the stress σ_U should not exceed the column yield stress, and the average stress over the cross section of the upright

$$\sigma_{U_{av}} = \frac{\sigma_U A_{U_e}}{A_U} \qquad (38)$$

should not exceed the allowable stress for a column with the slenderness ratio $h_U/2\rho$.

4.12. Web-to-flange rivets

The rivet load per inch run of beam is given by formula (34) as

$$R'' = \frac{S_W}{h_R}(1 + 0.414k)$$

where

h_R depth of beam measured between centroids of rivet patterns, top and bottom flanges

4.13. Upright-to-flange rivets

The end rivets must carry the load existing in the upright into the flange. If the gusset effect (decrease of upright load towards the end of the upright) is neglected, these loads are

for double uprights

$$P_U = \sigma_U A_U$$

for single uprights

$$P_U = \sigma_U A_{U_e}$$

(39)

4.14. Upright-to-web rivets

For double uprights, the upright-to-web rivets should be checked for two possibilities of failure, one due to shear caused by column bending, one due to tension in the rivets caused by the tendency of the web folds to force the two components of the upright apart.

To avoid shear failure, the total rivet shear strength (single shear strength of all rivets) for an upright of 24S-T3 alloy should be

$$R_R = \frac{100Qh_U}{bL_e} \text{ kips} \qquad (40)$$

where

Q static moment of cross section of one upright about an axis in the median plane of the web, inches^3

b width of outstanding leg of upright, inches

h_U/L_e ratio from formula (35), section 4.9

For uprights of other materials, it is suggested that the right-hand side of formula (40) be multiplied by the factor: Compressive yield stress of material divided by compressive yield stress of 24S-T3 alloy.

If the actual rivet strength R is less than the required strength R_R, the allowable stress for column failure (section 4.10, item (b)) must be multiplied by the reduction factor given in figure 21.

The strength necessary to avoid tension failures is given by the tentative criterion:

$$\text{Tensile strength of rivets per inch run} > 0.15t\sigma_{ult} \qquad (41)$$

where σ_{ult} is the tensile strength and t, the thickness of the web.

For single uprights, the tensile strength necessary to keep the folds of the web from lifting off the upright is given by the tentative criterion:

$$\text{Tensile strength of rivets per inch run} > 0.22t\sigma_{ult} \qquad (42)$$

The tensile strength of a rivet is defined as the tensile load that causes any failure; if the sheet is thin, failure will consist in the pulling of the rivet through the sheet. (See section 9.9 for data.)

No criterion for shear strength of the rivets on single uprights has been established; the criterion for tensile strength is probably adequate to insure a satisfactory design.

The pitch of the rivets on single uprights should be small enough to prevent inter-rivet buckling of the web (or the upright, if thinner than the web) at a compressive stress equal to $\sigma_{U_{max}}$. The pitch should also be less than $d/4$ in order to justify the assumption on edge support used in the determination of τ_{cr}. The two criteria for pitch are probably always fulfilled if the strength criteria are fulfilled and normal riveting practices are used.

4.15. Effective shear modulus

The effective (secant) shear modulus G_{IDT} of webs in incomplete diagonal tension is given by figure 22(a) for the elastic range. Figure 22(b) gives the plasticity correction factor G_e/G_{IDT} for webs of 24S-T3 alloy.

4.16. Secondary stresses in flanges

The compressive stress in a flange caused by the diagonal tension may be taken as

$$\sigma = - \frac{kS_W \cot \alpha}{2A_F}$$

The primary maximum bending moment in the flange (over an upright) is theoretically

$$M_{max} = kC_3 \frac{S_W d^2 \tan \alpha}{12h}$$

where C_3 is taken from figure 18. The secondary maximum moment, halfway between uprights, is half as large. Because these moments are highly localized, the block compressive strength is probably acceptable as the allowable value. The calculated moments are believed to be conservative and are often completely neglected in practice.

5. Structural Efficiency of Plane-Web Systems

In many problems of aircraft structural design, the over-all dimension of the component to be designed is fixed by aerodynamic or other considerations, and the load that it must carry is also known. These given requirements imply inherent limitations on the structural efficiency that may be achieved. Consider, for example, two compression members required to carry a load of 10 kips; the first one is specified to be 1 inch long, the second one 10 feet long. Obviously, the first one will be merely a compression block, which can be loaded to a very high stress and is thus very efficient. The second one will be a fairly slender column, which can carry only a low stress and is thus unavoidably rather inefficient.

As an aid in choosing the most efficient designs possible, Wagner suggested (reference 24) that the given parameters - load and dimension - be combined into a structural index having the dimensions of a stress (or any convenient power or function of a stress). For columns, the index would be P/L^2, and for shear webs, it would be S/h^2, but for convenience in plotting certain curves, the square root of these expressions is usually preferred; the structural index for shear webs is thus $\sqrt{S}/h$, where S is conventionally expressed in pounds and h in inches in order to obtain a convenient range of numbers. A web that is required to be very deep, but to carry only a small load may be termed "lightly loaded"; it has a low index value which connotes unavoidably low efficiency. A shallow web carrying a large load is "highly loaded"; it has a high structural index and can be designed to be more efficient than the lightly loaded web. A web 70 inches deep and carrying a load of 10,000 pounds (side of a flying-boat hull) would have an index value of 1.4; a web 10 inches deep and carrying a load of 100,000 pounds (web of a monospar fighter wing) would have an index value of 31.8. These two examples indicate roughly the range of the index value for conventional designs.

In order to obtain a general idea of the structural efficiency of plane webs in incomplete diagonal tension, systematic computations have been made for the following conditions:

(1) The material is either 24S-T3 for web and uprights, or Alclad 75S-T6 for the web and 75S-T6 for the uprights.

(2) The upright spacing is fixed at either one-fourth of the web depth or equal to the web depth.

(3) The cross section of the upright is an angle having legs of equal thickness but unequal width. The leg attached to the web is assumed to have a width-thickness ratio of 6, the outstanding leg a ratio of 12. Single as well as double uprights are investigated.

The allowable values used for web shear stresses are those shown in figure 19. The allowable upright stresses for forced crippling are taken from figure 20. The curve of allowable column stress is defined for 24S-T3 material by the Euler curve and a straight line tangent to it, starting at 52.5 ksi at zero length. For 75S-T6 uprights, the Euler formula is used with the tangent modulus substituted for Young's modulus.

With the design conditions thus fixed, web systems have been designed by a trial-and-error method to give simultaneous failure of the web and the uprights; the result may be termed "balanced designs." It has not been proved that a balanced design is necessarily the optimum (lightest) design, but spot checks on a number of designs have failed to disclose any cases where the efficiency could be improved by unbalance.

The results of the calculations are shown in figure 23. The upper diagrams show the structural efficiency, expressed as a nominal shear stress

$$\bar{\tau} = \frac{S}{h\left(t + \frac{A_U}{d}\right)}$$

that is to say, as the shear stress that would exist in the fictitious web obtained by adding the upright material in a uniformly distributed manner to the actual web. The upper limit for $\bar{\tau}$ is the allowable shear stress for webs with $k = 0$; at this limit, no stiffeners are required, the flanges alone being sufficient to make the web buckling stress equal to the stress at which the web fails in the connection to the flange.

The lower diagrams in figure 23 show the "stiffening ratio" A_U/dt. These diagrams are useful for finding a trial size of upright after the necessary web thickness has been estimated, as discussed in section 6. For double uprights on Alclad 75S-T6 webs, interpolation between the curves for $\frac{d}{h} = 1.0$ and $\frac{d}{h} = 0.25$ is not permissible for index values above about 10; a more complete set of curves is therefore given in figure 23(c).

For a given web material and index value, the stiffening ratio depends to some extent on the upright spacing (d/h) and on the type of upright (double or single). However, the efficiency of the web system as measured by $\bar{\tau}$ is practically independent of upright spacing and upright type for 24S-T3 webs. For 75S-T6 webs designed for an index

value greater than about 14, double uprights closely spaced $\left(\frac{d}{h} = 0.25\right)$ appear to give appreciably better efficiency than the other three arrangements, but the following practical considerations should be borne in mind.

At low values of diagonal tension (say $k < 0.05$), the calculations are very sensitive to changes in the web-buckling stress, the web allowable stress, and the shape of the upright (ratio b/t_U). Figure 24 shows the approximate relation between the index value, the thickness ratio h/t, and the factor k, based on the calculations for figure 23. Inspection of figure 24 shows that, for the web system under consideration $\left(75S\text{-}T6, \text{ double uprights}, \frac{d}{h} = 0.25\right)$, the value of $k = 0.05$ is already reached at an index value of about 15. For higher index values, the efficiency that can be counted upon in any given practical case is therefore somewhat doubtful; it may be only very little more than the efficiency of systems with single uprights and wider upright spacing, which are much more desirable for production.

Inspection of figure 24 shows that the thickness ratio of the web (h/t) depends only on the index value, in first approximation. Because the ratio h/t is more readily visualized than the index value, approximate (average) values of h/t are shown in figure 23 in addition to the index values. Inspection of this figure shows that thick and medium-thick webs occupy the largest part of the figure, while the thin webs are crowded together on the left side. Wagner recommended (reference 1) that webs be designed as diagonal-tension webs for index values less than 7 (and as shear-resistant webs for index values greater than 11). Webs that fall under Wagner's classification of diagonal-tension webs therefore occupy only a narrow strip on the left-hand edges of figure 23.

Each curve in figure 23 has two branches. On the right-hand branch, the uprights fail by forced crippling; on the left-hand branch, they fail by column bowing. (The sudden change in direction of the curves at their right-hand ends is caused by the "cut-off rule" regarding the critical shear stress given in note 2 of section 4.2.) Inspection of the figure shows that column failure becomes decisive only when the index value is quite low, about 4 or less, and the h/t ratio is correspondingly large (over 1000). In present-day practice, such thin webs are encountered only infrequently; upright failure by forced crippling therefore predominates in practice.

As long as failure by forced crippling remains decisive, the efficiencies shown in figure 23 can be improved somewhat by choosing more compact upright sections (lower b/t_U) than those chosen for the

calculations. The practical limitation will be the edge distance required for upright-to-web and upright-to-flange rivets.

Figure 25 shows a comparison of the most efficient web systems for the two materials considered. The curves represent faired envelopes for the range of upright spacing studied.

An often-debated question is the relative efficiency of sheet webs and truss webs. Figure 26 gives a comparison of 24S-T3 alloy sheet webs, Pratt truss webs, and Warren truss webs, based on a revision of the study made in reference 25. The truss-web members were assumed to be square tubes with a ratio $\frac{b}{t} = 24$ of the walls in order to eliminate local instability problems. The same allowable stresses (including the column curve) were used as for the sheet webs. Compression members were assumed to be pin-jointed for design purposes. For a number of trusses, sufficiently detailed designs were made to permit an estimate to be made of the weight added by the gussets and by the end-connection inefficiency of the web members. The tension members of the trusses were designed to be capable of carrying sufficient compression to enable the truss to carry a negative load equal to 40 percent of the positive load. (The sheet webs will carry 100-percent negative loads.)

Figure 26 shows that the Pratt truss is decidedly less efficient than a sheet web except over a very narrow range, but the Warren truss is somewhat more efficient than the sheet web over a considerable range of the index value. The following considerations, however, may influence the choice between the two types of shear webs:

(a) The method of designing sheet webs has been proved by about 200 tests covering a large range of proportions. There does not appear to be a single published strength test of a truss of the type considered. It is quite possible that the secondary stresses existing in trusses with riveted joints may reduce the actual efficiency below the theoretical value.

(b) In general, the designer is required to design a beam rather than a shear web alone. The allowable flange compressive stresses for a sheet-web beam are quite high (often above the yield stress), while the long unsupported chords of the Warren truss would have rather low allowable stresses. The efficiency of the tension chords is also lower in the truss because the web shears are introduced in concentrated form and thus necessitate large rivet holes through the flanges. Inefficiency of the flange might therefore counterbalance efficiency of the web.

(c) If the web to be designed is for the spar of a conventional wing with ribs, additional members must be added to the Warren truss

for attaching the ribs. On a sheet web, the uprights can be used for this purpose with little, if any, additional material being required. In addition, considerations of rib weight may require changes of the slopes of the truss diagonals, and the efficiency of the truss is fairly sensitive to such changes.

(d) The truss has generally poorer fatigue characteristics than the sheet web and is more expensive to manufacture.

(e) The truss gives access to the interior of the structure; this fact alone is often sufficient to overbalance all other considerations.

6. Design Procedure

For design, the following procedure is suggested:

With the given parameters S and h, the index $\sqrt{S}/h$ is calculated.

With the help of the efficiency curves in figure 23, a value of d/h is chosen (other design considerations affecting the spacing being considered, if necessary), and the choice between single or double stiffeners is made.

The appropriate lower diagram in figure 23 is used to find the stiffening ratio A_U/dt.

Figure 24 is used to find h/t and thus the web thickness t. (This figure was prepared from the computation data for figure 23.) Normally, the use of standard gages is required; the next-higher standard gage should be chosen, in general. If the ratio h/t cannot be estimated with sufficient accuracy from figure 24, use the figure to obtain an approximate value of k. Next, assume $\alpha_{PDT} = 40^\circ$ and use figure 19 to find an approximate value for τ_{all}. (Correct this, if necessary, for proper edge condition as specified in section 4.8). The required web thickness is then

$$t = \frac{S}{h_e \tau_{all}}$$

The area A_U can now be calculated, the values of d, t, and A_U/dt being known, and an upright having this area is chosen. Again, the next-higher standard area should be chosen unless the web thickness chosen is appreciably higher than the required thickness (i.e., nearly one gage-step higher).

As long as forced crippling is the decisive mode of failure of the upright, the formulas indicate no reason for choosing anything more complicated than an angle section for the upright. However, because the empirical formulas for forced crippling are not very accurate, it is quite possible that detailed experiments on a specific design may show some other cross sections to be somewhat better.

Attention is called to the fact that the allowable web stresses given by figure 19 are based on "minimum guaranteed" material properties which are considerably below the typical properties. The use of higher properties in design is permitted by the regulating agencies under some conditions; the allowable web stresses may then be increased in proportion.

The allowable stresses for uprights given in section 4 are also conservative; the degree of conservatism is discussed briefly in section 3.12 and in more detail in Part II (reference 2). The uncertainty is probably caused almost entirely by the weakness of the empirical formulas; variability of material properties is believed to be a very minor factor. Consequently, higher allowable stresses can be used for the uprights if the design is verified by a specific static test.

A final word of caution regarding figure 23 may not be amiss. The curves shown are strictly valid only when the stipulated allowable stresses are applicable and when the uprights have the stipulated cross section. Under other conditions, the curves will be somewhat different, and the differences may not be small; consequently, the charts should not be used as a means of strength analysis.

7. Numerical Examples

As numerical examples, a thin-web beam and a thick-web beam will be analyzed. Both beams were tested in the NACA research program; the failing loads measured in the tests will be used as "design ultimate loads" P.

Example 1. Thin-web beam.- The thin-web beam chosen as example 1 is beam I-40-4Da of Part II (reference 2) or reference 4. The uprights consist of two angles 0.750 × 0.625 × 0.125. The material of web and uprights is 24S-T3 aluminum alloy. The web is sandwiched between the flange angles. The flange-flexibility coefficient ω_d (formula (19a)) is 1.20.

Basic data: (All linear dimensions are in inches.)

$h_e = 41.4$ $\quad h_U = 38.6$ $\quad h_c = 37.1$

$d = 20.0$ $\quad d_c = 19.37$

$t = 0.0390$ $\quad t_U = 0.125$

$P = 30.3$ kips

Upright section $\begin{cases} A_U = 0.353 \text{ in.}^2 \\ \rho = 0.351 \end{cases}$

From these data:

$$\frac{A_U}{dt} = 0.454 \qquad h_e t = 1.61 \text{ in.}^2 \qquad \frac{t_U}{t} = 3.20$$

Buckling stress:

With $\frac{t_U}{t} = 3.20$ and $\frac{t_F}{t}$ large, figure 12(b) gives

$$R_h = R_d = 1.62$$

From figure 12(a), with $\frac{h_c}{d_c} = 1.91$

$$k_{ss} = 5.92$$

By formula (32)

$$\tau_{cr,elastic} = 5.92 \times 10.6 \times 10^3 \times \left(\frac{0.0390}{19.37}\right)^2 \times 1.62 = 0.416 \text{ ksi}$$

Figure 12(c) shows that $\tau_{cr,elastic} = \tau_{cr}$ for this stress; therefore,

$$\tau_{cr} = 0.416 \text{ ksi}$$

Web stress:

$$\tau = \frac{P}{h_e t} = \frac{30.3}{1.61} = 18.8 \text{ ksi}$$

Loading ratio:

$$\frac{\tau}{\tau_{cr}} = \frac{18.8}{0.416} = 45.2$$

Diagonal-tension factor:

From figure 13

$$k = 0.680$$

Upright stress:

From figure 14

$$\frac{\sigma_U}{\tau} = 0.90; \quad \sigma_U = 0.90(18.8) = 16.9 \text{ ksi}$$

Allowable upright stress for column failure:

The effective column length is, by formula (35),

$$L_e = \frac{38.6}{\sqrt{1.0 + 0.680^2(3 - 2 \times 0.519)}} = 28.0$$

$$\frac{L_e}{\rho} = \frac{28.0}{0.351} = 79.8$$

This is in the long-column range. Therefore $\sigma_{all} = \frac{\pi^2 E}{(L_e/\rho)^2} = 16.5$ ksi. This value would be the allowable stress for a solid-section column. The upright consists of two angles riveted together. By formula (40), the required rivet strength was computed as:

$$R_R = 8.56 \text{ kips}$$

The actual rivet strength was

$$R = 4.65 \text{ kips}$$

With the ratio $\frac{R}{R_R} = \frac{4.65}{8.56} = 0.545$, figure 21 gives a reduction factor 0.94. The allowable upright stress is therefore

$$\sigma_{all} = 16.5 \times 0.94 = 15.5 \text{ ksi}$$

Since the beam failed when the computed upright stress was 16.9 ksi (see heading "Upright Stress"), the allowable stress of 15.5 ksi was about 8 percent conservative.

Allowable upright stress for forced crippling:

With $\frac{d}{h_U} = 0.519$ and $k = 0.680$, figure 15 gives $\frac{\sigma_{U_{max}}}{\sigma_U} = 1.14$

$$\sigma_{U_{max}} = 1.14 \times 16.9 = 19.2 \text{ ksi}$$

From figure 20

$$\sigma_0 = 24.0 \text{ ksi}$$

The allowable stress is 25 percent greater than the existing stress.

Allowable web stress:

According to figure 16(a), with $\frac{\sigma_U}{\tau} = 0.90$ and $k = 0.680$,

$$\tan \alpha = 0.81$$

According to figure 17,

$$C_1 = 0.022$$

According to figure 18, with $\omega d = 1.20$,

$$C_2 = 0.01$$

Therefore

$$\tau'_{max} = \tau \left(1 + k^2 C_1\right)\left(1 + kC_2\right) = 18.8 \times 1.01 \times 1.01 = 19.2 \text{ ksi}$$

The allowable web stress according to figure 19(a) is 22.0 ksi which is 15 percent greater than the existing stress.

Note: The index value of the beam is $\frac{\sqrt{S}}{h} = \frac{\sqrt{30300}}{41.4} = 4.20$. Interpolation on figure 23(a) shows that a beam with this index value would be a balanced design if it had a ratio A_U/dt equal to 0.46 and that the uprights would fail by forced crippling.

The actual ratio A_U/dt is 0.454 and is thus very close to the value given by figure 23(a). However, the calculations for this figure are based on upright sections having b/t_U ratios of 6 and 12 for the attached and the outstanding legs, respectively. The actual sections

have ratios of 5 and 6, respectively; they are thus stockier than those assumed for figure 23(a). As a result, the detailed analysis shows that the uprights have excess margin against failure by forced crippling but are somewhat weak in column action. The detailed analysis thus shows that the design is slightly unbalanced and that beam failure should be caused by column failure of the uprights; this prediction agrees with the test result.

Example 2. Thick-web beam.- The thick-web beam chosen as example 2 is beam V-12-10S of Part II. The uprights are single angles 0.625 × 0.625 × 0.1283. The material is 24S-T3 aluminum alloy. The web is bolted (using washers) to the outside of the flange angles.

As in example 1, the test failing load will be used as "design ultimate load." Two sets of allowable stresses will be given for forced-crippling failure of the uprights and for web failure. The first set represents the values recommended for design use, obtained from the graphs or formulas quoted. The second set, given in parentheses following the first set, represents the "best possible estimate." The differences are as follows:

(a) The "best possible estimate" for the crippling allowable is based on the middle of the scatter band, while the "recommended for design" value represents the lower edge of the scatter band. The "best possible estimate" for crippling allowable is therefore $\frac{1}{0.8} = 1.25$ times the value given by formula (37).

(b) The "best possible estimate" for the web strength is obtained by multiplying the design allowable (fig. 19) by the factor: Actual tensile strength over specification strength (or 69.3/62) and by the factor 1.10 to obtain the average rather than the lower edge of the scatter band for the tests on shear webs. (See section 3.7.)

Basic data:

$h_e = 11.58$ in.	$h_U = 9.875$ in.	$h_c = 9.875$ in.
$d = 7.00$ ($=d_c$) in.	$t = 0.1043$ in.	$\rho = 0.182$ in.
$A_U = 0.1443$ in.^{2}	$t_U = 0.1283$ in.	$e = 0.251$ in.
$\omega d = 1.37$	$t_F = 0.3125$ in.	$A_F = 2.32$ in.^{2}
$P = 34.5$ kips		

Effective upright area:

$$A_{U_e} = \frac{0.1443}{1 + \left(\frac{0.251}{0.182}\right)^2} = 0.0497 \qquad \frac{A_{U_e}}{dt} = 0.0681$$

Buckling stress:

$$\frac{t_U}{t} = 1.23 \qquad R_h = 0.93$$

$$\frac{t_F}{t} = 3.00 \qquad R_d = 1.62$$

$$\frac{h_c}{d} = 1.50 \qquad k_{ss} = 6.70$$

$$\tau_{cr,elastic} = 6.70 \times 10.6 \times 10^3 \left(\frac{0.1043}{7}\right)^2 \left[0.93 + \frac{1}{2}(1.62 - 0.93)\left(\frac{2}{3}\right)^3\right]$$

$$= 16.55 \text{ ksi}$$

According to figure 12(c):

$$\tau_{cr} = 16.10 \text{ ksi}$$

Stress analysis:

$$\tau = \frac{34.5}{11.58 \times 0.1043} = 28.56 \text{ ksi}$$

$$\frac{\tau}{\tau_{cr}} = 1.77$$

$k = 0.123$ (from fig. 13 or formula (27a))

$$\frac{\sigma_U}{\tau} = 0.227 \qquad \sigma_U = 6.48 \text{ ksi}$$

$$\frac{\sigma_{U_{max}}}{\sigma_U} = 1.30 \qquad \sigma_{U_{max}} = 8.34 \text{ ksi}$$

Column failure of uprights:

A $\frac{5}{8} \times \frac{5}{8}$ angle with an effective length less than 9.9 inches is evidently in no danger of column failure at a stress of 6.48 ksi.

Forced-crippling failure:

$$\frac{t_U}{t} = 1.23 \qquad \sigma_o = 7.0\ (8.75)\ \text{ksi}$$

Comparison of the two values of σ_o with $\sigma_{U_{max}}$ shows that the "design allowable" value (7.0 ksi) would have predicted upright failure at a load about 16 percent lower than the test failing load, while the "best possible estimate" of 8.75 ksi would have predicted upright failure at a load 4.5 percent higher than the test load. In the test, the web ruptured, but these figures indicate that upright failure might have contributed to the web failure or else would have been the primary cause of failure if the web had been slightly stronger.

Web failure:

$$\frac{2A_F}{h_e t} = 3.84$$

From figure 16(b): $\alpha_{PDT} \approx 29^\circ$

From figure 19(a): $\tau_{all} = 25\ (30.75)$ ksi

The actual web stress at failure (web rupture) was computed to be 28.56 ksi. (The correction for effect of flange flexibility is negligible.) The "design allowable" value of 25 ksi therefore would have predicted the failure too low (conservatively) by about 12 percent. The "best possible estimate" of 30.75 ksi would have predicted the failure about 8 percent too high. If the correction for actual material properties had been made, but not the correction for scatter in shear-web tests, the prediction would have been very close.

Note: According to the "best possible estimates," failure of the uprights should have precipitated failure of the beam at a load less than 4 percent lower than that causing web failure. In the test report, failure was attributed to web failure. It appears, therefore, that the design was very closely balanced.

The index value for this beam is $\frac{\sqrt{34500}}{11.58} = 16.0$. According to figure 23(a), this index value would require a ratio A_U/dt of about 0.26, while the actual ratio was only 0.198. This high efficiency of the test beam is attributable to the use of an upright section having a b/t_U ratio of 5, which is considerably more compact than the section assumed for the calculations leading to figure 23(a).

CURVED-WEB SYSTEMS

The analysis of diagonal tension in curved-web systems utilizes the methods developed for plane-web systems. The discussion is therefore kept brief except for new problems introduced by the curvature. The circular cylinder under torque loading is the simplest case and is used as the basis of discussion.

8. Theory of Pure Diagonal Tension

If a fuselage were built as a polygonal cylinder and subjected to torque loads (fig. 27(a)), the theory of diagonal tension would evidently be applicable and require only minor modifications. If the fuselage were built with a circular-section skin, but polygonal rings (fig. 27(b)), the sheet would begin to "flatten" after buckling and would approach the shape of the polygonal cylinder more and more as the load increases. In the limit, the theory of pure diagonal tension would be applicable, but in the intermediate stages, the theory developed for plane webs evidently would not be directly applicable. In an actual fuselage, the rings are circular, not polygonal (fig. 27(c)); consequently, all the tension diagonals of one sheet bay cannot lie in one plane, even when the diagonal tension is fully developed; an additional complication therefore exists.

In order to derive a theory of pure diagonal tension in circular cylinders with a minimum of complications, it is necessary to consider special cases. Wagner has given fundamental relations (reference 5) for two cases: cylinders with panels long in the axial direction ($d > 2h$, see fig. 27(d)) between closely spaced stiffeners $\left(h < \frac{1}{3} R\right)$, and cylinders with panels long in the circumferential direction ($h > 2d$, fig. 27(e)) between closely spaced rings $\left(d < \frac{1}{3} R\right)$. In the first case, the majority of the tension diagonals lie in the surface planes of the "polygonalized" cylinder; in the second case, the majority of the tension diagonals lie on a hyperboloid of revolution.

In the development of the theory of pure diagonal tension for plane webs, it was pointed out that all the stresses are known as soon as the angle α of the folds is known. The fundamental formula for finding this angle is formula (14), which may be transformed by dividing numerator and denominator by Young's modulus into

$$\tan^2\alpha = \frac{\epsilon - \epsilon_x}{\epsilon - \epsilon_y} \tag{43}$$

This formula can also be applied to the diagonal-tension field formed by an originally curved panel on the basis of the following considerations.

Imagine a panel long in the axial direction (fig. 27(d)) to be cut along one long edge and both curved edges. If the panel were now flattened out, the cut long edge would be separated from the stringer by a distance Δ equal to the difference between the length of the arc and the length of the chord, which is approximately

$$\Delta = \frac{1}{24}\frac{h^3}{R^2}$$

(The restriction to closely spaced stiffeners, $h < \frac{1}{3}R$, is made in order to permit the use of this formula.) The same configuration would have been obtained if the panel had been made flat originally and then compressed by the amount Δ. The change from a circular section to a polygonal section that takes place while the diagonal tension develops is therefore equivalent to a compressive strain Δ/h in the rings, and formula (43) may be used to compute the angle α for a curved panel by writing

$$\epsilon_y = \epsilon_{RG} - \frac{1}{24}\left(\frac{h}{R}\right)^2$$

The formula thus becomes

$$\tan^2\alpha = \frac{\epsilon - \epsilon_{ST}}{\epsilon - \epsilon_{RG} + \frac{1}{24}\left(\frac{h}{R}\right)^2} \tag{44}$$

For the panel long in the circumferential direction, the relations are more involved, but the final result again takes a simple form (reference 5)

$$\tan^2\alpha = \frac{\epsilon - \epsilon_{ST}}{\epsilon - \epsilon_{RG} + \frac{1}{8}\left(\frac{d}{R}\right)^2 \tan^2\alpha} \qquad (45)$$

If the restrictions as to the ratio d/h are disregarded, and both formulas are applied to a cylinder with square panels ($d = h$), it will be seen that the "flattening-out" terms become equal and the formulas give identical results if

$$\tan^2\alpha = \frac{1}{3}$$

or

$$\alpha = 30^\circ$$

which is a fairly representative angle for curved webs. It may be assumed, then, in view of the empirical factors contained in the theory of incomplete diagonal tension, that for practical purposes formula (44) may be used if $\frac{d}{h} > 1.0$ and formula (45), if $\frac{d}{h} < 1.0$. The tests available so far tend to confirm the assumption that no limitations need be placed on the aspect ratio d/h of the panels. Until further data become available, however, it would be well to limit the subtended arc of the panel to a right angle $\left(h = \frac{\pi}{2} R\right)$ unless the ring spacing is very small; it should also be noted that the investigations of the panel long in the circumferential direction made to date are very sketchy.

When the strains on the right-hand side of formula (44) are expressed in terms of the applied shear stress by using the basic formulas

$$\sigma_{ST} = -\frac{\tau th \cot\alpha}{A_{ST}} \quad ; \quad \sigma_{RG} = -\frac{\tau td \tan\alpha}{A_{RG}} \quad ; \quad \sigma = \frac{2\tau}{\sin 2\alpha}$$

the formula becomes a transcendental equation for α and may be written in the form

$$\left(1 + R_R\right)\tan^4\alpha + A \tan^3\alpha = 1 + R_S \qquad (d > h) \qquad (44a)$$

where

$$A = \frac{1}{24}\left(\frac{h}{R}\right)^2 \frac{E}{\tau} \quad ; \quad R_S = \frac{ht}{A_{ST}} \quad ; \quad R_R = \frac{dt}{A_{RC}}$$

Similarly, formula (45) becomes

$$B \tan^5\alpha + \left(1 + R_R\right)\tan^4\alpha = 1 + R_S \qquad (h > d) \qquad (45a)$$

where

$$B = \frac{1}{8}\left(\frac{d}{R}\right)^2 \frac{E}{\tau}$$

Graphs based on these formulas are shown in figure 28.

The effective shear modulus of a cylinder in pure diagonal tension is obtained by the basic formula (23a), modified only to suit the notation for curved-web systems

$$\frac{E}{G_{PDT}} = \frac{dt}{A_{RG}} \tan^2\alpha + \frac{ht}{A_{ST}} \cot^2\alpha + \frac{4}{\sin^2 2\alpha} \qquad (46)$$

It will be noted that the formulas given contain the actual areas of the stringers and rings. In practice, these stringers and rings are probably always single; in the case of plane webs, single uprights enter into all equations with an effective area given by formula (22), but the following considerations indicate that the actual areas should be used, in general, for the analysis of cylinders.

Consider a cylinder of closed circular cross section (fig. 27(c)) with closely spaced rings under the action of torques applied at the two ends; the rings as well as the stringers are assumed to be riveted to the skin. The rings in such a structure are evidently in simple hoop compression that balances the circumferential component of the diagonal tension; the eccentricity of the rings does not affect the hoop compression, the load actually being applied to the ring in the form of a uniformly distributed radial pressure. Consequently, the actual area of the rings should be used in the calculations.

The stringers are loaded eccentrically by the skin, but they cannot bow from end to end; they are constrained by the rings to remain in a straight line, except for secondary bowing between the rings and local disturbances in the vicinity of stations where the magnitude of the

shear load changes. In the main, then, the stringers act as though they are under central axial loads, and their actual areas should correspondingly be used.

When the rings are "floating" (fig. 29(a)), the radial pressure exerted by the skin tension is transmitted to the rings in the form of forces P_r concentrated at the stringers. The circular beam under hoop compression and isolated radial forces shown in figure 29(a) are statically equivalent to the straight beam shown in figure 29(b), a continuous beam under uniform load. The maximum bending moment in the ring (under the stringer) is therefore

$$M_{RG} = \frac{1}{12} P_r h$$

By statics, with sufficient accuracy if $\frac{h}{R} < 1$,

$$P_r = P_{RG} \frac{h}{R} = \tau t d \tan \alpha \frac{h}{R}$$

therefore

$$M_{RG} = \tau t \frac{h^2 d}{12R} \tan \alpha \tag{47}$$

For the remainder of this section, the discussion is confined to cylinders with panels long in the axial direction ($d > h$).

Because of the polygonal shape acquired by the cross section of the cylinder as the diagonal tension develops, each tension diagonal experiences a change in direction as it crosses a stringer. Consequently, each tension diagonal exerts an inward (radial) pressure on the stringer. The magnitude of this pressure per running inch of the stringer is

$$p = \frac{\tau t h}{R} \tan \alpha \tag{48}$$

If this pressure were distributed uniformly along the length of the stringer, the primary peak bending moment in the stringer (at the junction with a ring) would be given by the formula

$$M_{ST} = \tau t \frac{h d^2}{12R} \tan \alpha \tag{49}$$

A secondary peak moment would exist half-way between rings; its magnitude would be one-half of the primary peak.

For several reasons, the radial pressure p is not uniform. The first and most important reason is as follows. The derivation of formula (48) for p assumes that every tension diagonal experiences the same change in direction as it crosses the stringer; this is the condition that would exist if the "rings" of the cylinder were built as polygons. Since the rings are actually circular (or curved), a portion of the tension diagonals near each end of a panel will be forced to remain more or less in the original cylindrical surface and will thus experience little change in direction. The radial pressure is therefore less near the ends than given by the simple formula; as a result, the primary peak bending moment may be much less, and the secondary peak somewhat less than indicated by the formulas based on a uniform distribution of the pressure. Other reasons for nonuniform distribution of the pressure are sagging of the stringers, possibly sagging of the rings, and nonuniformity of skin stress.

The effects of nonuniform distribution of the radial pressure could perhaps be estimated under the condition of pure diagonal tension considered here, but the calculations would be tedious and would probably require additional approximations. Under the practical condition of incomplete diagonal tension, additional large difficulties would arise. In any event, elaboration of the procedures for computing bending moments is not likely to be worthwhile in view of the empirical nature of the theory of incomplete diagonal tension.

9. Engineering Theory of Incomplete Diagonal Tension

9.1. Calculation of web buckling stress.- Theoretical coefficients for computing the buckling stress τ_{cr} in the elastic range, based on the assumption of simply supported edges (reference 26) are given in figure 30. Over the limited range of available tests, these theoretical formulas have given better results than any empirical formulas for buckling of curved sheet, particularly when the appearance of stringer (compressive) stresses was used as the criterion for sheet buckling. It should be noted, however, that in the limiting case of flat sheet it has been found necessary to modify the theoretical coefficients by means of empirical restraint coefficients (section 4.2). Logically, analogous modifications should also be made for slightly curved sheet (small values of Z in fig. 30), but no recommendations can be made at present concerning a suitable procedure.

9.2. Basic stress theory.- As pointed out in section 8, the geometric change of shape from a circular to a polygonal cylinder with $d > h$ is equivalent to producing a compressive strain in the

rings, and a similar consideration applies when $h > d$. The development of the diagonal tension therefore proceeds more rapidly in a curved web than in a plane web, and the empirical relation between the diagonal-tension factor k and the loading ratio τ/τ_{cr} must be generalized. Analysis of test data has shown (reference 27) that they can be fitted fairly well by the generalized formula

$$k = \tanh\left[\left(0.5 + 300\frac{td}{Rh}\right)\log_{10}\frac{\tau}{\tau_{cr}}\right] \qquad (50)$$

with the auxiliary rules:

(a) If $h > d$, replace d/h by h/d.

(b) If d/h (or h/d) is larger than 2, use 2.

Figure 13 shows equation (50) in graphical form.

With the same assumptions as in plane diagonal tension, the stresses and strains in stringers and rings are given by the formulas

$$\sigma_{ST} = -\frac{k\tau \cot\alpha}{\frac{A_{ST}}{ht} + 0.5(1 - k)} \quad ; \quad \epsilon_{ST} = \frac{\sigma_{ST}}{E} \qquad (51)$$

$$\sigma_{RG} = -\frac{k\tau \tan\alpha}{\frac{A_{RG}}{dt} + 0.5(1 - k)} \quad ; \quad \epsilon_{RG} = \frac{\sigma_{RG}}{E} \qquad (52)$$

For floating rings, the factor $0.5(1 - k)$ representing effective skin in formula (52) is omitted.

The web strain ϵ is obtained by formula (30d). A graph for evaluating this strain in the usual range of design proportions is given in figure 31. In curved diagonal-tension fields, the longitudinal and the transverse stiffening ratio are in most cases of the same order of magnitude. The stringer stress and the ring stress thus depend on three parameters, the two stiffening ratios and the radius of curvature. With this number of parameters, it is impracticable to prepare an analysis chart for curved diagonal-tension fields corresponding to figure 14; the analysis must therefore be made by solving the equations in the manner described in section 3.2 for the general case of plane

diagonal tension. A first estimate of α is made; equations (51), (52), and (30d) are solved; the resulting values of ϵ, ϵ_{ST}, and ϵ_{RG} are substituted into formula (44) (or (45)) to obtain an improved value of α, and so forth.

As a first approximation to the angle α, the value α_{PDT} for pure diagonal tension given by figure 28 may be used. A better first approximation to α is obtained if the angle α_{PDT} taken from figure 28 is multiplied by the ratio α/α_{PDT} given by figure 32. This curve represents the average of the scatter band obtained by plotting the ratios α/α_{PDT} for a number of webs with proportions varied within the usual design range. In general, the value of α obtained in this manner will be within 2° to 3° of the final value found by successive approximation. Analysts with some experience generally dispense with the use of figures 28 and 32 and simply assume an initial value of the angle α.

The stresses given by formulas (51) and (52) are average stresses that correspond to the value σ_U given by formula (30a). The maximum stresses are obtained, as for plane webs, by multiplication with the ratio σ_{max}/σ given by figure 15. It is possible that these ratios may require modification for strongly curved panels. As mentioned in the discussion of plane webs, direct experimental verification of the ratio is extremely difficult because of the difficulty of separating the compression stress from the stress due to bending and the stress due to forced local deformation.

The effective shear modulus of curved webs in incomplete diagonal tension is computed by formulas (31a) and (31b), with A_{RG} substituted for A_{U_e} and A_{ST} substituted for $2A_F$. In order to be consistent with the assumption that the "polygonization" takes place immediately after buckling in cylinders with $d > h$, the polygon section should be used in the calculations. Thus, for a circular cylinder with equally spaced stringers, the shear flow due to torque and the torsion constant should be computed by the formulas

$$q = \frac{T}{2\pi R^2\left(1 - \frac{1}{6}\varphi^2\right)}$$

$$J = 2\pi R^3 t\left(1 - \frac{7}{24}\varphi^2\right)$$

where φ is the angle subtended by two stringers. The reduction factors in the brackets are approximate but are sufficiently accurate for values of φ up to about $\frac{1}{2}$ radian (12 or more stringers, uniformly spaced). It may be noted that the percentage correction for J is roughly twice as large as for q.

9.3. Accuracy of basic stress theory.- Because the development of diagonal tension in curved webs depends on more parameters than in plane webs, and because the test specimens are more expensive to construct and test, it has not been feasible to check the behavior of curved webs experimentally as thoroughly as for plane webs. An effort has been made to check a sufficient number of extreme cases to insure reasonable reliability over the usual range of designs, but very few checks have been made to date with $h > d$. The reliability of the basic stress theory appears to be about the same as for plane-web systems except for the effective shear modulus, which is somewhat overestimated for curved webs.

9.4. Secondary stresses.- The primary maximum bending moment in a floating ring can be calculated by using expression (47), which is valid for pure diagonal tension, and multiplying it by the diagonal-tension factor k. The secondary maximum, which is equal to one-half of the primary maximum and occurs half-way between stringers, has been checked experimentally in one case and agreed very closely with the computed value.

The maximum bending moment in a stringer can similarly be calculated by using expression (49) and multiplying it by the factor k. However, as pointed out in the discussion of expression (49), this formula cannot be regarded as reliable. There have been very few attempts to check these moments by strain measurements. Such a check is extremely difficult because the effective width of skin working with the stringer is not known with sufficient accuracy, and consequently it is difficult to separate bending from compressive stresses. Even more difficult is the problem of allowing for the local bending stresses due to forced deformation of the stringer cross sections. Taken at face value, the few data available indicate that the secondary peak moment (half-way between rings) may agree roughly with the calculated value (one-half of the primary peak). The primary peak at the rings, however, appears to be even less than the calculated secondary peak. The analysis of available strength tests on cylinders has also led to the conclusion that the maximum moment appears to be no larger than the calculated secondary peak. It is suggested, therefore, that the bending moment in the stringer at the ring as well as the moment at the half-way station be computed by formula (49), with the factor k added and the factor 12 replaced by 24.

9.5. Failure of the web.- The nominal shear stress τ at which a curved web (or skin of a cylinder) ruptures would be given directly by the curves of figure 19 if the diagonal tension were uniformly distributed. For plane webs, nonuniformity of stress distribution is allowed for by the stress-concentration factor C_2 (formula (33b)) which is calculated by Wagner's theory of flange-flexibility effects. For curved-web systems, no corresponding theory has been developed; the factor C_2 is thus necessarily taken to be zero. In order to compensate for the error introduced by this assumption, the allowable stress taken from figure 19 is multiplied by an empirical reduction factor which depends on the properties of the stringers and rings. From analogy with the plane-web case, it would seem that the reduction factor should depend primarily on the bending stiffnesses of stringers and rings. However, for the tests available to date, much better correlation was achieved by using the stiffening ratios involving the areas as parameters.

The allowable ultimate value for the shear stress τ in a curved web is thus given by the empirical expression (reference 27)

$$\tau_{all} = \tau^*_{all} (0.65 + \Delta) \tag{53}$$

where

$$\Delta = 0.3 \tanh \frac{A_{RG}}{dt} + 0.1 \tanh \frac{A_{ST}}{ht} \tag{54}$$

The value τ^*_{all} is given by figure 19; the quantity Δ may be read from figure 33. It may be noted that τ_{all} can exceed τ^*_{all}, because the quantity Δ can exceed the value 0.35 if the stringers and rings are heavy. The explanation lies in the fact that a grid-system of stringers and rings can absorb some shear; the effect is analogous to the portal-frame effect in plane-web systems.

In section 4.8, it is stated that the basic allowable values of shear stress for plane webs may be increased 10 percent if the web is attached by rivets assumed to remain tight in service. All the curved webs tested also developed this higher strength, but the number of tests is small.

It should be noted that section 4 also states that the rivets are assumed to be not of any countersunk (flush) type because no applicable tests are available; this statement holds for curved webs as well as for plane webs.

9.6. General instability.- As a check against the danger of collapse of the cylinder by general instability, the empirical criterion developed by Dunn (reference 28) is available. This criterion gives the shear stress τ_{inst} at which instability failure will occur and is shown graphically in figure 34. The full lines indicate the region covered by the test points, which lie close to the lines with very few exceptions. No explanation was found for the sudden shift from one line to the other. The radii of gyration ρ_{ST} and ρ_{RG} should be computed on the assumptions that the full width of sheet acts with the stringer or ring, respectively, and that the sheet is flat, because the empirical criterion was obtained under these assumptions. Graphs for evaluating radii of gyration for stringer-sheet combinations are generally given in stress manuals and are therefore not given here.

9.7. Strength of stringers.- Geometrically, the stringers of a cylinder correspond to the flanges of a plane-web beam, and the rings correspond to the uprights of the beam. Functionally, however, the stringers as well as the rings of a cylinder under torque load act essentially like the uprights of a beam; the strength analysis of stringers therefore involves the same considerations as the design of uprights.

In the discussions on plane-web beams, it was shown that uprights can fail either by forced crippling or by column action, and that forced crippling dominates over most of the practical range of design proportions. The problem of column failure was therefore treated rather briefly, and the problem of interaction between column failure and forced crippling was only mentioned.

In curved-web systems with many rather light stringers, the problem is unfortunately not so simple. The investigations made to date are hardly more than exploratory, but they indicate that column action may be relatively more important than in plane webs for the following reasons:

(a) The angle of diagonal tension is lower in curved webs than in plane webs (20° to 30° against 40°, roughly); the stringers therefore receive a relatively higher load than the uprights.

(b) The bracing action which a plane web exerts against column buckling is absent in curved webs. In fact, the radial component of the diagonal tension applies a transverse load to the stringer, which acts therefore as a beam-column rather than as a column.

The importance of column action of the stringers arising from these causes is increased greatly by the necessity of designing cylinders such as fuselages to carry bending moments as well as torque loads.

In view of the great importance of column action in stringers, it would be highly desirable to have rather complete and reliable methods of predicting this type of failure. Most of the customary methods are adaptations of those developed for "free" columns not attached to webs. These methods are highly unreliable because

(a) the twisting mode of failure is greatly altered by attachment to a web, and

(b) the skin usually buckles well before ultimate failure takes place. The forced local buckling of the stringer section induced by the skin buckles materially reduces the resistance against column buckling or twisting unless the stringer is unusually sturdy, that is to say, unusually resistant to forced buckling.

The problems involved are very complex, and very little useful information is available even for the much simpler problem of the stiffened cylinder in compression. A purely empirical solution is hardly feasible in view of the many parameters involved. Substantial progress in the analysis methods for torsion cylinders can therefore be expected only when an adequate theory of the compression cylinder has been developed.

For the time being, the following checks are suggested in addition to the check against general instability discussed in section 9.6.

(1) The strength against forced crippling should be checked in the same manner as for uprights on plane webs.

(2) A check should be made against column failure. For Euler buckling normal to the skin, fixed-end conditions can probably be assumed to exist at the rings. The column curve established in the usual manner (using the local crippling stress for the stringer section as allowable for $\frac{L}{\rho} = 0$) probably requires some reduction to allow for the effect of skin buckles unless the ratio t_{ST}/t is larger than 3. Consideration should be given to the possibility of twisting failure if the column curve is obtained by computation. Some allowance should be made for beam-column effect.

(3) The maximum compressive stress in the stringer should be computed as the sum of the stress σ_{ST} (computed in accordance with section 10.4) and the stress caused by the bending moment M_{ST} (section 10.5).

9.8. Strength of rings.- Floating rings should be designed to carry the combined effect of the hoop compression σ_{RG} (section 10.4)

and of the bending due to the moment M_{RG} (section 10.6) at the juncture with the stiffener. A check at the station midway between stiffeners (where the moment is only half as large, but of opposite sign) may be necessary if the cross section of the ring is such that the allowable stresses in the outer and the inner fibers differ greatly.

Rings riveted to the skin should be checked against forced crippling in the same manner as the stringers. No recommendations can be made at present concerning checks against instability failures other than that given in section 9.6 for general instability. For the tests available, the two checks (for forced crippling and general instability) used in conjunction gave adequate strength predictions, but the number of tests is very small because the rings were usually overdesigned in order to force stringer or web failure.

Unless the stringers are made intercostal (which leads to loss of efficiency in bending strength of the cylinder and is therefore seldom done) the rings must be notched to permit the stringers to pass through. At the notch, the ring stress is increased because the cross section is reduced; this effect is aggravated by the suddenness of the reduction, that is to say, a stress-concentration effect exists. The free edge of the notch should therefore be checked against local crippling failure. In the tests of reference 29, all specimens (representing fuselage side walls) failed in this manner. If the stringer is connected to the ring by a clip-angle of sufficient length riveted to the web of the ring, the net section at the notch is increased, and the edge of the notch can readily be stiffened so much that there is no danger of this type of failure. No specific recommendations on this problem can be made at present because no adequate tests are available.

9.9. Web attachments.- For the edge of a panel riveted to a stringer, the required rivet shear strength per inch run is taken as

$$R'' = q\left[1 + k\left(\frac{1}{\cos \alpha} - 1\right)\right] \tag{55}$$

This formula is obtained from formula (10) with the assumption used to obtain formula (34). For an edge riveted to a ring, cos α is replaced by sin α.

If the sheet is continuous across a stiffening member, but the shear flow changes at the member, the rivets evidently need be designed only to carry the difference $(R_1'' - R_2'')$ between the adjacent panels. In such cases, neither the factor k nor the angle α for the lower-stressed panel is likely to be needed for other purposes. In order to eliminate the necessity of calculating these values for the purpose of

rivet design, simplified criteria may be used and should be adequate for practical purposes.

Rivets should fulfill the criterion for tensile strength given by expression (42). Curved surfaces are encountered mostly on the outer surface of the airframe, where flush rivets are often required for aerodynamic reasons. Flush rivets usually develop a low tensile strength because they pull through the sheet; the check for tensile strength is therefore important.

Data for the tensile strength of protruding-head rivets taken from reference 30 are given in figure 35. Data for some types of flush rivets, taken from reference 31, are given in figure 36. These data are for so-called NACA rivets, in which the countersunk head is formed from the rivet shank in the driving operation and then milled off flush. For "conventional" rivets with preformed countersunk heads, the tensile strengths were found to be from 10 to 20 percent lower for some test series (reference 31). Additional data on flush rivets may be found in references 31 and 32.

9.10. Repeated buckling.- It has been found experimentally that a load in excess of the buckling load will cause a lowering of the buckling stress for the next application of the load. Thus, in a series of tests on curved panels (reference 33), the buckling stress was lowered as much as 30 percent after 10 loads, and as much as 40 percent after 60 load applications. The maximum applied shear stress was of the order of 50 percent in excess of the buckling stress; in the worst case, it was near the probable proportional limit, but in the great majority of cases it was well below this limit. The reason for the lowering of the buckling stress therefore presumably must be sought in large but highly localized sheet bending stresses associated with the buckle formation ("plastic hinges").

In static tests made in the aircraft industry, standard practice appears to be to apply the test load in steps; after each step, the load is removed in order to check for permanent set. Thus, any shear web will have been buckled a number of times before the ultimate load is reached. The calculations, on the other hand, use formulas for buckling stresses that can be considered as valid only for the case where the test load is increased continuously until failure occurs. In the test, then, the diagonal tension will be more fully developed than predicted, and consequently failure will take place at a lower load than predicted.

The magnitude of the error in the predicted strength depends on the degree to which the diagonal tension is developed at failure, that is to say, on the magnitude of the diagonal-tension factor k, on the type of failure, and on the history of the loadings.

The prediction of sheet failure in curved-web systems is not sensitive to moderate errors in k, although somewhat more sensitive than for plane webs, as inspection of figure 19 indicates. The prediction of stringer or ring failure by forced crippling is not sensitive because an overestimate of k leading to an overestimate of the stresses developed also leads to an overestimate of the allowable stresses. (For balanced designs, a given small percentage error in k results in about one-third as much error in the predicted load.) The prediction of a column failure in a stringer, however, is presumably much more sensitive because the allowable stress in this case is presumably independent of k.

The angle of twist of a cylinder is extremely sensitive to small errors in k, or T/T_{cr}, in the vicinity of the buckling torque. An addition of 20 percent to the buckling torque may double or triple the angle of twist. Since previous buckling or other factors can easily cause a 20-percent error in the estimated buckling torque, it is evident that the calculated angle of twist can be in error by 100 to 200 percent in the region from, say, $0.8T_{cr}$ to $1.5T_{cr}$.

At the present, there are no methods available for estimating any of the effects of repeated buckling quantitatively.

10. Formulas and Graphs for Strength Analysis of Curved-Web Systems

No attempt should be made to use the following formulas until sections 8 and 9 have been carefully read.

10.1. Critical shear stress

The critical shear stress τ_{cr} is obtained with the aid of figure 30 and figure 12(c). Note that d is the distance between rings riveted to the skin (not floating). Use judgment in reducing τ_{cr} if $Z < 10$ and t_{ST}/t $\left(\text{or } t_{RG}/t\right) < 1.3$.

10.2. Nominal shear stress

When $d > h$, the nominal shear stress τ for post-buckling conditions is calculated as though the sheet were unbuckled and flat between stringers.

10.3. Diagonal-tension factor

The diagonal-tension factor k is obtained from figure 13, or by formula (50). The spacing d is measured between rings riveted to the skin.

When $h > d$, the nominal shear stress may be calculated (in general) as though the sheet were unbuckled.

10.4. Stresses, strains, and angle of diagonal tension

By formulas (51), (52), (30d), (44), and (45), respectively,

$$\sigma_{ST} = - \frac{k\tau \cdot \cot \alpha}{\frac{A_{ST}}{ht} + 0.5(1 - k)} \quad ; \quad \epsilon_{ST} = \frac{\sigma_{ST}}{E}$$

$$\sigma_{RG} = - \frac{k\tau \tan \alpha}{\frac{A_{RG}}{dt} + 0.5(1 - k)} \quad ; \quad \epsilon_{RG} = \frac{\sigma_{RG}}{E}$$

(For floating rings, omit $0.5(1 - k)$ in the last expression; use actual ring spacing for d.)

$$\epsilon = \frac{\tau}{E}\left[\frac{2k}{\sin 2\alpha} + \sin 2\alpha(1 - k)(1 + \mu)\right]$$

(Use fig. 31 to evaluate ϵ.)

$$\tan^2\alpha = \frac{\epsilon - \epsilon_{ST}}{\epsilon - \epsilon_{RG} + \frac{1}{24}\left(\frac{h}{R}\right)^2} \qquad (d > h)$$

$$\tan^2\alpha = \frac{\epsilon - \epsilon_{ST}}{\epsilon - \epsilon_{RG} + \frac{1}{8}\left(\frac{d}{R}\right)^2 \tan^2\alpha} \quad ; \quad (h \geq d)$$

The equations are solved simultaneously by successive approximation.

10.5. Bending moments in stringers

The suggested design value for the moment in a stringer at the rings as well as halfway between rings is

$$M_{ST} = k\tau t \frac{hd^2}{24R} \tan \alpha$$

10.6. Bending moment in floating ring

The primary maximum moment in a floating ring (at the junction with a stringer) is

$$M_{RG} = k\tau t \frac{h^2 d}{12R} \tan \alpha$$

The secondary maximum half-way between stringers is half as large.

10.7. Strength of web

Obtain: α_{PDT} from figure 28 (or by formula (44a) or (45a))

τ^*_{all} from figure 19

Δ from figure 33

Then, by formula (53),

$$\tau_{all} = \tau^*_{all} (0.65 + \Delta)$$

The value τ_{all} may be increased 10 percent for rivets that remain tight in service. It is not applicable without special verification if rivets are of any flush type.

10.8. Strength check, stringers and rings

Check for general instability (fig. 34).

Check stringers against column failure. See section 9.7 for suggestions.

Check against forced crippling as follows: For stringers, compute $\sigma_{ST_{max}}$, with σ_{max}/σ from figure 15. Allowable value is σ_o from figure 20 (single uprights). For rings (not floating), check similarly with $\sigma_{RG_{max}}$.

On notched rings, check edge of notch against buckling.

If rings are floating, assume $\sigma_{ST_{max}}$ equals σ_{ST}.

Design floating rings to carry combination of hoop compression (formula (52) or section 10.4) and bending moment (section 10.6).

10.9. Riveting

For edges of panel along stringer, the required rivet shear strength per inch run is, by formula (55),

$$R'' = q\left[1 + k\left(\frac{1}{\cos \alpha} - 1\right)\right]$$

For edge riveted to ring, replace $\cos \alpha$ by $\sin \alpha$.

Rivets should be checked for tensile strength (which includes rivet pulling through the sheet as one possible mode of failure). The tentative criterion for tensile strength is given by expression (42) as

$$\text{Tensile strength of rivets per inch run} > 0.22t\sigma_{ult}$$

For tensile strengths of rivets, see figures 35 and 36.

11. Combined Loading

The preceding sections have dealt with the problem of designing a shell subjected to pure torque loading. They may also be used for designing a shell subjected to transverse loads producing bending, provided the shell is so short that the axial stresses produced by bending are small compared with the shear stresses. If the shell is not very short, however, a number of problems of combined loading arise. As a first step toward the solution of these problems, the cylinder subjected to torsion and compression has been investigated in reference 34, and the following method of analysis has been found to yield reasonable accuracy.

The critical shear stress is calculated with the aid of figure 30. This stress is now denoted by $\tau_{cr,0}$, where the additional subscript zero indicates the condition of shear acting alone. Next, the critical compressive stress is calculated and denoted by $\sigma_{cr,0}$. Because the classical theory of compression buckling of curved sheet is in poor agreement with tests, the theoretical buckling coefficients should be modified by an empirical factor (reference 35). In figure 37, the values $\tau_{cr,0}$ and $\sigma_{cr,0}$ are plotted on a σ-τ diagram. These two points are connected by an "interaction curve." Each point on the interaction curve characterizes a pair of critical stresses σ_{cr} and τ_{cr} that, acting in conjunction, will produce buckling of the sheet. This curve has been drawn from the equation

$$\frac{\sigma_{cr}}{\sigma_{cr,0}} + \left(\frac{\tau_{cr}}{\tau_{cr,0}}\right)^2 = 1 \tag{56}$$

which describes the interaction with sufficient accuracy (reference 35).

Let σ denote the compressive stress that would exist in the cylinder if the sheet did not buckle (i.e., remained fully effective) under the action of the design compressive load P. Similarly, let τ denote the shear stress that would exist if the sheet did not buckle under the action of the design torque T. The values of σ and τ establish the point C in the σ-τ diagram of figure 37. The line drawn from C to the origin intersects the interaction curve at point D. The critical stresses σ_{cr} and τ_{cr} characterized by point D are used in the following steps. For convenience of notation, there are also used the interaction factors

$$R^C = \frac{\sigma_{cr}}{\sigma_{cr,0}} \quad ; \quad R^T = \frac{\tau_{cr}}{\tau_{cr,0}} \tag{57}$$

With the aid of the ratios

$$A = \frac{\tau_{cr,0}}{\sigma_{cr,0}} \quad ; \quad B = \frac{\tau}{\sigma}$$

which can be computed directly from the dimensions of the structure and the specified design loads, the interaction factors can be written in the form

$$R^T = -\frac{A}{2B} + \sqrt{\frac{A^2}{4B^2} + 1} \quad ; \quad R^C = \frac{A}{B} R^T$$

The total stringer stress is the sum of the stringer stress due to the compressive load P and the stringer stress due to the diagonal tension caused by the torque, or

$$\sigma_{ST} = \sigma^C{}_{ST} + \sigma^T{}_{ST} \tag{58}$$

The stress $\sigma^C{}_{ST}$ is computed by the formula

$$\sigma^C{}_{ST} = \frac{P}{n(A_{ST} + ht\eta^C)} \tag{59}$$

The load P must be taken as negative because it is compressive; n is the number of stringers, A_{ST} is the area of one stringer, and η^C is the effective-width factor. This factor is taken as the Kármán-Sechler expression for effective width (reference 36), multiplied by the ratio R^C in order to make allowance for the presence of the torque loading; thus

$$\eta^C = R^C 0.89 \sqrt{\frac{\sigma_{cr}}{\sigma^C{}_{ST}}} \tag{60}$$

If expression (60) is substituted into equation (59), a quadratic equation is obtained which yields

$$\sigma^C{}_{ST} = \frac{P}{nA_{ST}} - 2D^2 + 2D\sqrt{D^2 - \frac{P}{nA_{ST}}} \tag{61}$$

where

$$D = 0.445 \frac{ht}{A_{ST}} R^C \sqrt{-\sigma_{cr}} \tag{62}$$

The stress σ^T_{ST} is computed by formula (51), modified by the ratio R^T, in order to allow for the presence of the compressive load P; the modified formula is

$$\sigma^T_{ST} = - \frac{k\tau \cot \alpha}{\frac{A_{ST}}{ht} + 0.5(1 - k)R^T} \tag{63}$$

The interaction factors R^C and R^T, by definition, describe the interaction between compression and torque at the instant of buckling. Their use in formulas (60) and (63) to describe the interaction on the effective width is fundamentally arbitrary. However, in the usual design range, the effect of moderate errors in estimating the effective width is unimportant; any reasonable method for estimating the effect of interaction on effective width is therefore acceptable for the time being.

The stress in a ring is computed, according to reference 34, by the unmodified formula (52). This procedure is, in principle at least, open to some question; it would seem that some interaction factor should be added in the denominator, as was done in equation (63). In the tests made to date, the rings were relatively large; for this reason, and because the ring stresses are proportional to tan α (instead of cot α as the stringer stresses), the experimental ring stresses were too low to afford a sensitive check on this point.

The diagonal strain in the sheet is computed by equation (30d), on the implied assumption that it is not modified significantly by the compressive force carried by the sheet. The angle α is computed by formula (44) or (45), the strain ϵ_{ST} being computed from the total compressive stress σ_{ST} given by expression (58). The diagonal-tension factor k is obtained from figure 13 by using τ_{cr} $\left(\text{not } \tau_{cr,0}\right)$.

The stress computation for the case of combined loading thus differs from that for the case of pure torque loading in the following items:

(1) The critical stress is reduced by interaction

(2) The stringer stress due to the load P must be added; this calculation involves an interaction factor

(3) The calculation of the stringer stress due to the torque involves an interaction factor

Concerning item (1), there is ample theoretical and experimental evidence to justify the belief that the calculation is sufficiently accurate for design purposes. The factors used in items (2) and (3) are arbitrary, but they have only a very minor effect except for low loading ratios. Consequently, the accuracy with which the stresses can be computed under combined loading might be expected to be about the same as for pure-torque loading, as long as the ratio τ/τ_{cr} is greater than 2, and this expectation was fulfilled in the tests of reference 34.

The question of allowable stresses for failure is more problematical. The allowable value of skin shear stress is probably not changed significantly by added compression, but there is no experimental evidence on this score. As far as true column failure of the stringers is concerned, it would be immaterial whether the compressive stress in the stringer arises directly from the axial load P, or indirectly (through diagonal-tension action) from the torque; in other words, column failure would be assumed to take place when the total stringer stress given by expression (58) reaches the column allowable value. The condition of true column failure would only exist, however, if the cross section of the stringer were completely immune to forced deformations induced by skin buckles. As mentioned previously, the problem of interaction between forced deformation and column failure is probably more serious in curved than in plane webs, and fragmentary data indicate that no practical stringer section may be completely free from interaction effects.

Since it appears that there will be some interaction in most cases, the investigation of reference 34 was carried out in the region where the interaction is clearly large; namely, on stringers designed to fail by forced crippling in the case of pure-torque loading. Five cylinders of identical construction were built; one was tested in pure compression, one in pure torsion, and the other three in combined compression and torsion. The results were fitted by the interaction formula

$$\left(\frac{T}{T_o}\right)^{1.5} + \frac{P}{P_o} = 1.00 \qquad (64)$$

where T and P are the torque and the compressive load that cause stringer failure when acting simultaneously, T_o is the torque causing stringer failure when acting alone, and P_o is the compressive load causing stringer failure when acting alone. When this formula is used,

it is not necessary to compute the stringer stress by the method described previously for combined loading; a stringer-stress computation is made only for the case of a pure torque to calculate T_o. Ideally, the load P_o would also be calculated, but at present it would be safer to obtain this load by a compression test on one bay of the complete cylinder, or on a sector of this bay large enough to contain at least five stringers.

12. General Applications

The discussions and formulas for curved diagonal tension have been given on the assumption that the structure considered is a circular cylinder. Evidently, more general types of structure may be analyzed by the same formulas by the usual device of analyzing small regions or individual panels. The questions of detail procedure that will arise must be answered by individual judgment, because more general methods are not available at present. The results will obviously be more uncertain, for instance, if there are large changes in shear flow from one panel to the next. It should be borne in mind that in such cases problems in stress distribution exist even when the skin is not buckled into a diagonal-tension field; the existence of these problems is often overlooked because elementary theories are normally used to compute the shear flows.

13. Numerical Examples

As numerical examples of strength analyses of curved diagonal-tension webs, two cylinders will be analyzed that were tested in the investigation of reference 34. The cylinders were of nominally identical construction and differed only in loading conditions. They had 12 stringers of Z-section and rings also of Z-section. The rings were notched to let the stringers pass through them. Clip angles were used to connect the stringers to the rings and at the same time to reinforce the edge of the notch. The analysis will be made for the test loads that produced failure. The third example illustrates the calculation of the angle of twist for the cylinder used in the first example.

Example 1. Pure torsion.- The example chosen is cylinder 1 of reference 34. The material is 24S-T3 aluminum alloy.

Basic data:

$R = 15.0$ in. $\quad t = 0.0253$ in. $\quad d = 15.0$ in.

$E = 10.6 \times 10^3$ ksi $\quad \mu = 0.32 \quad h = 7.87$ in.

$$\pi R^2\left(1 - \frac{1}{6}\varphi^2\right) = 675 \qquad G = 4.0 \times 10^3 \text{ ksi}$$

Stringers: Z-section $\frac{3}{4} \times 1 \times \frac{3}{4} \times 0.040$; $A_{ST} = 0.0925$ in.^{2}

Rings: Z-section $\frac{3}{4} \times 2 \times \frac{3}{4} \times 0.081$; $A_{RG} = 0.251$ in.^{2}

Nominal shear stress:

$$\tau = \frac{388}{2 \times 675 \times 0.0253} = 11.36 \text{ ksi}$$

Buckling stress:

$$Z = \frac{7.87^2}{15.0 \times 0.0253}\sqrt{1 - 0.32^2} = 155$$

From figure 30: $k_s = 35$

$$\tau_{cr} = 35 \frac{\pi^2 \times 10.6 \times 10^3 \times 7.87^2}{12 \times 15^2 \times 155^2} = 3.50 \text{ ksi}$$

Loading ratio:

$$\frac{\tau}{\tau_{cr}} = \frac{11.36}{3.50} = 3.24$$

Diagonal-tension factor:

$$300 \frac{td}{Rh} = 300 \frac{0.0253 \times 15.0}{15.0 \times 7.87} = 0.965$$

From figure 13: $k = 0.63$

First approximation for angle of diagonal tension:

$$R_R = \frac{dt}{A_{RG}} = \frac{15.0 \times 0.0253}{0.251} = 1.513$$

$$R_S = \frac{ht}{A_{ST}} = \frac{7.87 \times 0.0253}{0.0925} = 2.155$$

$$\frac{1 + R_S}{1 + R_R} = 1.256$$

$$\frac{\frac{h}{R}\sqrt{\frac{E}{\tau}}}{\sqrt{1 + R_R}} = \frac{\frac{7.87}{15.0}\sqrt{\frac{10.6 \times 10^3}{11.36}}}{\sqrt{1 + 1.513}} = 10.1$$

From figure 28(a): $\alpha_{PDT} = 32.3^\circ$

From figure 32: $\frac{\alpha}{\alpha_{PDT}} = 0.90$

$$\alpha = 32.3^\circ \times 0.90 = 29.0^\circ$$

Stress and strain formulas:

From formulas (51) and (52):

$$\sigma_{ST} = -\frac{0.63 \times 11.36}{0.465 + 0.5(1 - 0.63)} \cot \alpha = -11.03 \cot \alpha \text{ ksi}$$

$$\epsilon_{ST} = -1.04 \times 10^{-3} \cot \alpha$$

$$\sigma_{RG} = -\frac{0.63 \times 11.36 \tan \alpha}{0.660 + 0.5(1 - 0.63)} = -8.46 \tan \alpha \text{ ksi}$$

$$\epsilon_{RG} = -0.800 \times 10^{-3} \tan \alpha$$

$$\frac{1}{24}\left(\frac{h}{R}\right)^2 = \frac{1}{24}\left(\frac{7.87}{15.0}\right)^2 = 11.48 \times 10^{-3}$$

$$\frac{I}{E} = 1.07 \times 10^{-3}$$

First cycle:

$$\alpha = 29^\circ \qquad \tan \alpha = 0.554 \qquad \cot \alpha = 1.805$$

From figure 31:

$$\frac{\epsilon E}{\tau} = 1.90 \quad ; \quad \epsilon = 1.90 \times 1.07 \times 10^{-3} = 2.035 \times 10^{-3}$$

$$\epsilon_{ST} = -1.04 \times 10^{-3} \times 1.805 = -1.875 \times 10^{-3}$$

$$\epsilon_{RG} = -0.800 \times 10^{-3} \times 0.554 = -0.444 \times 10^{-3}$$

According to formula (44):

$$\tan^2\alpha = \frac{2.035 + 1.875}{2.035 + 0.440 + 11.48} = 0.280$$

$$\tan \alpha = 0.529$$

Second cycle:

The final value of α is closer to the computed value of the preceding cycle than to the initially assumed value; therefore, take as the next approximation

$$\tan \alpha = 0.529 + \frac{1}{4}(0.554 - 0.529) = 0.535$$

$$\cot \alpha = 1.87 \qquad \alpha = 28^\circ 10'$$

From figure 31:

$$\frac{\epsilon E}{\tau} = 1.92 \quad ; \quad \epsilon = 1.92 \times 1.07 \times 10^{-3} = 2.054 \times 10^{-3}$$

$$\epsilon_{ST} = -1.04 \times 10^{-3} \times 1.87 = -1.945 \times 10^{-3}$$

$$\epsilon_{RG} = -0.800 \times 10^{-3} \times 0.535 = -0.427 \times 10^{-3}$$

$$\tan^2\alpha = \frac{2.054 + 1.945}{2.054 + 0.427 + 11.48} = 0.286$$

$$\tan \alpha = 0.535$$

The computed value of $\tan \alpha$ checks the assumed value; the second cycle is therefore the final one.

Stresses:

$$\sigma_{ST} = \epsilon_{ST} \times E = -1.945 \times 10^{-3} \times 10.6 \times 10^{3} = -20.6 \text{ ksi}$$

$$\sigma_{RG} = \epsilon_{RG} \times E = -0.427 \times 10^{-3} \times 10.6 \times 10^{3} = -4.54 \text{ ksi}$$

Note: The last strain measurements in the test were taken at 99 percent of the failing torque. The extrapolation to 100 percent gave a stringer stress of -20.20 ksi, which is numerically less than the calculated value by 2 percent.

Web strength:

The calculated skin stress being 11.36 ksi, inspection of figure 19(a) shows that there is a large margin (about 50 percent) against skin rupture.

Stringers, column failure:

The radius of gyration of the stringer section is 0.408 inch; therefore,

$$\frac{d}{2\rho} = 18.4$$

This slenderness ratio is so low that there is obviously a large margin against column failure at the computed value of stringer stress.

Stringers, forced-crippling failure:

From figure 15: $\frac{\sigma_{max}}{\sigma} = 1.16$

$$\sigma_{ST_{max}} = -20.6 \times 1.16 = -23.85 \text{ ksi}$$

$$\frac{t_{ST}}{t} = \frac{0.0404}{0.0253} = 1.60$$

From figure 20: $\sigma_o = -22.3$ ksi

Note: The "design allowable" value of the stringer stress (-22.3 ksi) is 7 percent greater than the calculated value of -23.85 ksi. Therefore, the calculation would have predicted failure at a torque 7 percent lower than the actual failing torque, that is, the calculation is 7 percent conservative. The "best possible estimate" of the allowable stress (based on the middle of the scatter band instead of the lower edge) would be 25 percent higher than the "design allowable" value; a strength prediction based on this value thus would have been 18 percent unconservative.

Example 2. Combined loading.- The example chosen to demonstrate the analysis of a cylinder under combined torsion and compression is cylinder 5 of reference 34. In order to simplify the demonstration by making use of partial results obtained in example 1, it will be assumed that the dimensions given for example 1 apply; actually, some of the dimensions differed by as much as 2 percent.

Basic data:

Dimensions as in example 1.

$T = 303$ inch-kips $\qquad P = -13.5$ kips

Compression area:

$$12 \text{ stringers} = 12 \times 0.0925 = 1.11 \text{ in.}^2$$

$$\text{Sheet } (100\%) = \pi \times 30 \times 0.0253 = 2.38 \text{ in.}^2$$

$$\text{Total } 3.49 \text{ in.}^2$$

Basic stresses:

$$\tau_{cr,0} = 3.50 \text{ ksi} \quad \text{(see example 1)}$$

$$\sigma_{cr,0} = -5.95 \text{ ksi}$$

The latter value is computed according to the recommendations of reference 35 with an empirical reduction factor.

At the design loads, the nominal stresses are

$$\sigma = \frac{-13.5}{3.49} = -3.87 \text{ ksi}$$

$$\tau = \frac{303}{34.2} = 8.86 \text{ ksi}$$

Interaction factors:

From formulas (57):

$$A = \frac{3.50}{-5.95} = -0.588 \qquad B = \frac{8.86}{-3.87} = -2.29$$

$$R^T = 0.878 \qquad R^C = 0.228$$

$$\tau_{cr} = 0.878 \times 3.50 = 3.07 \text{ ksi} \qquad \sigma_{cr} = -0.228 \times 5.95 = -1.356 \text{ ksi}$$

Compressive stress due to axial load:

From formulas (62) and (61), respectively

$$D = 0.445 \times 2.155 \times 0.228 \times \sqrt{1.356} = 0.254$$

$$\sigma^C_{ST} = -10.55 \text{ ksi} \qquad \epsilon^C_{ST} = -0.996 \times 10^{-3}$$

Diagonal-tension factor:

$$\frac{\tau}{\tau_{cr}} = \frac{8.86}{3.07} = 2.88 \qquad k = 0.59$$

Stress and strain formulas:

From formula (63):

$$\sigma^T_{ST} = -\frac{0.59 \times 8.86 \cot \alpha}{0.465 + 0.5(1 - 0.59) \times 0.878} = -8.10 \cot \alpha \text{ ksi}$$

$$\epsilon^T_{ST} = -0.764 \times 10^{-3} \cot \alpha$$

From formula (52):

$$\sigma^T_{RG} = -\frac{0.59 \times 8.86 \tan \alpha}{0.660 + 0.5(1 - 0.59)} = -6.05 \tan \alpha \text{ ksi}$$

$$\epsilon_{RG} = -0.570 \times 10^{-3} \tan \alpha$$

Computation cycle:

Only the last cycle will be shown here. This computation is essentially the same as for a case of pure torsion (example 1), except that the stringer strain due to axial load $\left(\epsilon^C_{ST}\right)$ is added to the strain due to the torque $\left(\epsilon^T_{ST}\right)$.

The first approximation to the angle α may be obtained by disregarding the compression, that is to say, in the same manner as in example 1. An analyst with some experience may improve this approximation by adding a correction for the effect of the axial load (compression load will steepen the angle).

Assume $\alpha = 28^\circ 30'$; $\tan \alpha = 0.543$; $\cot \alpha = 1.84$

From figure 31:

$$\frac{\epsilon E}{\tau} = 1.86 \quad ; \quad \epsilon = 1.86 \times \frac{8.86}{10.6 \times 10^3} = 1.552 \times 10^{-3}$$

From the strain formulas:

$$\epsilon^T_{ST} = -0.764 \times 10^{-3} \times 1.84 = -1.405 \times 10^{-3}$$

$$\epsilon_{RG} = -0.570 \times 10^{-3} \times 0.543 = -0.310 \times 10^{-3}$$

$$\tan^2\alpha = \frac{1.552 + 1.405 + 0.996}{1.552 + 0.310 + 11.48} = 0.296$$

$$\tan \alpha = 0.544$$

This result agrees with the assumed value within the accuracy of calculation and thus constitutes the final value.

By the stress formulas

$$\sigma^T_{ST} = \frac{-8.10}{0.544} = -14.90 \text{ ksi}$$

Therefore the total stringer stress is

$$\sigma_{ST} = -14.90 - 10.55 = -25.45 \text{ ksi}$$

The value measured (on a cylinder with slightly different actual dimensions) was -25 ksi.

Failure:

Since the torque is much less than in example 1 (pure-torque case), there is a wide margin against web rupture.

The margin against stringer failure is evaluated by formula (64). According to test (reference 34), the cylinder failed under pure compression at $P_o = 42.0$ kips. Under pure torque, the test gave $T_o = 388$ inch-kips: (the calculated value of T_o (example 1) is 7 percent lower). Thus, with the "design loads" $T = 303$ inch-kips and $P = 13.5$ kips

$$\left(\frac{T}{T_o}\right)^{1.5} + \frac{P}{P_o} = \left(\frac{303}{388}\right)^{1.5} + \frac{13.5}{42.0} = 1.01$$

Note: Because the "design loads" T and P used in this example were actually test failing loads and because the interaction curve was based on a series of tests on cylinders of these dimensions, the calculated value of 1.01 indicates that the analytical expression chosen for the interaction curve fits this particular test very well.

Example 3. Angle of twist.- In this example, the angle of twist will be calculated for the cylinder of example 1 at the failing torque.

According to example 1:

$$\tan \alpha = 0.535 \quad ; \quad \cot \alpha = 1.87 \quad ; \quad \sin 2\alpha = 0.832 \quad ; \quad k = 0.63$$

By formula (31b):

$$\frac{E}{G_{DT}} = \frac{4}{0.832^2} + \frac{0.535^2}{0.660 + 0.5(1 - 0.63)} + \frac{1.87^2}{0.465 + 0.5(1 - 0.63)}$$

$$\frac{E}{G_{DT}} = 5.77 + 0.34 + 5.39 = 11.50$$

$$G_{DT} = \frac{E}{11.50} = \frac{10.6 \times 10^3}{11.50} = 0.922 \times 10^3 \text{ ksi}$$

By formula (31a):

$$\frac{1}{G_{IDT}} = \frac{0.37}{4 \times 10^3} + \frac{0.63}{0.922 \times 10^3} = 0.0925 \times 10^{-3} + 0.683 \times 10^{-3}$$

$$= 0.775 \times 10^{-3}$$

$$G_{IDT} = 1.29 \times 10^3 \text{ ksi}$$

The torsion constant for the polygon section is

$$J = 2 \times \pi \times 15^3 \times 0.0253\left(1 - \frac{7}{24} \times 0.524^2\right) = 492$$

For a length of 60 inches, the angle of twist is

$$\frac{TL}{G_{IDT}J} = \frac{388 \times 60}{1.29 \times 10^3 \times 492} = 0.0366 \text{ radian}$$

Langley Aeronautical Laboratory
National Advisory Committee for Aeronautics
Langley Field, Va., October 5, 1951

APPENDIX

PORTAL-FRAME EFFECT

In the stress analysis of plate girders of constant depth, it is customary to assume that the shear web carries the entire shear. This assumption is usually a very good one, but it may become inaccurate under some conditions. If the flanges are heavy and deep, the portion of the shear carried by the flanges may become appreciable; this condition is aggravated by the yielding of the web-to-flange attachments and of the web, when the formulas of the elementary beam theory begin to break down.

The tip bay of a plate girder is usually reinforced by a web doubler plate. If the unreinforced portion of the web is removed completely, there remains a "portal frame" (fig. 38) consisting of the two flanges connected by a built-up transverse member. This portal frame can carry a shear load which may be appreciable compared with the shear load carried in the web. A rough approximation of the portal-frame shear may be obtained under the following assumptions:

(a) The transverse member in the frame is sufficiently stiff to maintain the right angles between this member and the flanges

(b) The deflections of the portal frame and of the shear web are independent of each other except at the tip

The deflection of the shear web under a load of unit magnitude is

$$\delta_1 = \frac{L}{htG_e}$$

The deflection of the portal frame under a load of unit magnitude is approximately

$$\delta_2 = \frac{L^3}{24EI}$$

where I is the moment of inertia of one flange. Under assumption (b), the ratio of the shear carried by the web to the total shear is

$$\frac{S'}{S} = \frac{1}{1 + \frac{\delta_1}{\delta_2}} = \frac{1}{1 + \frac{24EI}{L^2htG_e}}$$

Test evidence suggests that it would be wise not to count on portal-frame effect in routine strength predictions (Part II, section 2.4). Conversely, however, it would seem wise to reduce allowable web stresses deduced from special tests if the flanges of the test beam are much stiffer than those in the actual airplane structure.

REFERENCES

1. Wagner, Herbert: Flat Sheet Metal Girders with Very Thin Metal Web. Part I - General Theories and Assumptions. NACA TM 604, 1931.

Wagner, Herbert: Flat Sheet Metal Girders with Very Thin Metal Web. Part II - Sheet Metal Girders with Spars Resistant to Bending. Oblique Uprights - Stiffness. NACA TM 605, 1931.

Wagner, Herbert: Flat Sheet Metal Girders with Very Thin Metal Web. Part III - Sheet Metal Girders with Spars Resistant to Bending. The Stress in Uprights - Diagonal Tension Fields. NACA TM 606, 1931.

2. Kuhn, Paul, Peterson, James P., and Levin, L. Ross: A Summary of Diagonal Tension. Part II - Experimental Evidence. NACA TN 2662, 1952.

3. Timoshenko, S.: Theory of Elastic Stability. McGraw-Hill Book Co., Inc., 1936.

4. Kuhn, Paul, and Peterson, James P.: Strength Analysis of Stiffened Beam Webs. NACA TN 1364, 1947.

5. Wagner, H., and Ballerstedt, W.: Tension Fields in Originally Curved, Thin Sheets during Shearing Stresses. NACA TM 774, 1935.

6. Kuhn, Paul: Loads Imposed on Intermediate Frames of Stiffened Shells. NACA TN 687, 1939.

7. Kuhn, Paul: Investigations on the Incompletely Developed Plane Diagonal-Tension Field. NACA Rep. 697, 1940.

8. Kuhn, Paul, and Chiarito, Patrick T.: The Strength of Plane Web Systems in Incomplete Diagonal Tension. NACA ARR, Aug. 1942.

9. Levin, L. Ross, and Sandlin, Charles W., Jr.: Strength Analysis of Stiffened Thick Beam Webs. NACA TN 1820, 1949.

10. Koiter, W. T.: Het schuifplooiveld bij groote overschijdingen van de knikspanning (Theoretical Investigation of the Diagonal Tension Field of Flat Plates). Rep. S.295, Nationaal Luchtvaartlaboratorium, Amsterdam, Oct. 1944.

11. Denke, Paul H.: Strain Energy Analysis of Incomplete Tension Field Web-Stiffener Combinations. Jour. Aero. Sci., vol. 11, no. 1, Jan. 1944, pp. 25-40.

12. Denke, Paul H.: Analysis and Design of Stiffened Shear Webs. Jour. Aero. Sci., vol. 17, no. 4, April 1950, pp. 217-231.

13. Levy, Samuel, Fienup, Kenneth L., and Woolley, Ruth M.: Analysis of Square Shear Web above Buckling Load. NACA TN 962, 1945.

14. Levy, Samuel, Woolley, Ruth M., and Corrick, Josephine N.: Analysis of Deep Rectangular Shear Web above Buckling Load. NACA TN 1009, 1946.

15. Leggett, D. M. A.: The Buckling of a Square Panel under Shear When One Pair of Opposite Edges is Clamped, and the Other Pair is Simply Supported. R. & M. No. 1991, British A.R.C., 1941.

16. Iguchi, S.: Die Knickung der rechteckigen Platte durch Schubkräfte. Ing.-Archiv, Bd. IX, Heft 1, Feb. 1938, pp. 1-12.

17. Smith, R. C. T.: The Buckling of Plywood Plates in Shear. Rep. SM. 51, Council for Sci. and Ind. Res., Div. Aero., Commonwealth of Australia, Aug. 1945.

18. Kromm, A.: Stabilität von homogenen Platten und Schalen im elastischen Bereich. Ringbuch der Luftfahrttechnik, Bd. II, Art. A10, May 1940.

19. Stowell, Elbridge Z.: Critical Shear Stress of an Infinitely Long Plate in the Plastic Region. NACA TN 1681, 1948.

20. Buchert, Kenneth P.: Stability of Alclad Plates. NACA TN 1986, 1949.

21. Levin, L. Ross: Ultimate Stresses Developed by 24S-T and Alclad 75S-T Aluminum-Alloy Sheet in Incomplete Diagonal Tension. NACA TN 1756, 1948.

22. Kuhn, Paul: Ultimate Stresses Developed by 24S-T Sheet in Incomplete Diagonal Tension. NACA TN 833, 1941.

23. Kuhn Paul, and Moggio, Edwin M.: The Longitudinal Shear Strength Required in Double-Angle Columns of 24S-T Aluminum Alloy. NACA RB 3E08, 1943.

24. Wagner, Herbert: Remarks on Airplane Struts and Girders under Compressive and Bending Stresses. Index Values. NACA TM 500, 1929.

25. Ochiltree, David W.: Comparison of Structural Efficiencies of Diagonal-Tension Webs and Truss Webs of 24S-T Aluminum Alloy. NACA RB L5F25, 1945.

26. Batdorf, S. B., Stein, Manuel, and Schildcrout, Murry: Critical Shear Stress of Curved Rectangular Plates. NACA TN 1348, 1947.

27. Kuhn, Paul, and Griffith, George E.: Diagonal Tension in Curved Webs. NACA TN 1481, 1947.

28. Dunn, Louis G.: Some Investigations of the General Instability of Stiffened Metal Cylinders. VIII - Stiffened Metal Cylinders Subjected to Pure Torsion. NACA TN 1197, 1947.

29. Thorn, K.: Spannungsmessungen an gekrümmten Schubwänden eines Schalenrumpfes. Jahrb. 1937 der deutschen Luftfahrtforschung, R. Oldenbourg (Munich), pp. I 459 - I 463.

30. Schuette, Evan H., Bartone, Leonard M., and Mandel, Merven W.: Tensile Tests of Round-Head, Flat-Head, and Brazier-Head Rivets. NACA TN 930, 1944.

31. Mandel, Merven W., and Bartone, Leonard M.: Tensile Tests of NACA and Conventional Machine-Countersunk Flush Rivets. NACA ARR L4F06, 1944.

32. Schuette, Evan H., and Niles, Donald E.: Data on Optimum Length, Shear Strength, and Tensile Strength of Age-Hardened 17S-T Machine-Countersunk Rivets in 75S-T Sheet. NACA TN 1205, 1947.

33. Kuhn, Paul, and Levin, L. Ross: An Empirical Formula for the Critical Shear Stress of Curved Sheets. NACA ARR L5A05, 1945.

34. Peterson, James P.: Experimental Investigation of Stiffened Circular Cylinders Subjected to Combined Torsion and Compression. NACA TN 2188, 1950.

35. Batdorf, S. B., Schildcrout, Murry, and Stein, Manuel: Critical Combinations of Shear and Longitudinal Direct Stress for Long Plates with Transverse Curvature. NACA TN 1347, 1947.

36. Sechler, Ernest E., and Dunn, Louis G.: Airplane Structural Analysis and Design. John Wiley & Sons, Inc., 1942.

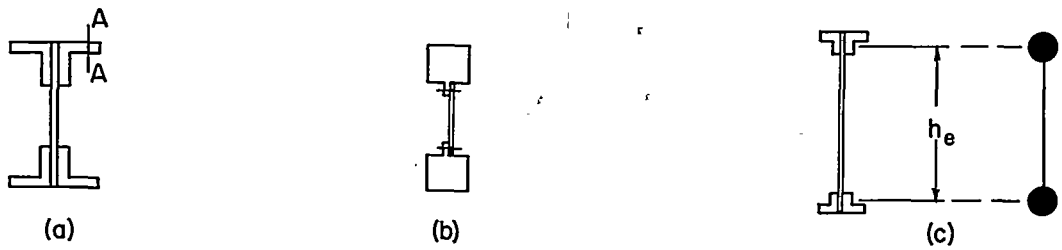

Figure 1.— Cross sections of built-up beams.

Figure 2.— (See next page.)

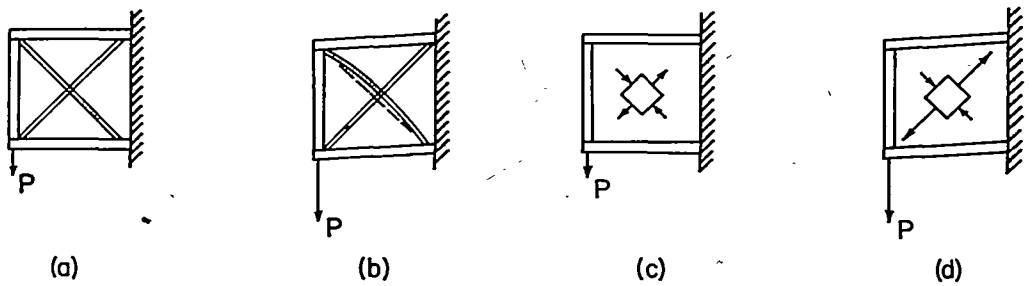

Figure 3.— Principle of diagonal tension.

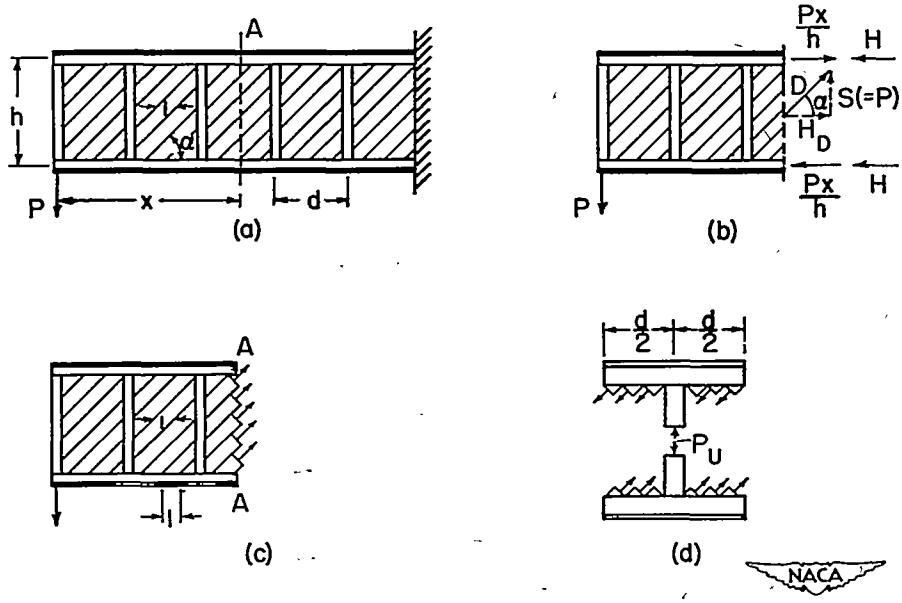

Figure 4.— Forces in diagohal-tension beam.

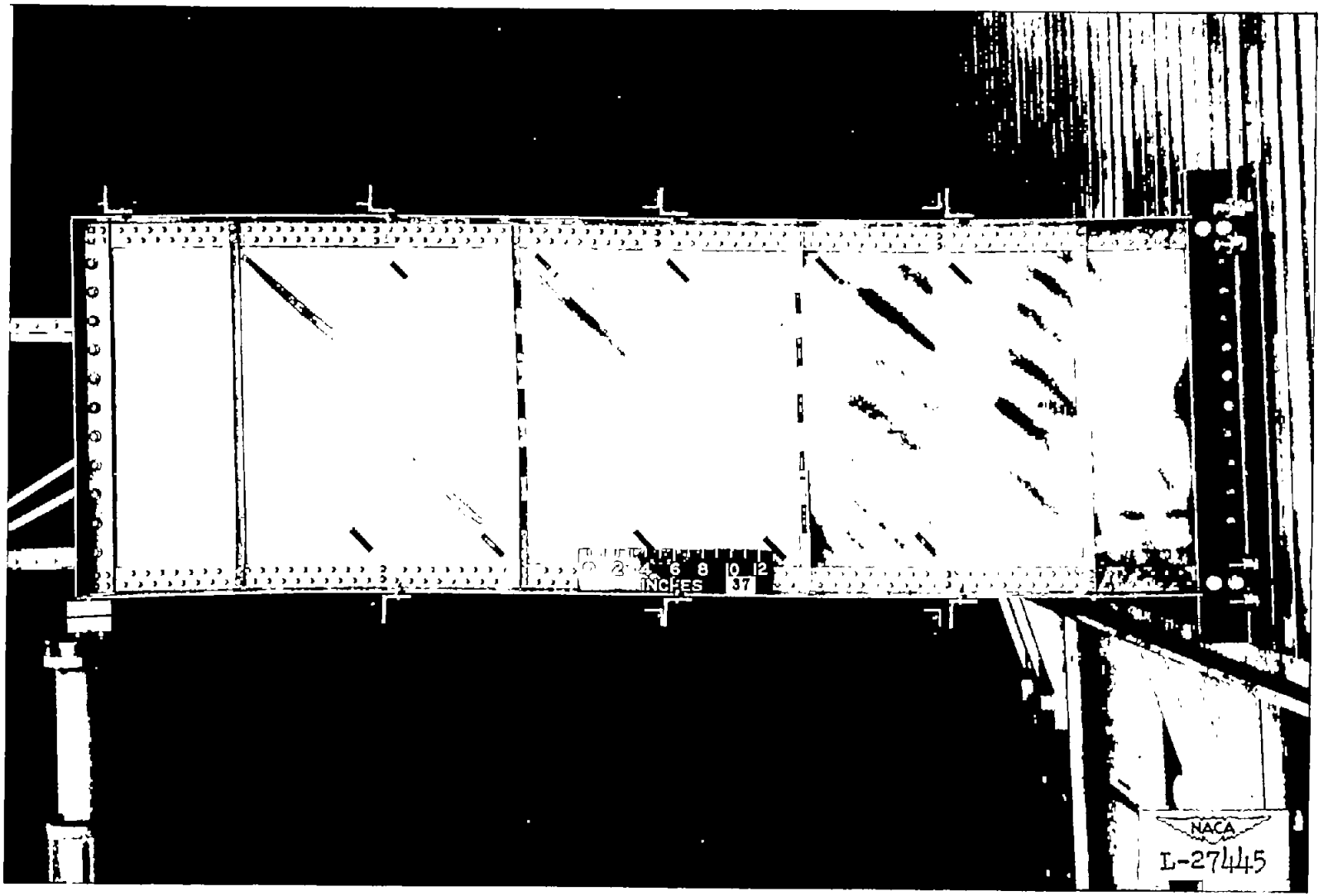

Figure 2.- Diagonal-tension beam.

Figure 5.– Secondary actions in diagonal–tension beams.

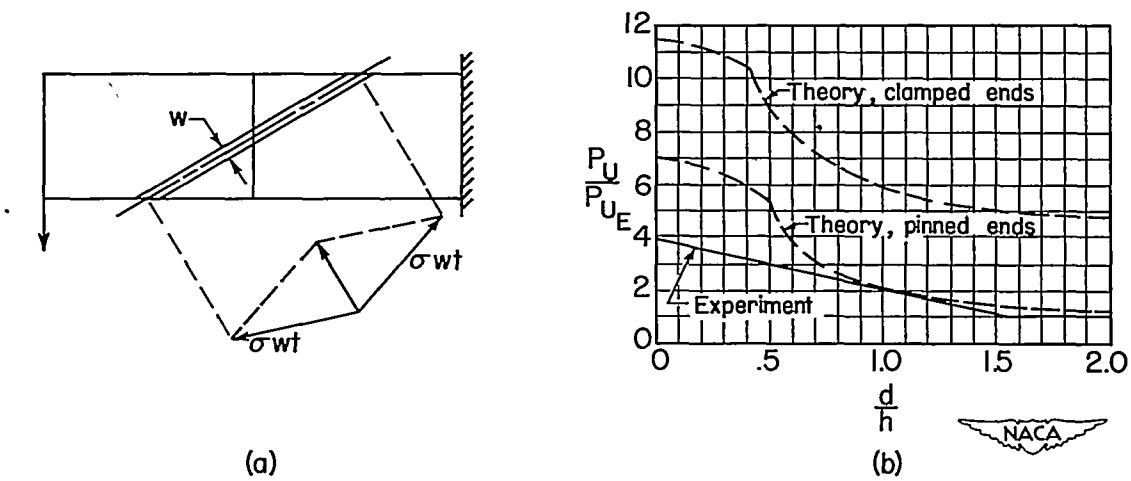

Figure 6.– Effect of diagonal tension on column length of uprights.

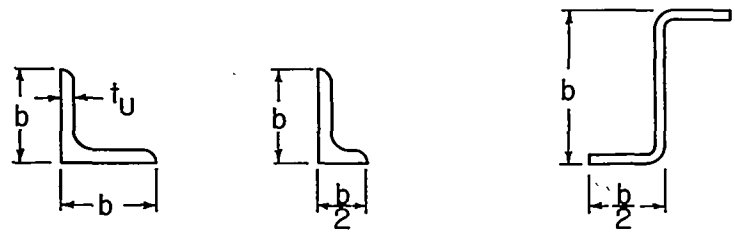

$\frac{A_{U_e}}{A_U}$				$\frac{b}{t_U}$
.51	.41	.40	.44	8
.57	.46	.40	.44	16

NACA

Figure 7.– Ratio of effective to actual area of uprights.

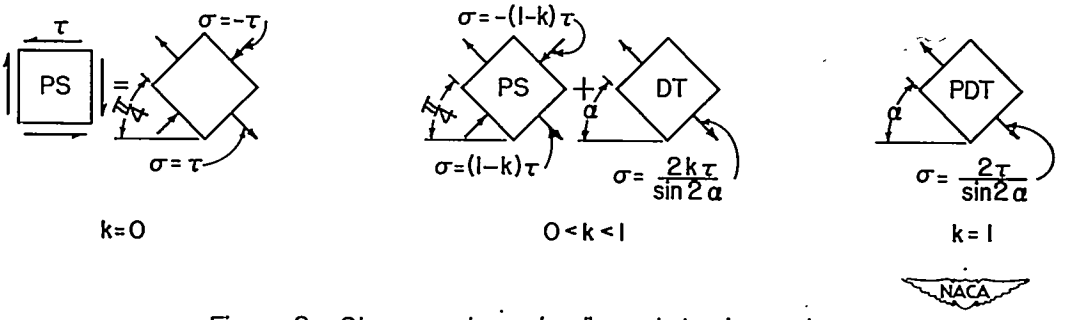

Figure 8.– Stress systems in diagonal-tension webs.

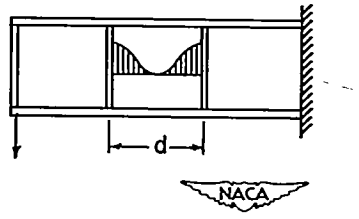

Figure 9.– Assumed distribution of vertical compressive stresses in sheet just buckled.

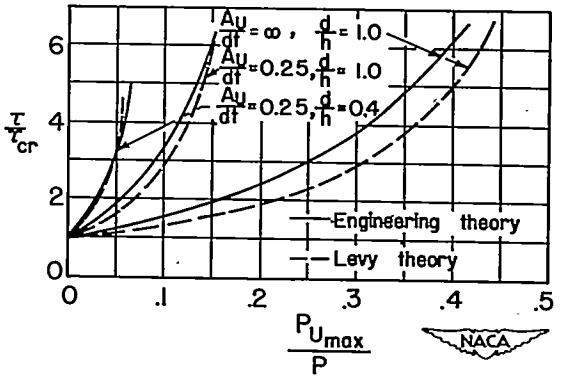

Figure 10.– Upright forces by two theories. $P_{U_{max}} = \sigma_{U_{max}} A_U$.

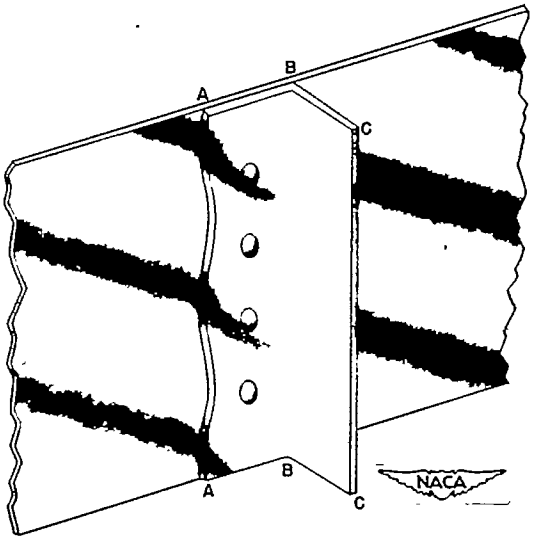

Figure 11.– Failure of upright by forced crippling.

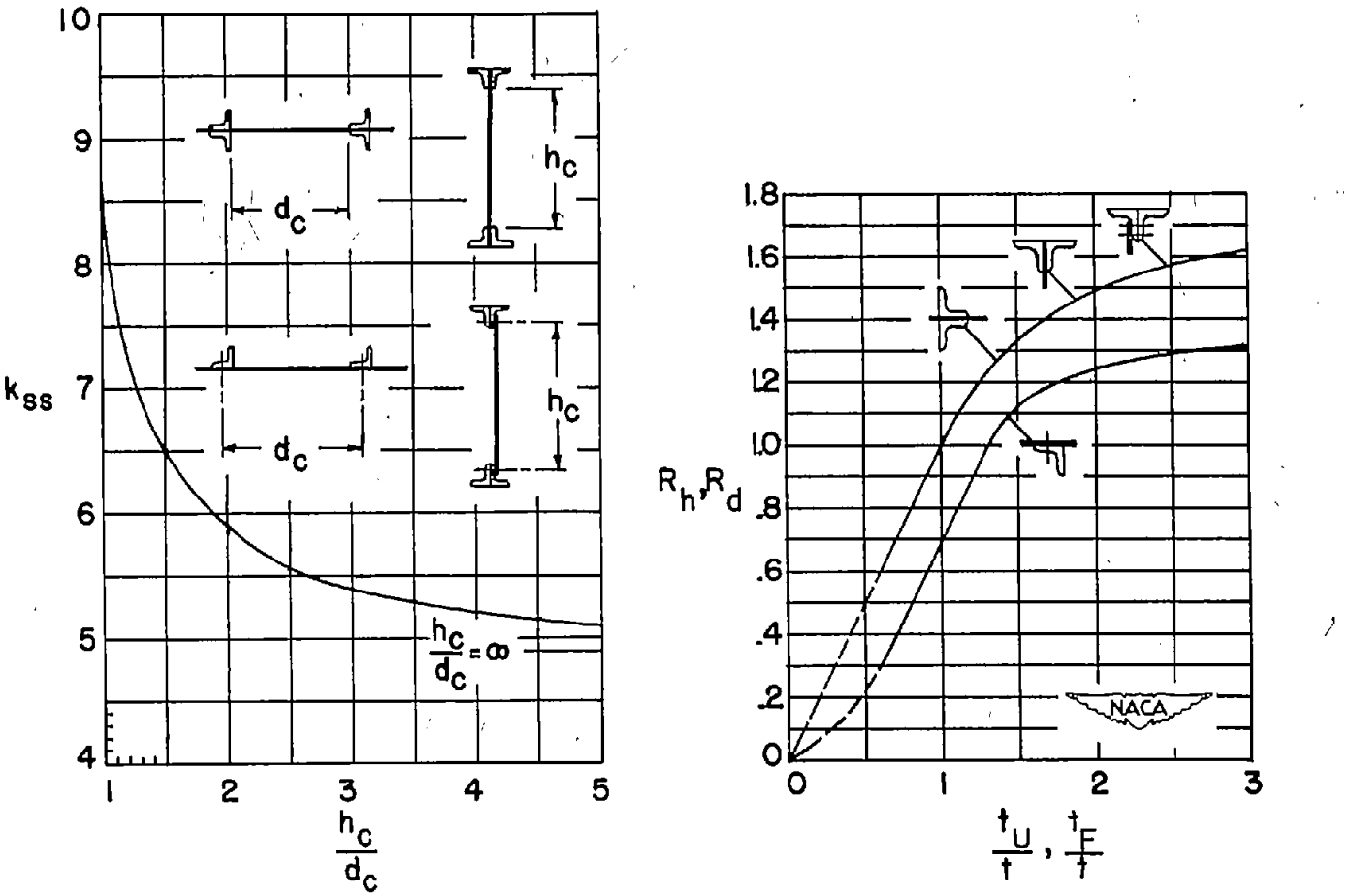

(a) Theoretical coefficients for plates with simply supported edges. (b) Empirical restraint coefficients.

Figure 12. — Graphs for calculating buckling stress of webs.

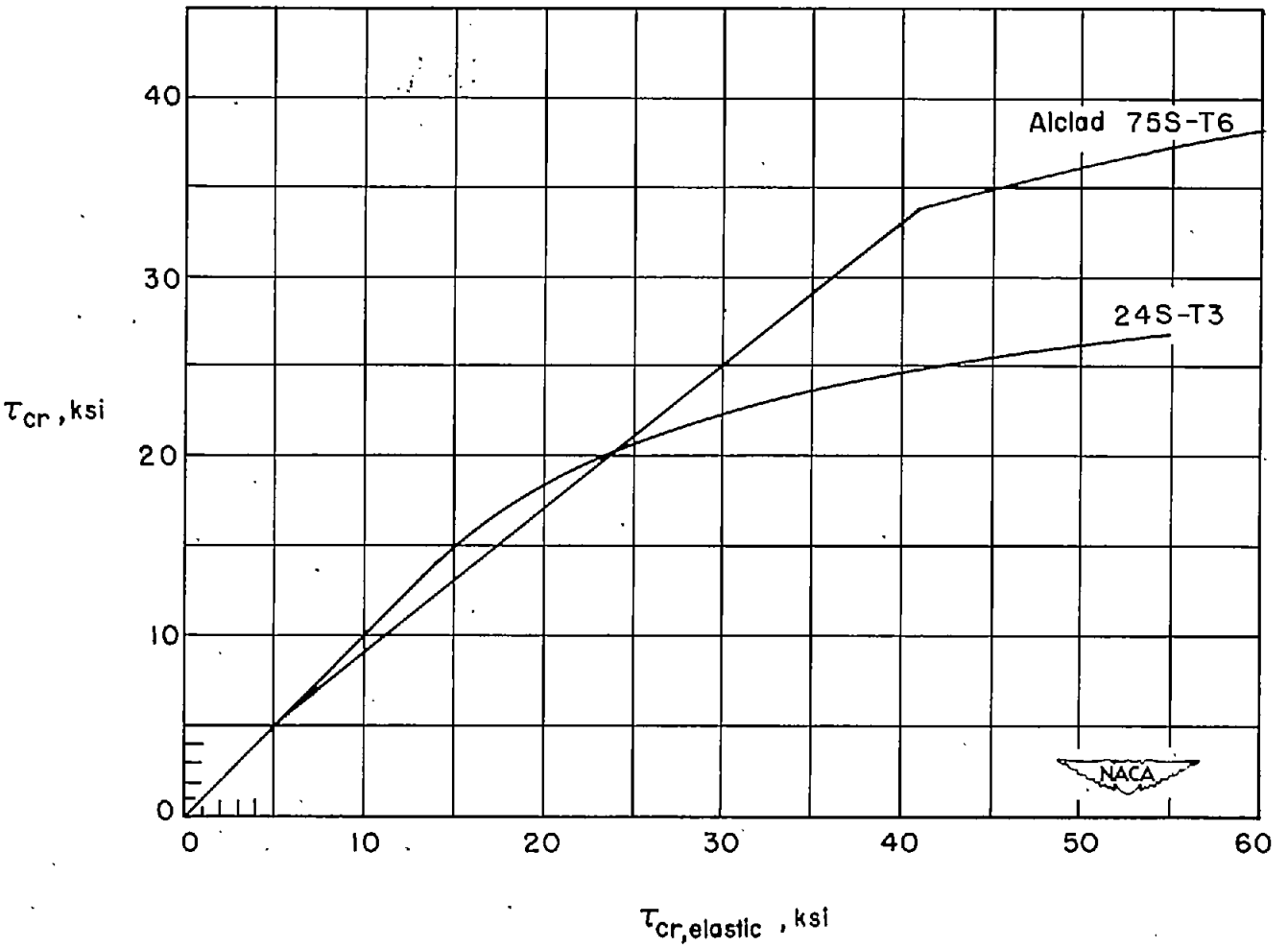

(c) Plasticity correction.

Figure 12.— Concluded.

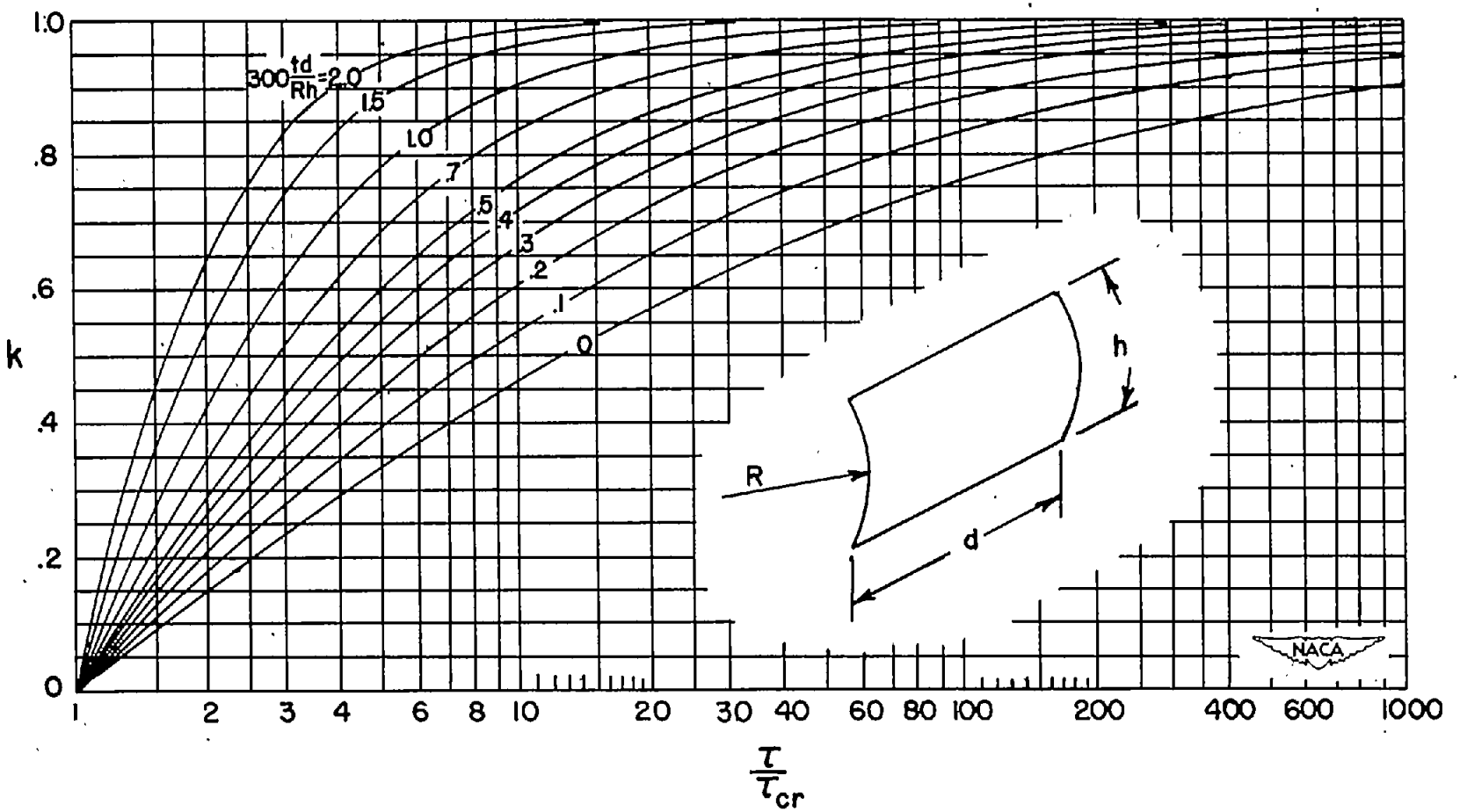

Figure 13.– Diagonal–tension factor k. (If h>d, replace $\frac{td}{Rh}$ by $\frac{th}{Rd}$; if $\frac{d}{h}$ $\left(\text{or } \frac{h}{d}\right) > 2$, use 2.)

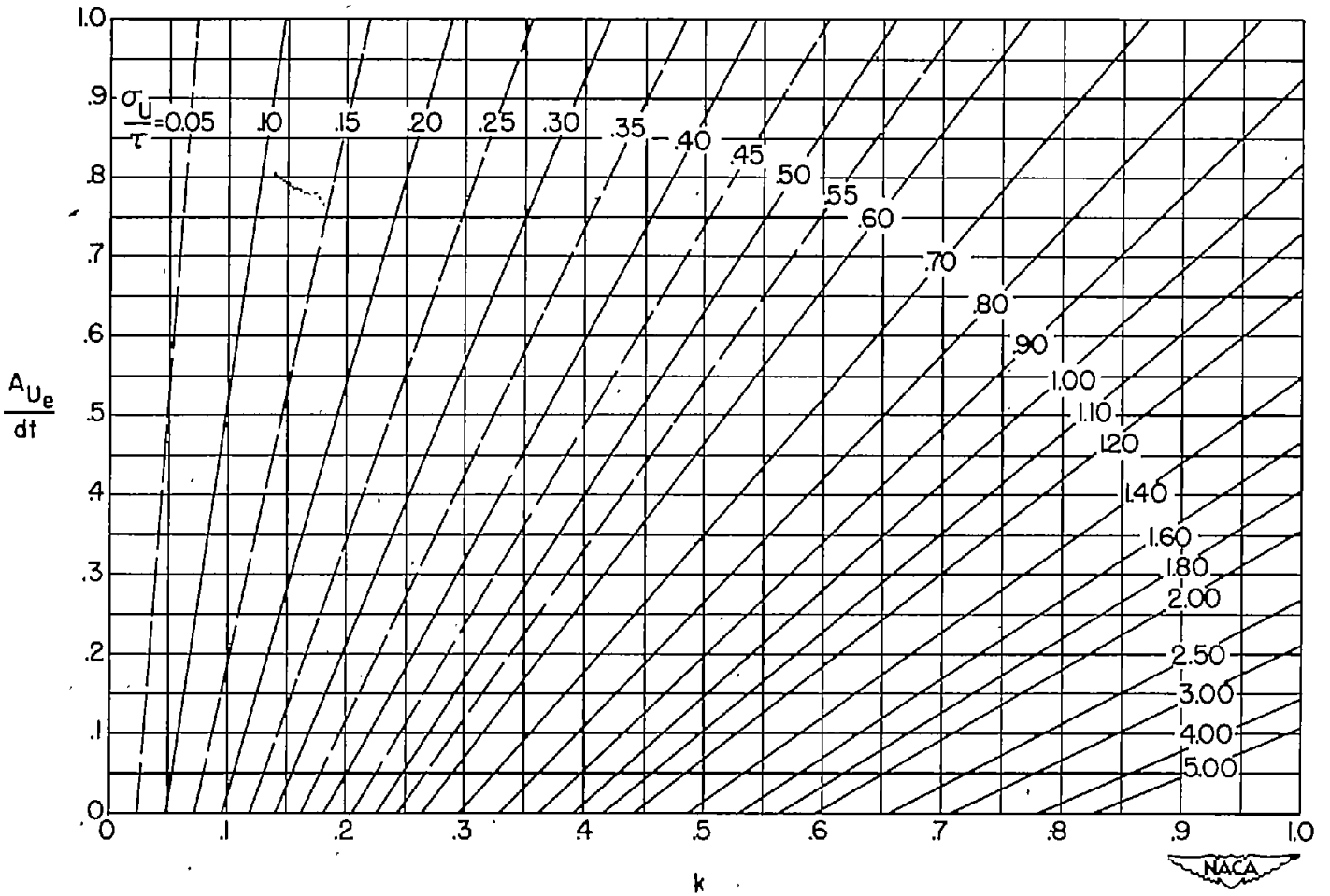

Figure 14.-Diagonal-tension analysis chart.

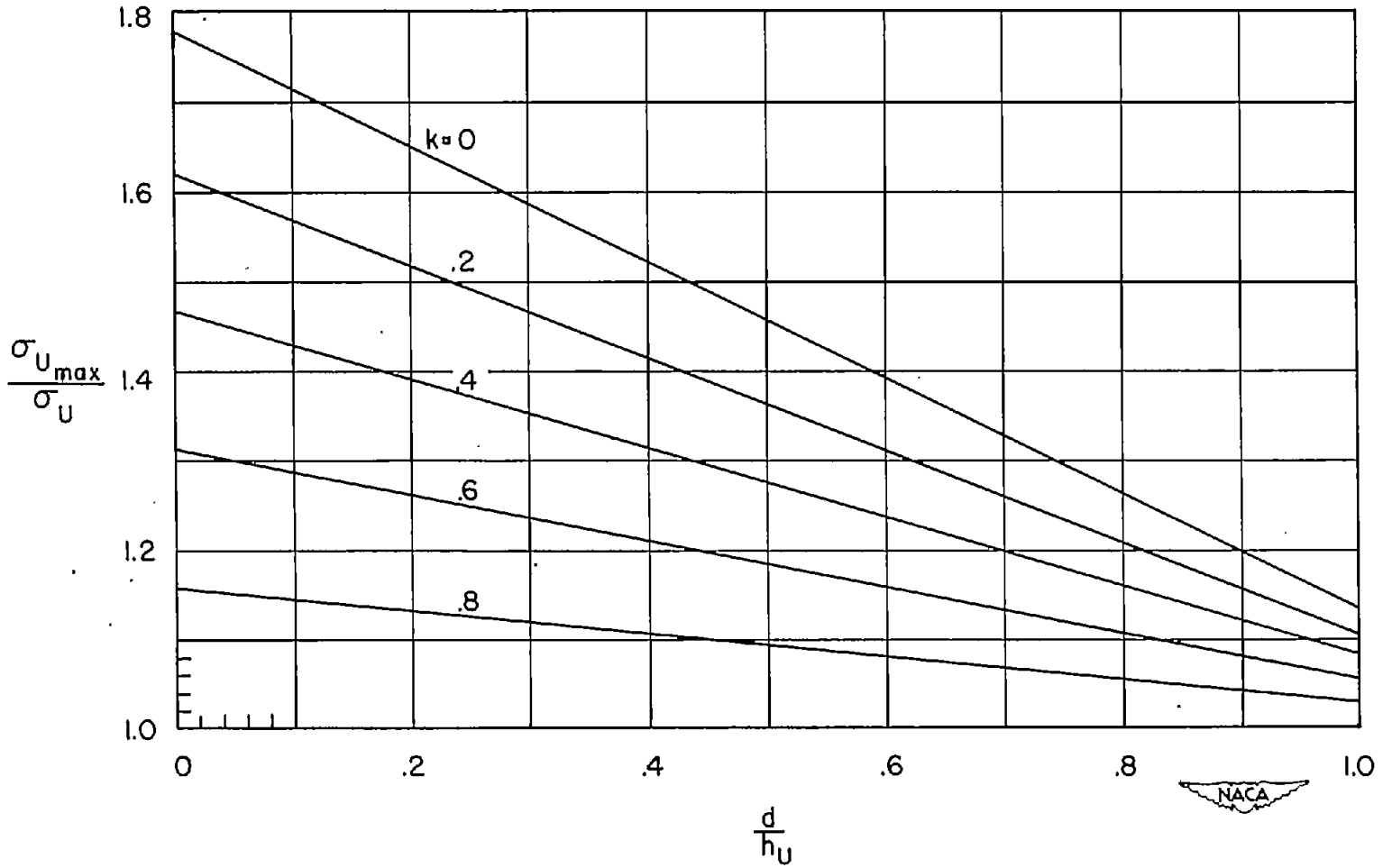

Figure 15.— Ratio of maximum stress to average stress in web stiffener.

Note for use on curved webs:
For rings, read abscissa as $\frac{d}{h}$; for stringers, read abscissa as $\frac{h}{d}$.

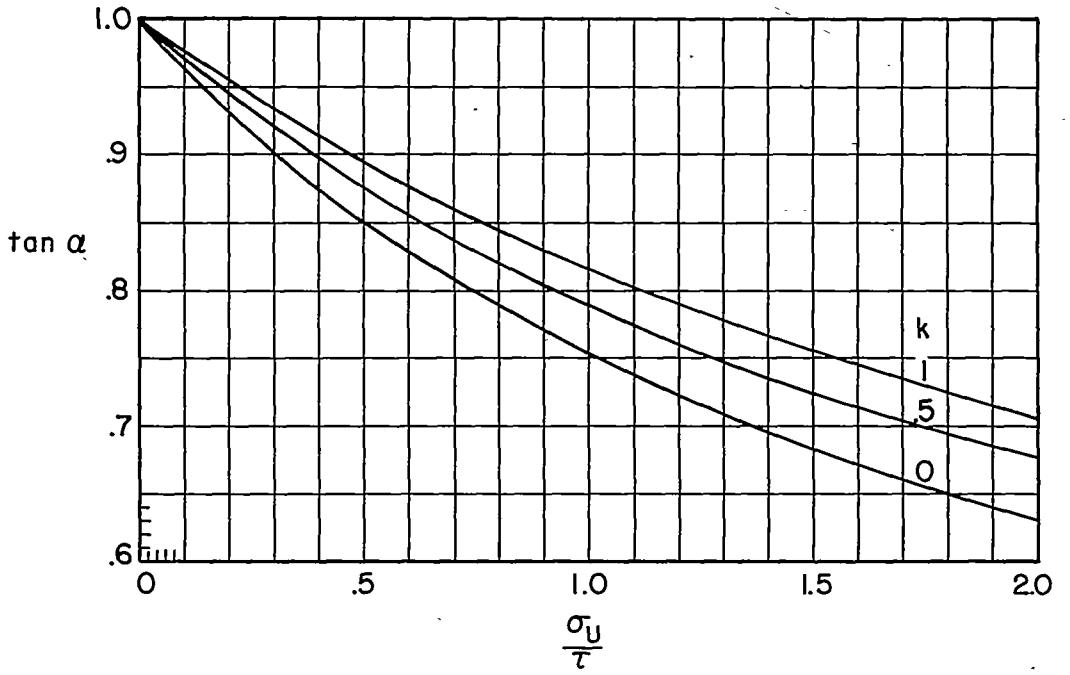

(a) Incomplete diagonal tension.

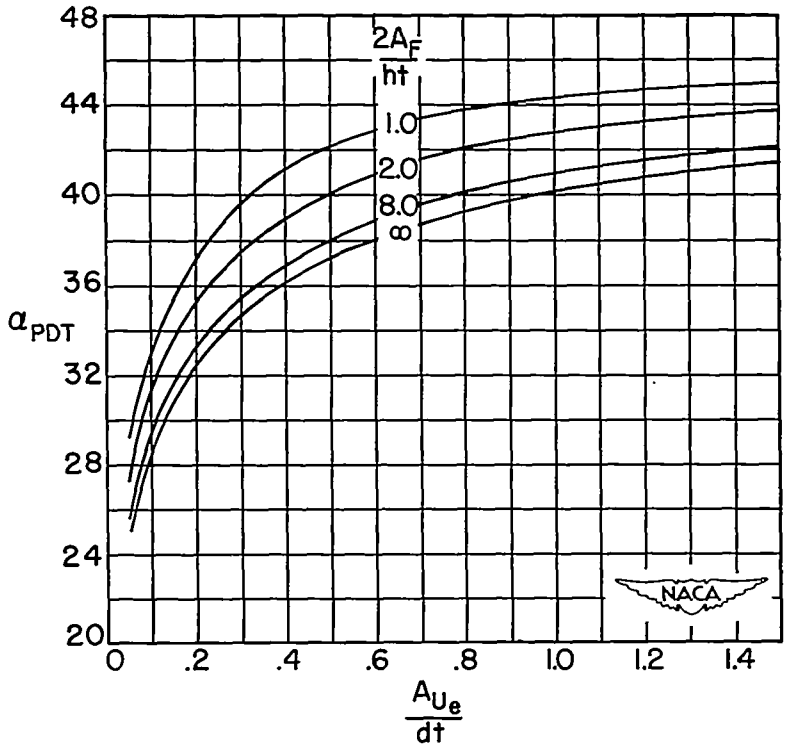

(b) Pure diagonal tension.

Figure 16.– Angle of diagonal tension.

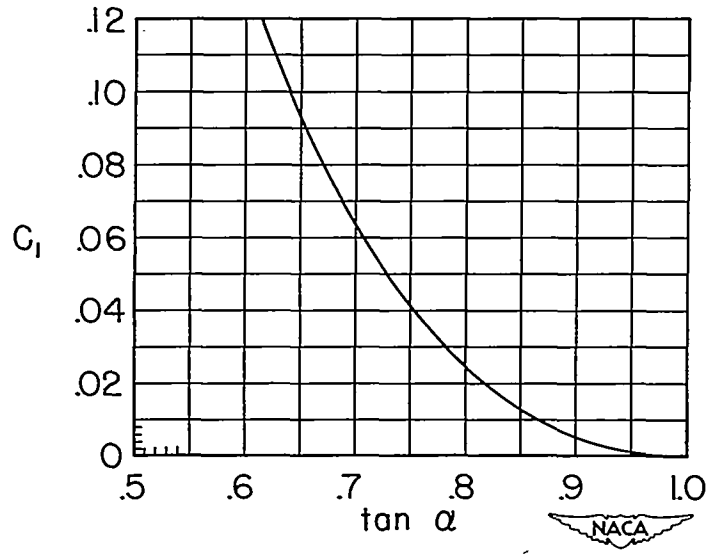

Figure 17.- Angle factor C_1.

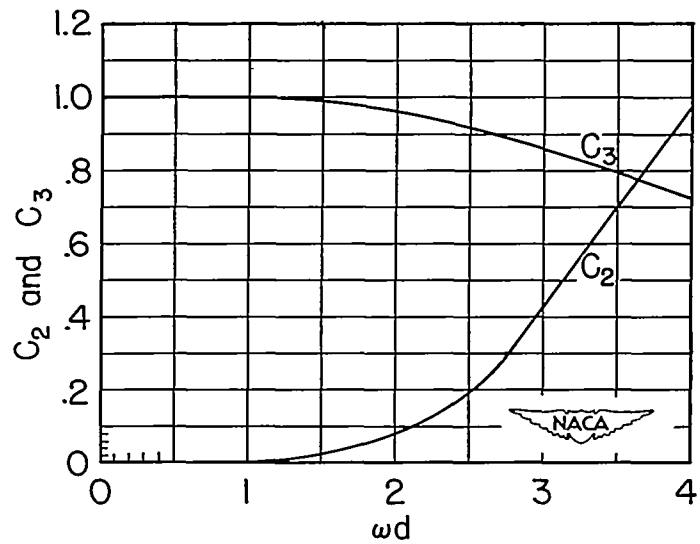

Figure 18.-Stress-concentration factors C_2 and C_3.

$$\left(\omega d = 0.7d \sqrt[4]{\frac{t}{(I_C + I_T) h_e}}\right)$$

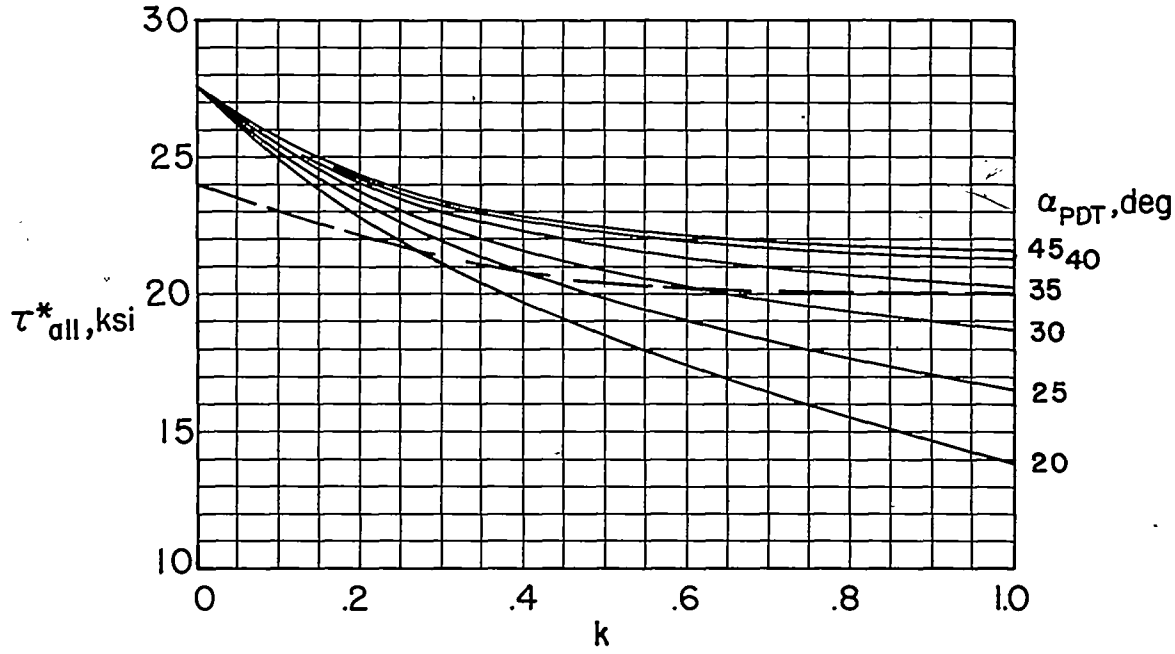

(a) 24S-T3 aluminum alloy. σ_{ult} = 62 ksi.
Dashed line is allowable yield stress.

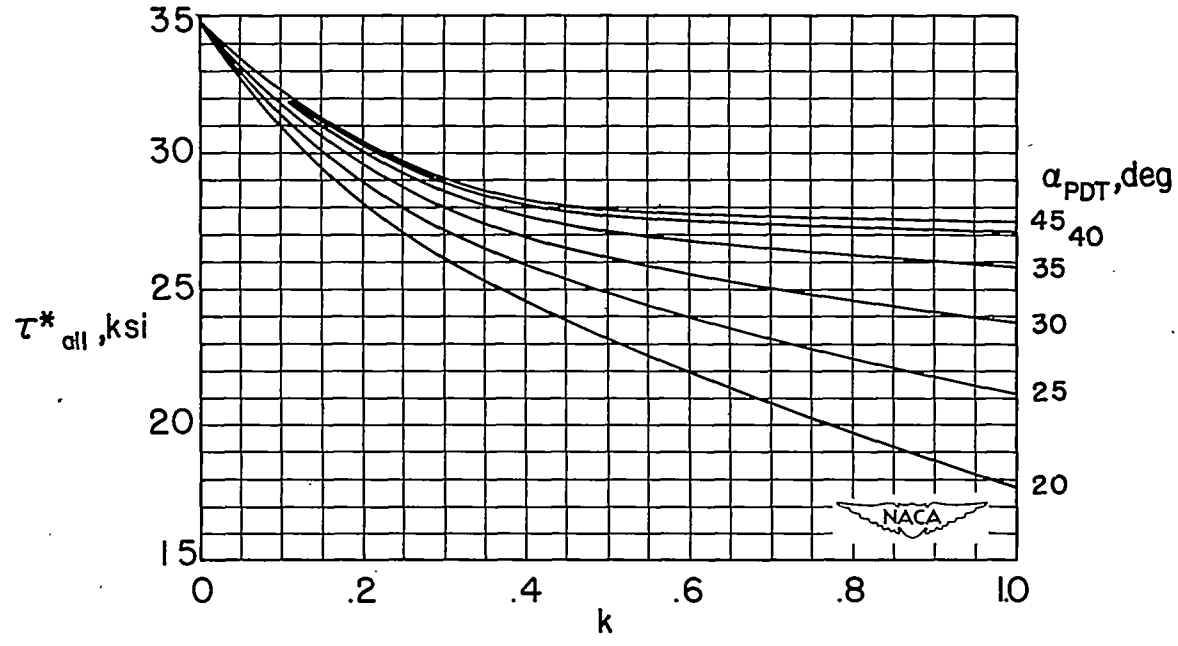

(b) Alclad 75S-T6 aluminum alloy. σ_{ult} = 72 ksi.

Figure 19.— Basic allowable values of τ_{max}.

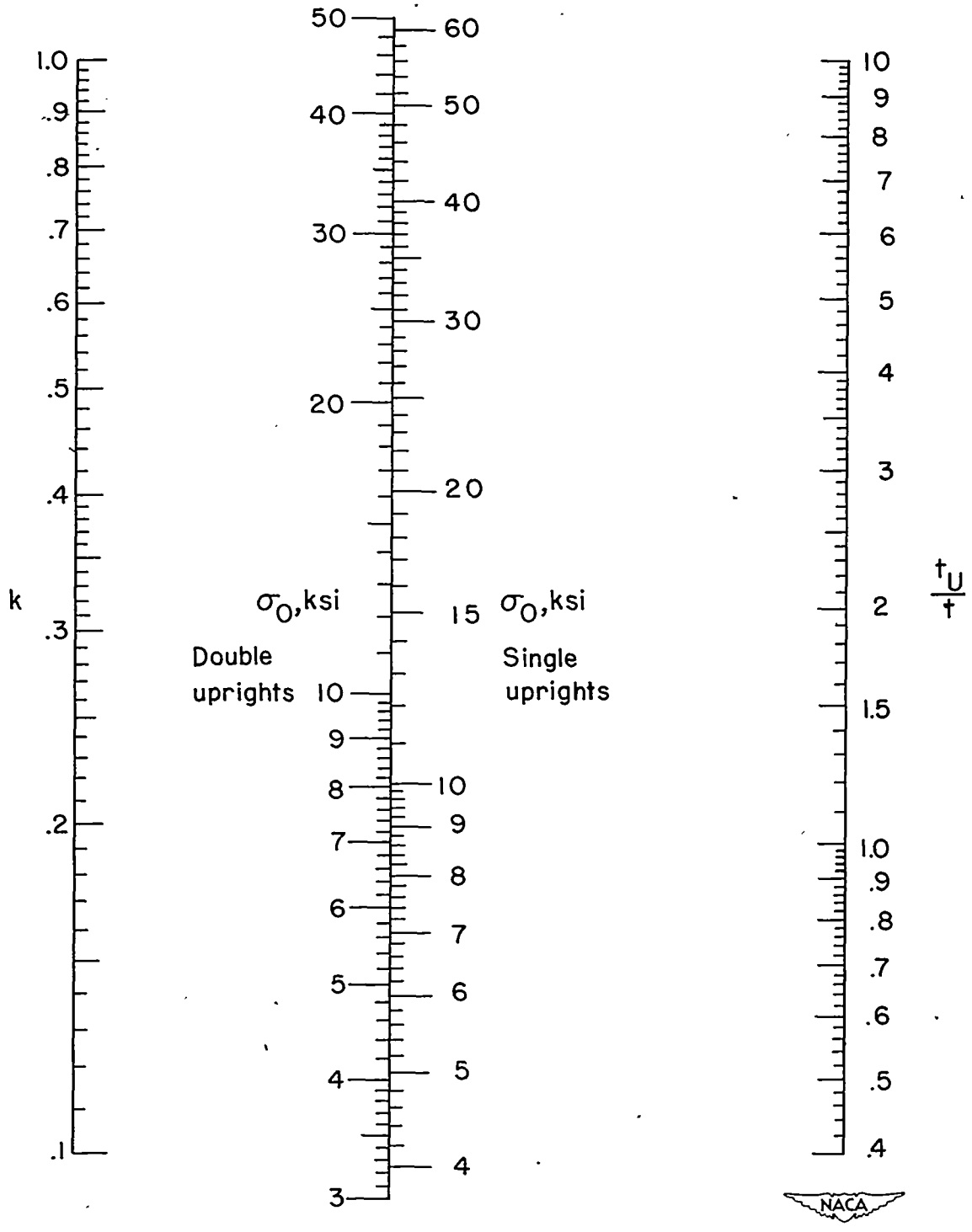

(a) 24S-T3 aluminum alloy.

Figure 20.— Nomogram for allowable upright stress (forced crippling).

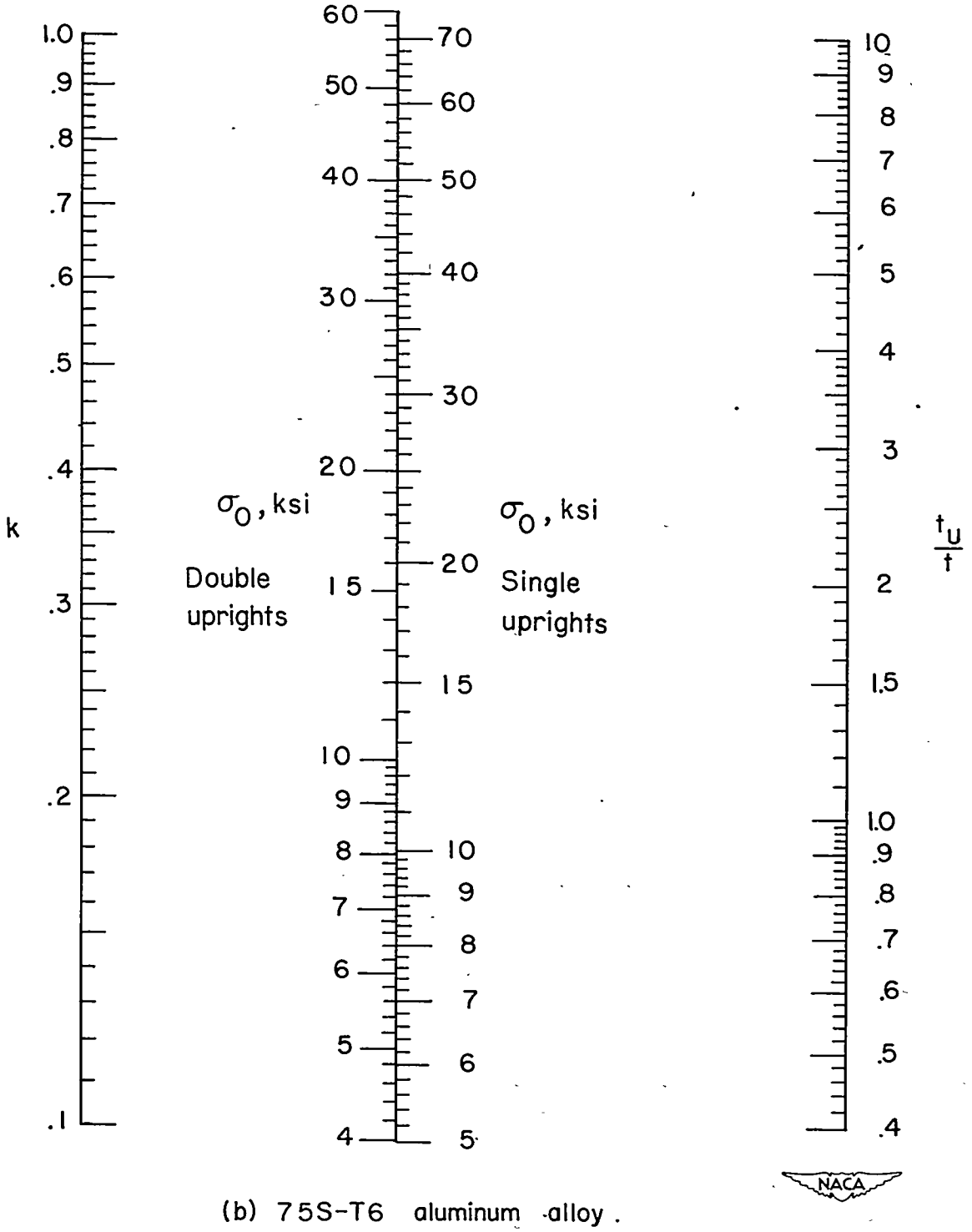

(b) 75S-T6 aluminum alloy.

Figure 20.— Concluded.

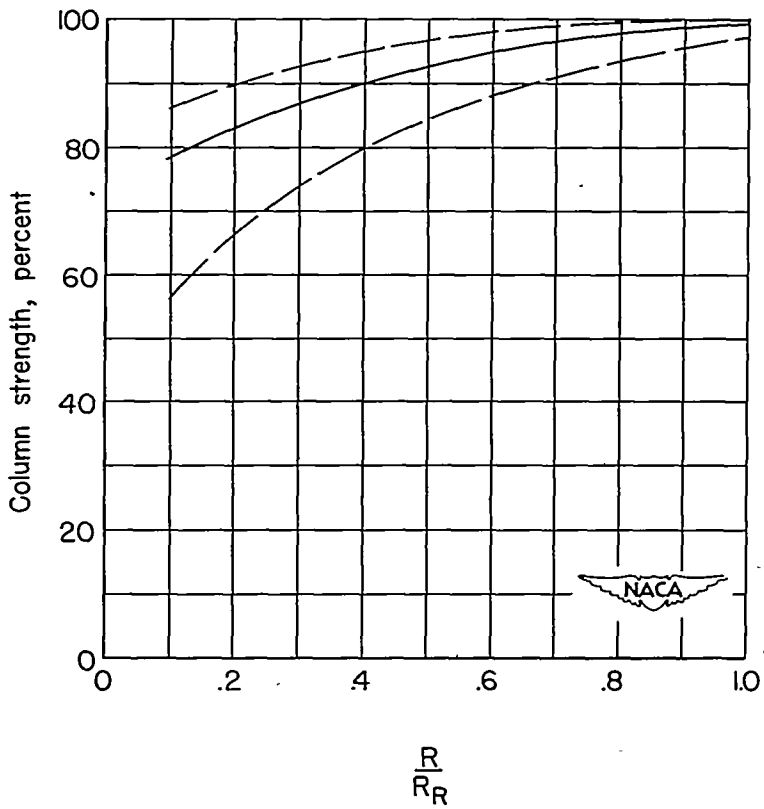

Figure 21.-Strength of riveted columns.

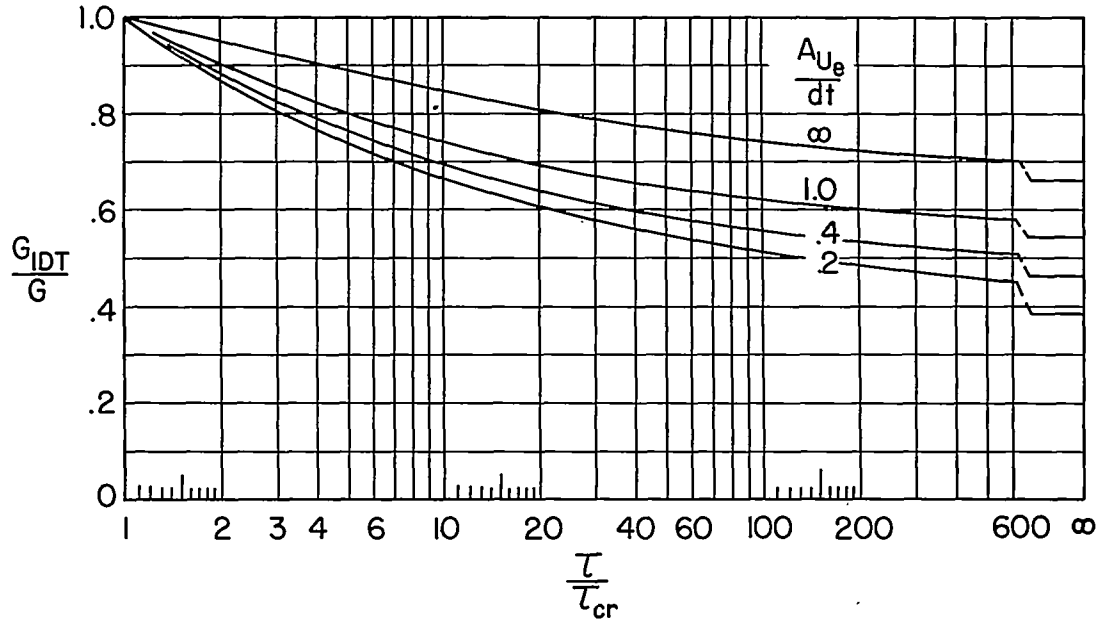

(a) Modulus ratio for elastic web.

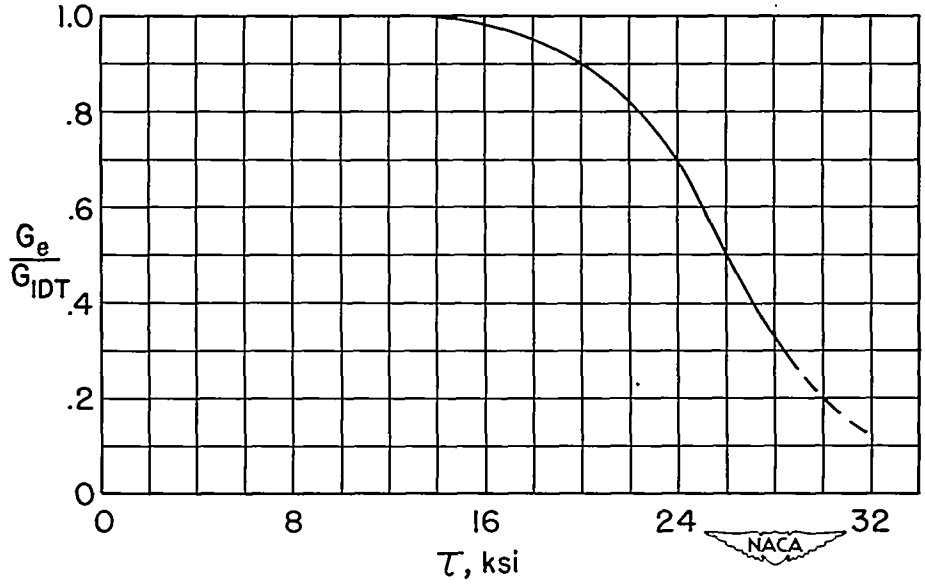

(b) Plasticity correction for 24S-T3 aluminum alloy.

Figure 22.— Effective shear modulus of diagonal-tension webs.

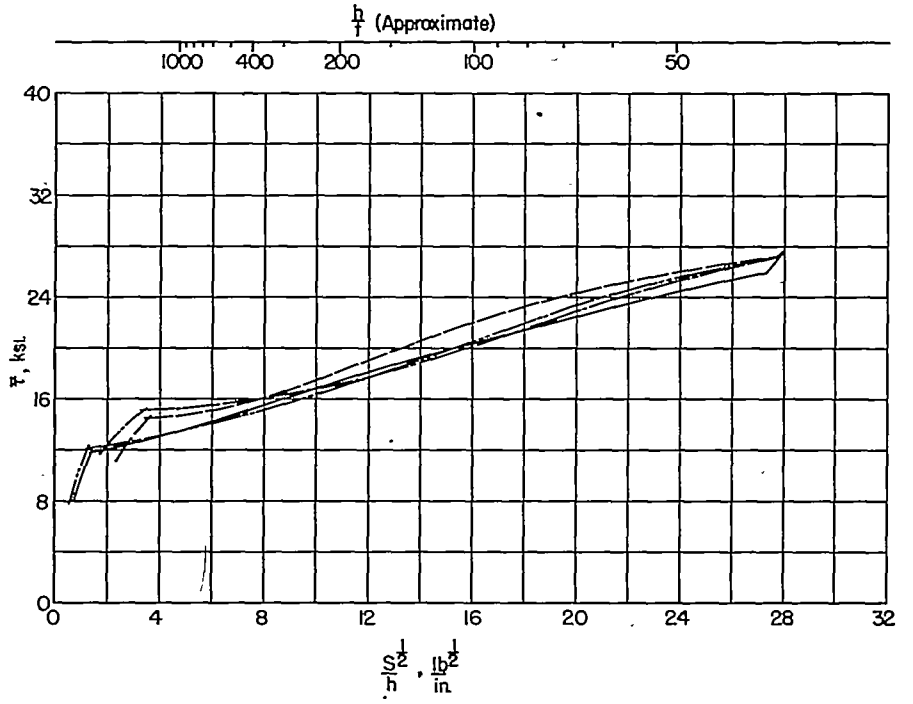

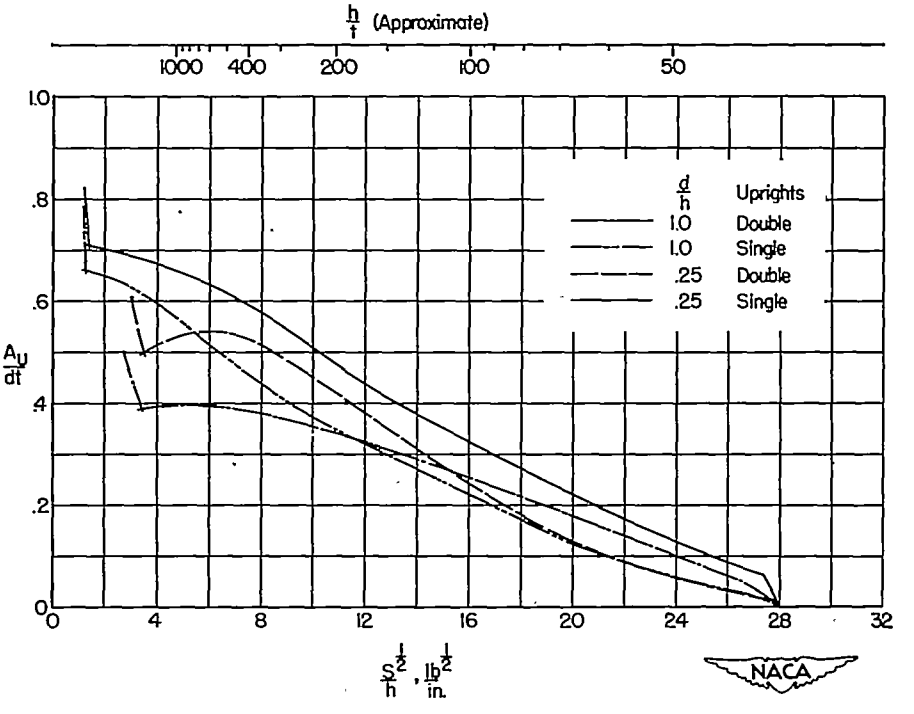

(a) 24S-T3 web and uprights.

Figure 23.-Structural efficiencies and stiffening ratios for diagonal-tension webs.

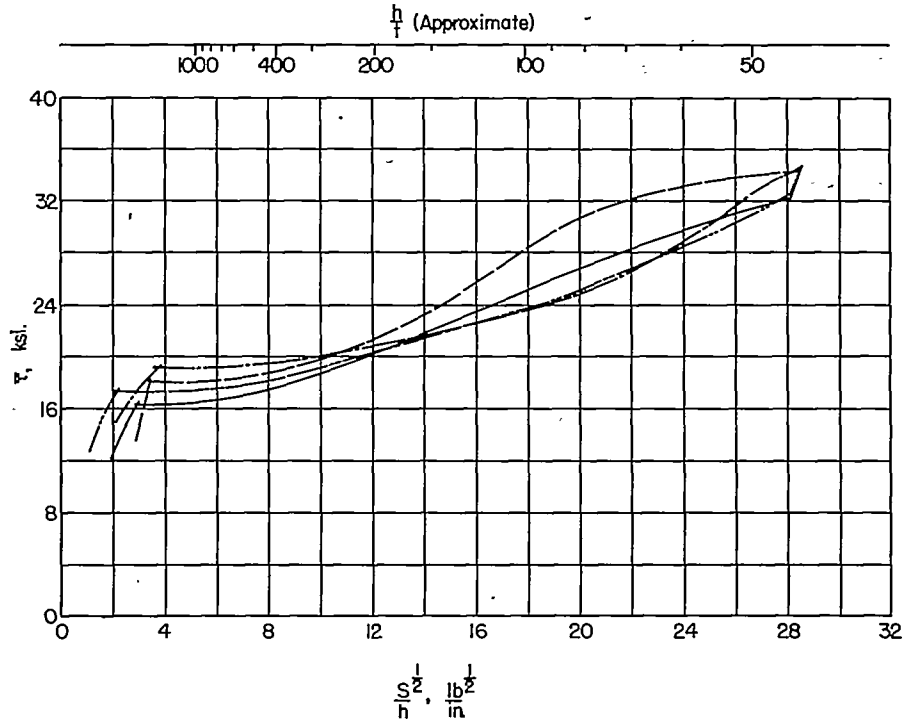

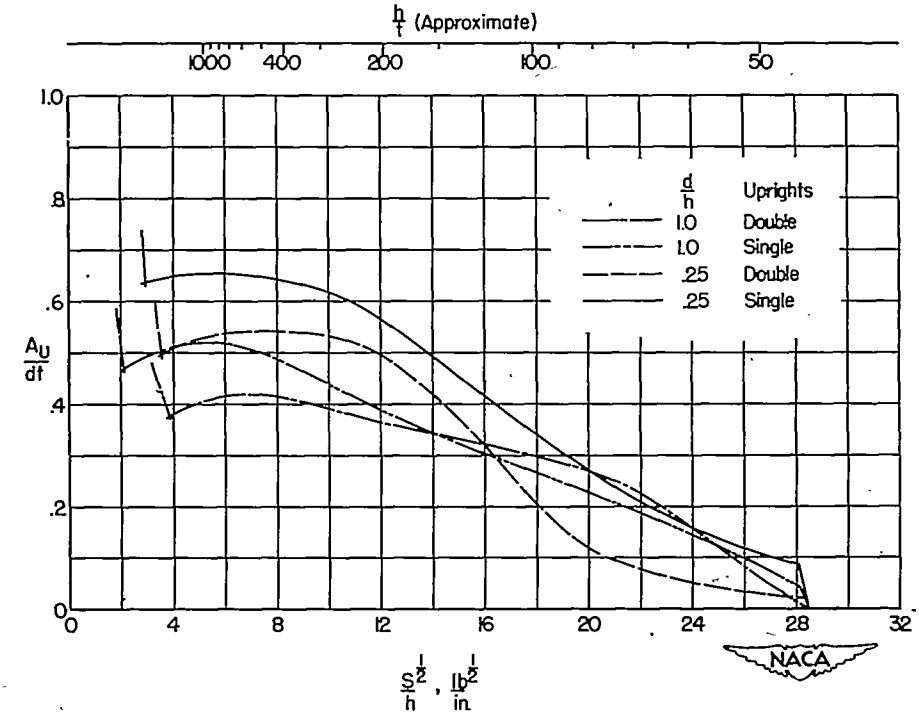

(b) Alclad 75S-T6 web and 75S-T6 uprights.

Figure 23.-Continued.

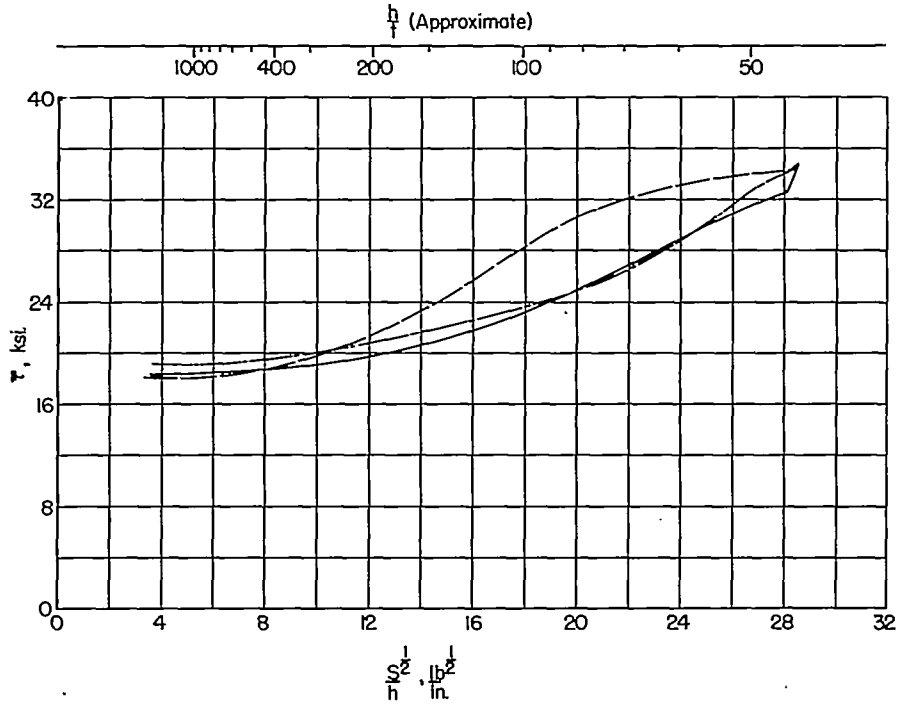

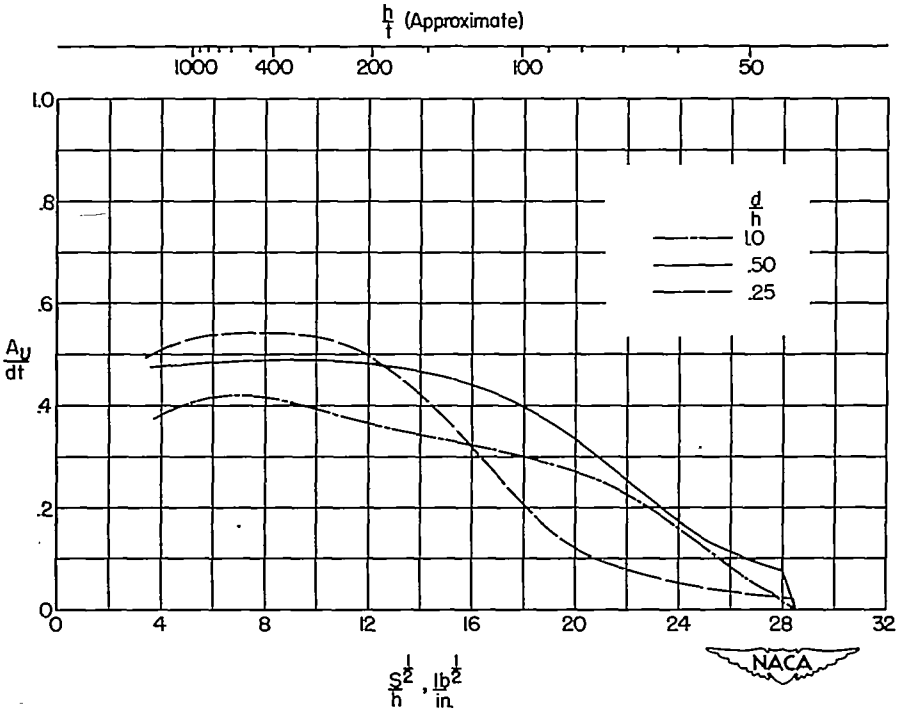

(c) Alclad 75S-T6 web and 75S-T6 double uprights.

Figure 23.- Concluded.

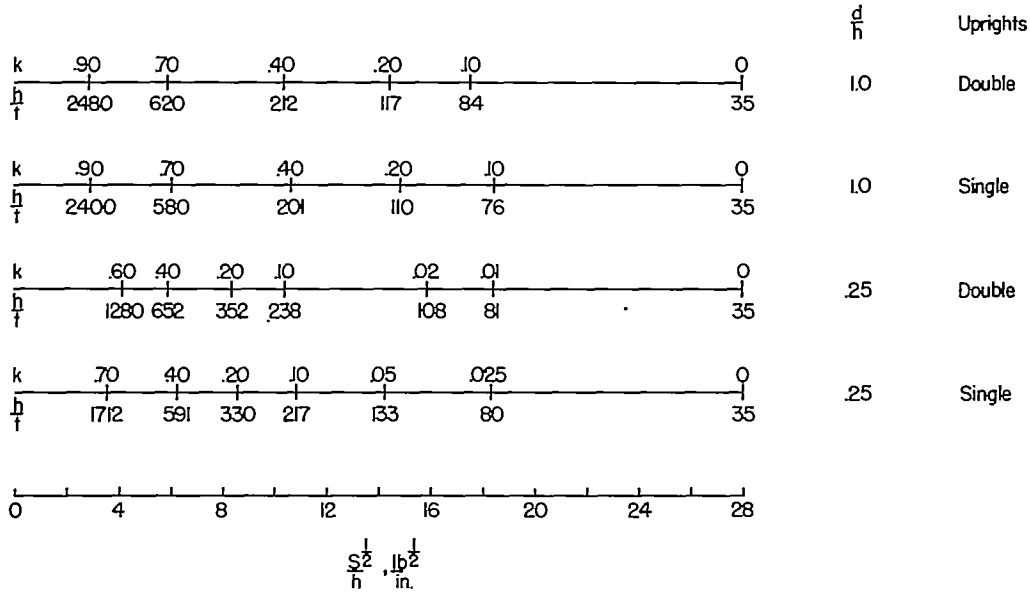

(a) 24S-T3 web and uprights.

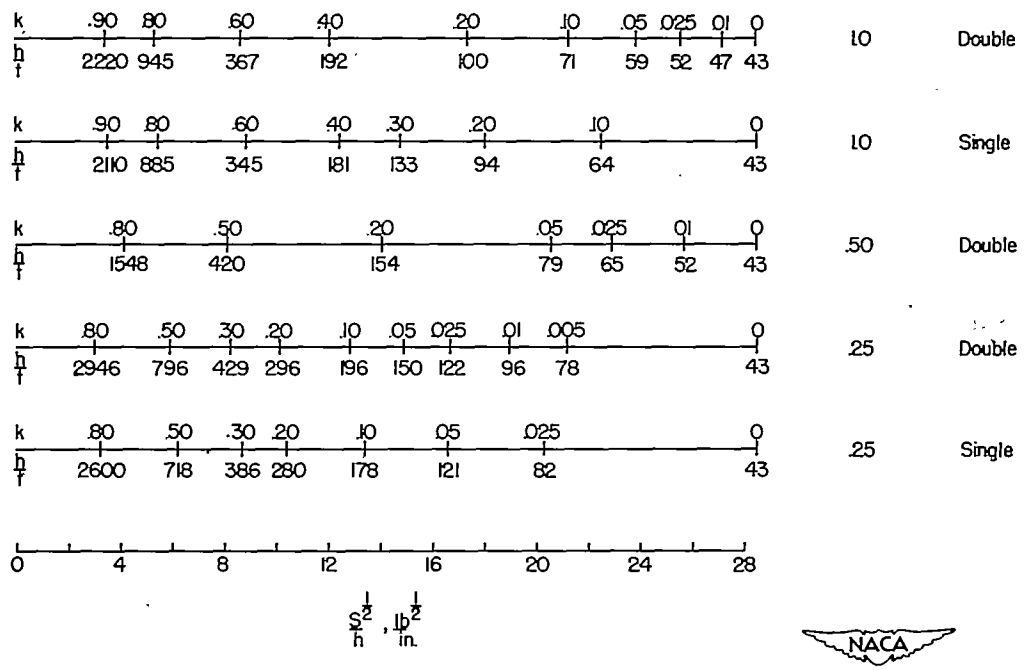

(b) Alclad 75S-T6 web and 75S-T6 uprights.

Figure 24.-Approximate relation between index value, depth-thickness ratio, and factor k.

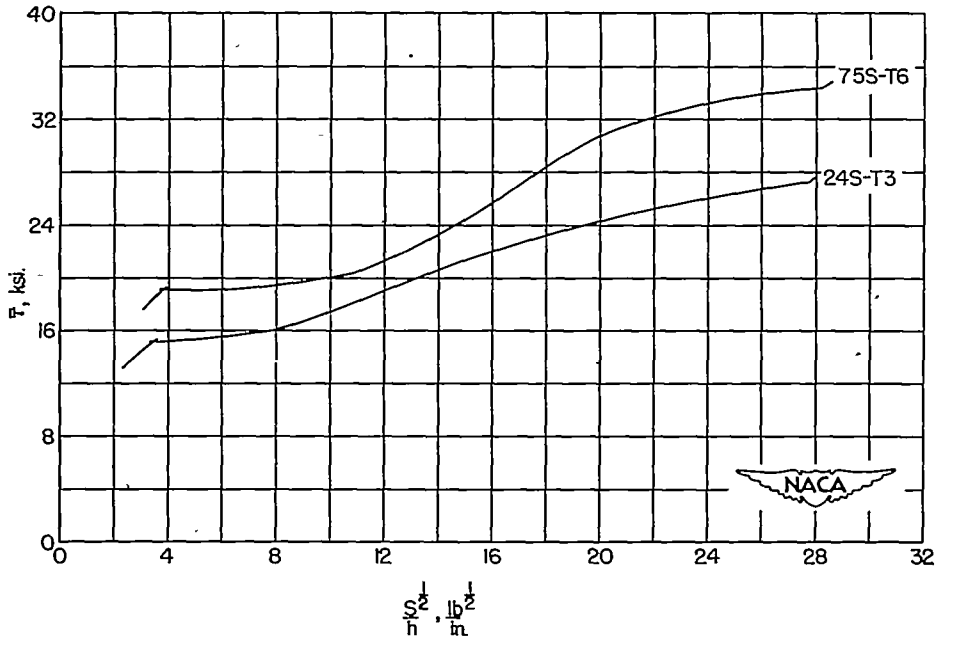

Figure 25.- Most efficient web systems ($0.25 < \frac{d}{h} < 1.0$)

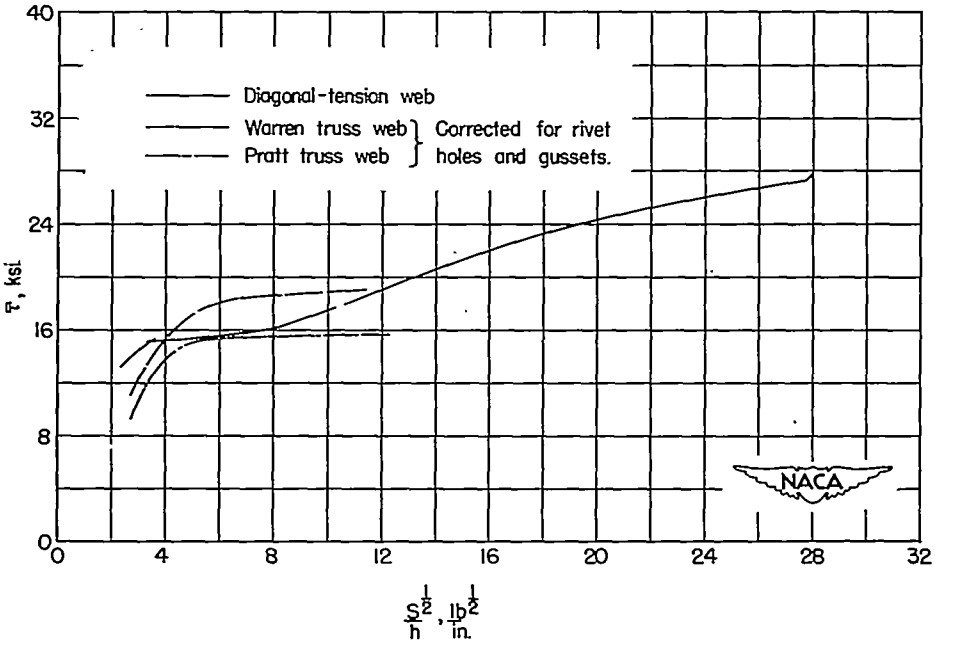

Figure 26 - Structural efficiencies of diagonal-tension webs and truss webs of 24S-T3 aluminum alloy. (Truss webs carry 40 % reversed load.)

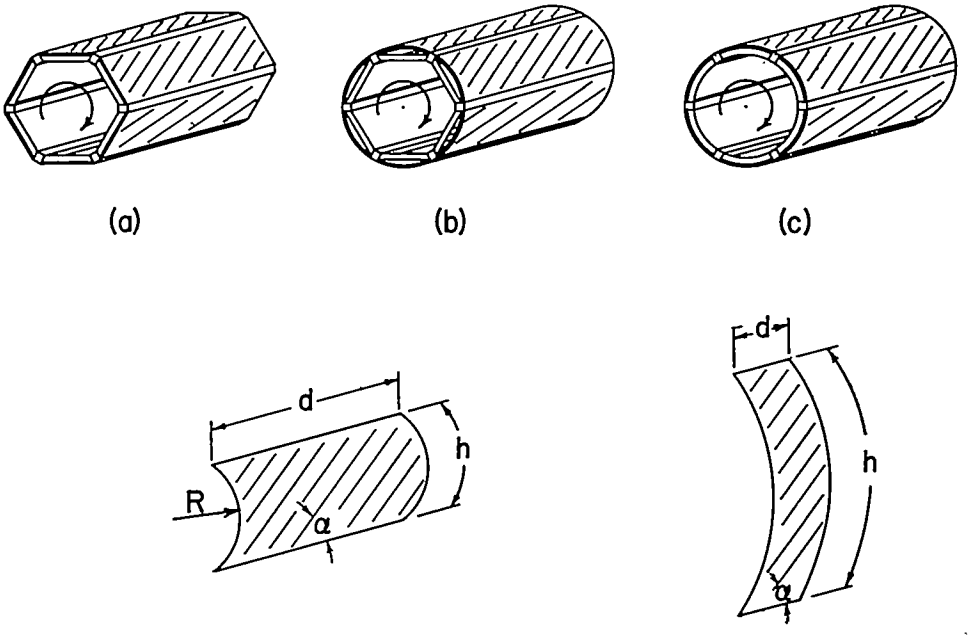

Figure 27.- Diagonal tension in curved webs.

Figure 28.- See next page.

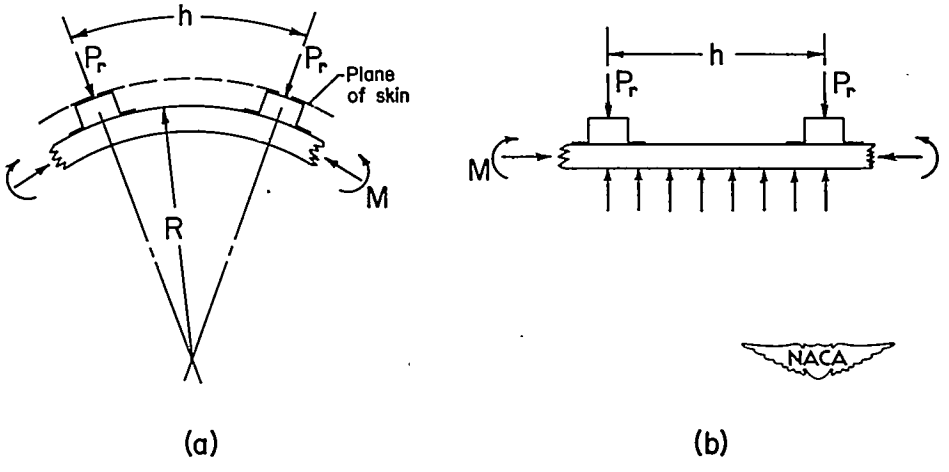

Figure 29.- Forces on floating rings.

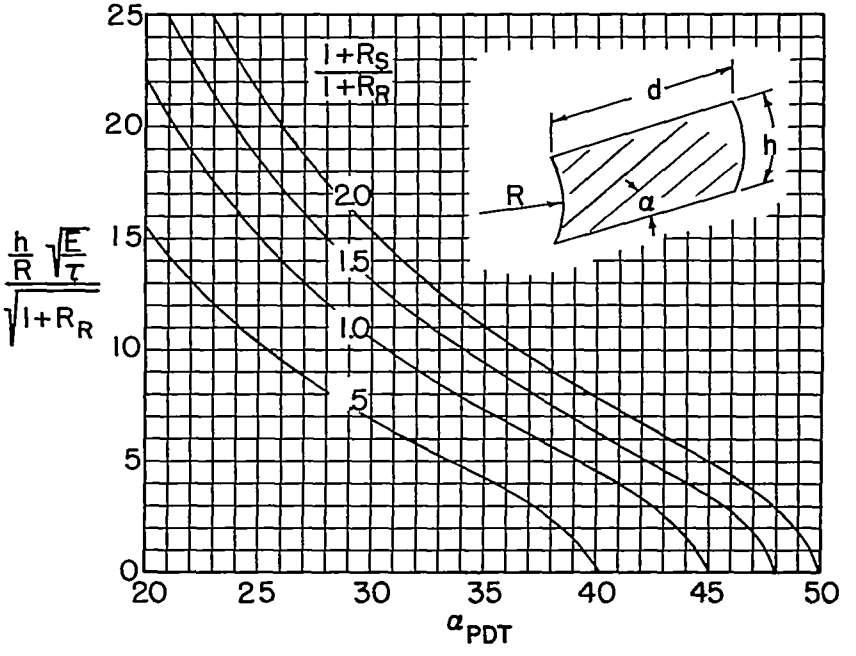

(a)

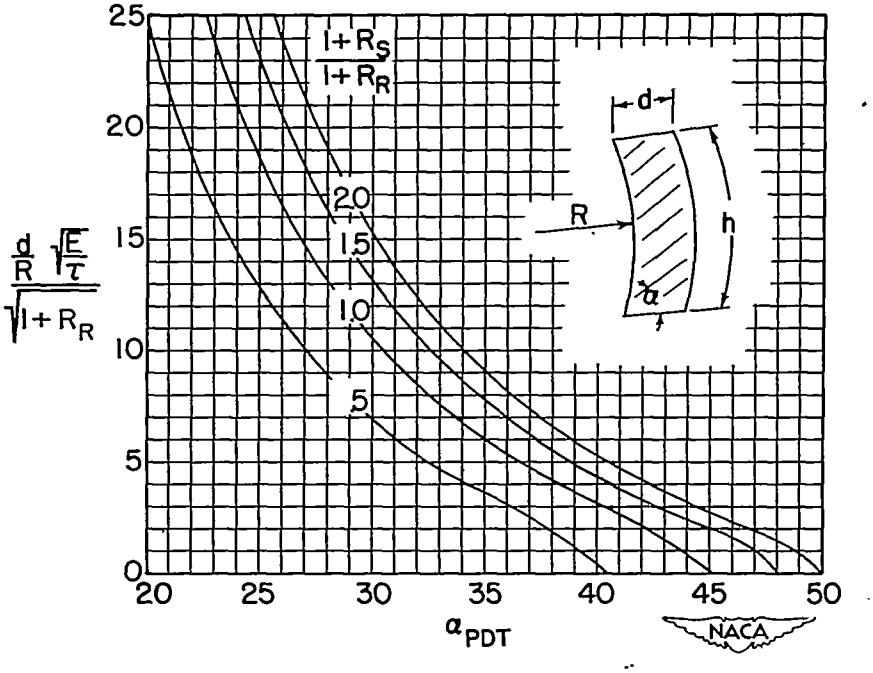

(b)

Figure 28.– Angle of pure diagonal tension.

$$R_R = \frac{dt}{A_{RG}} \; ; \; R_S = \frac{ht}{A_{ST}}$$

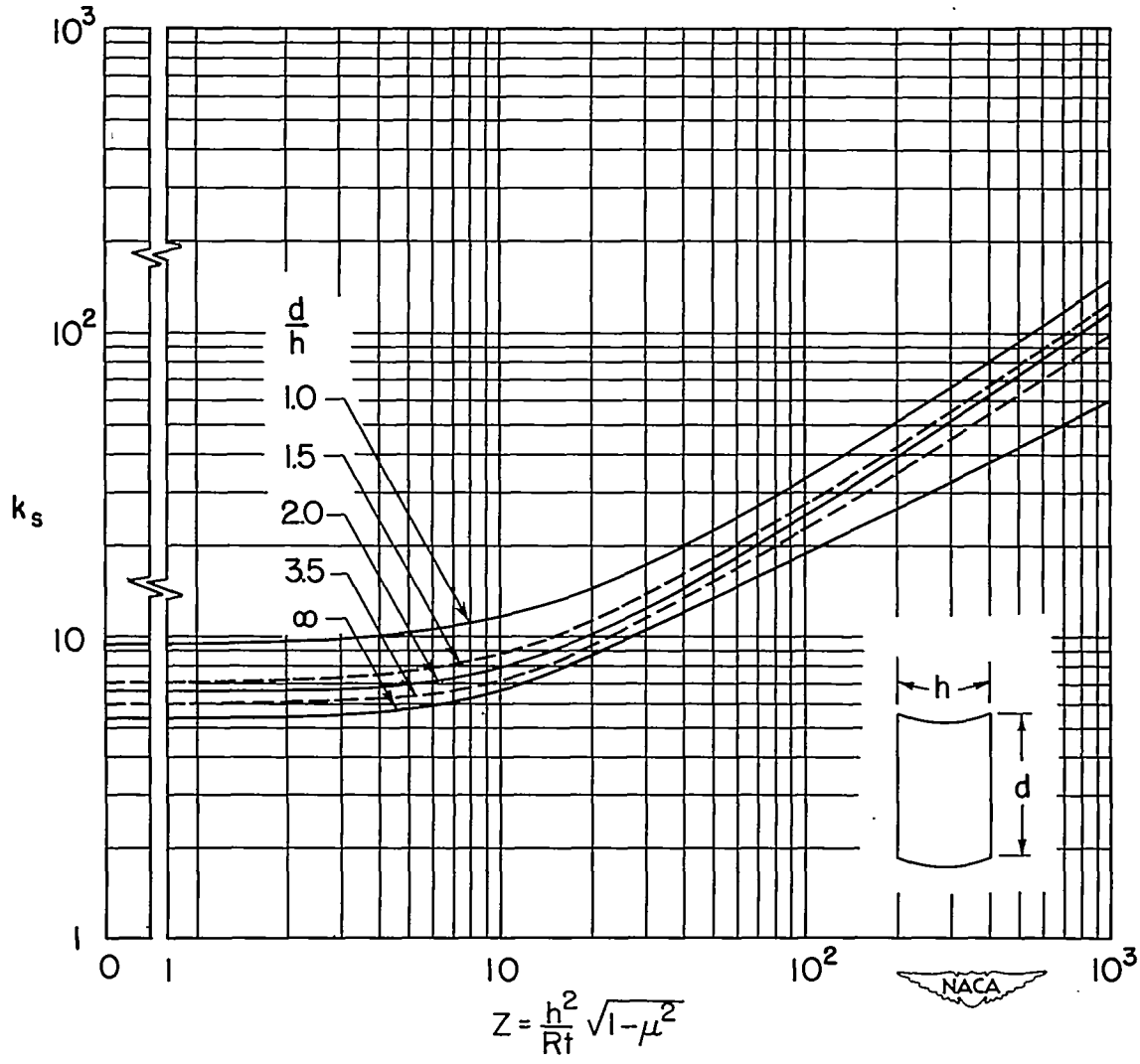

(a) Plates long axially ($d \geq h$). $\tau_{cr,elastic} = k_s \frac{\pi^2 E h^2}{12 R^2 Z^2}$.

Figure 30.– Critical shear-stress coefficients for simply supported curved plates.

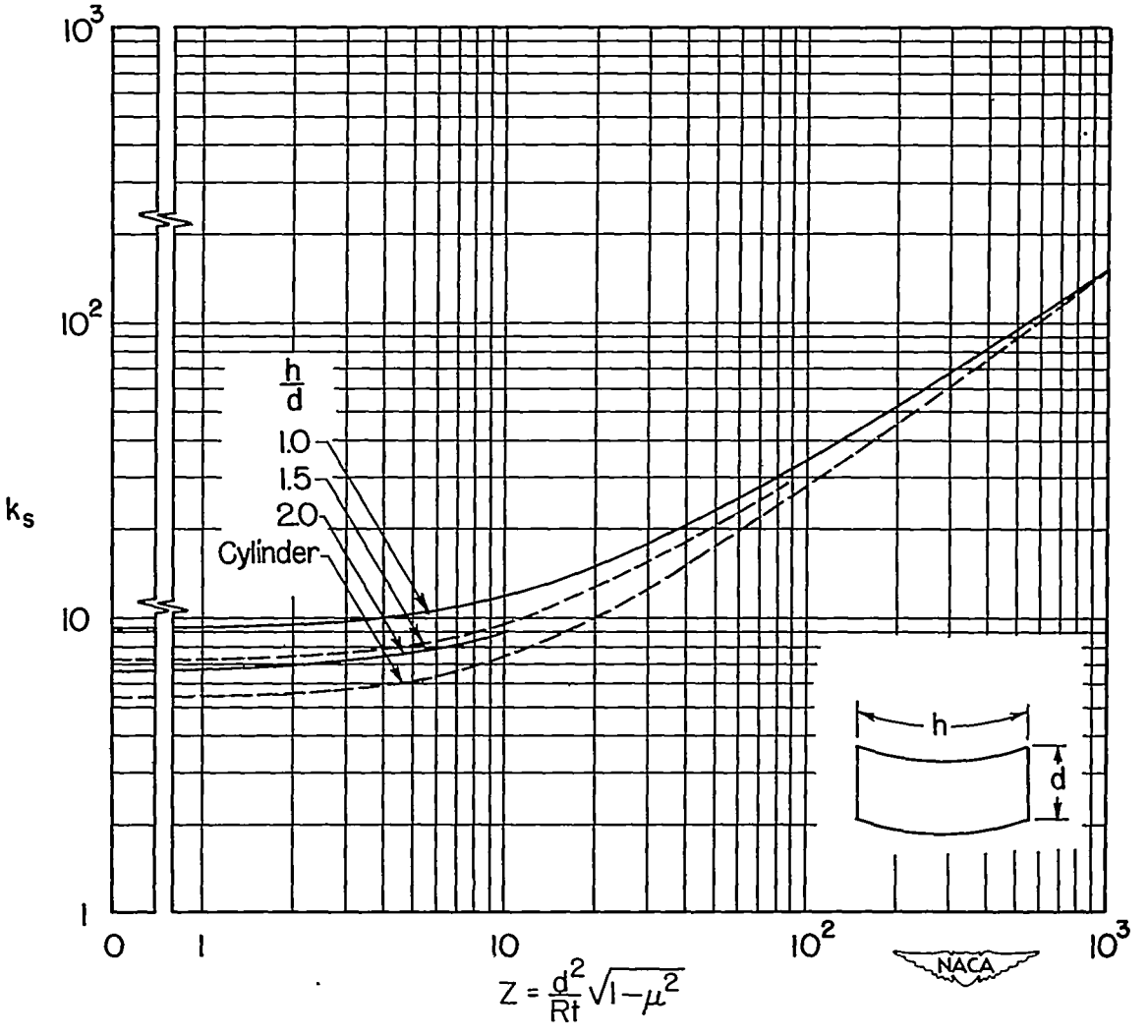

(b) Plates long circumferentially ($h \geq d$). $\tau_{cr,elastic} = k_s \frac{\pi^2 E d^2}{12 R^2 Z^2}$.

Figure 30.– Concluded .

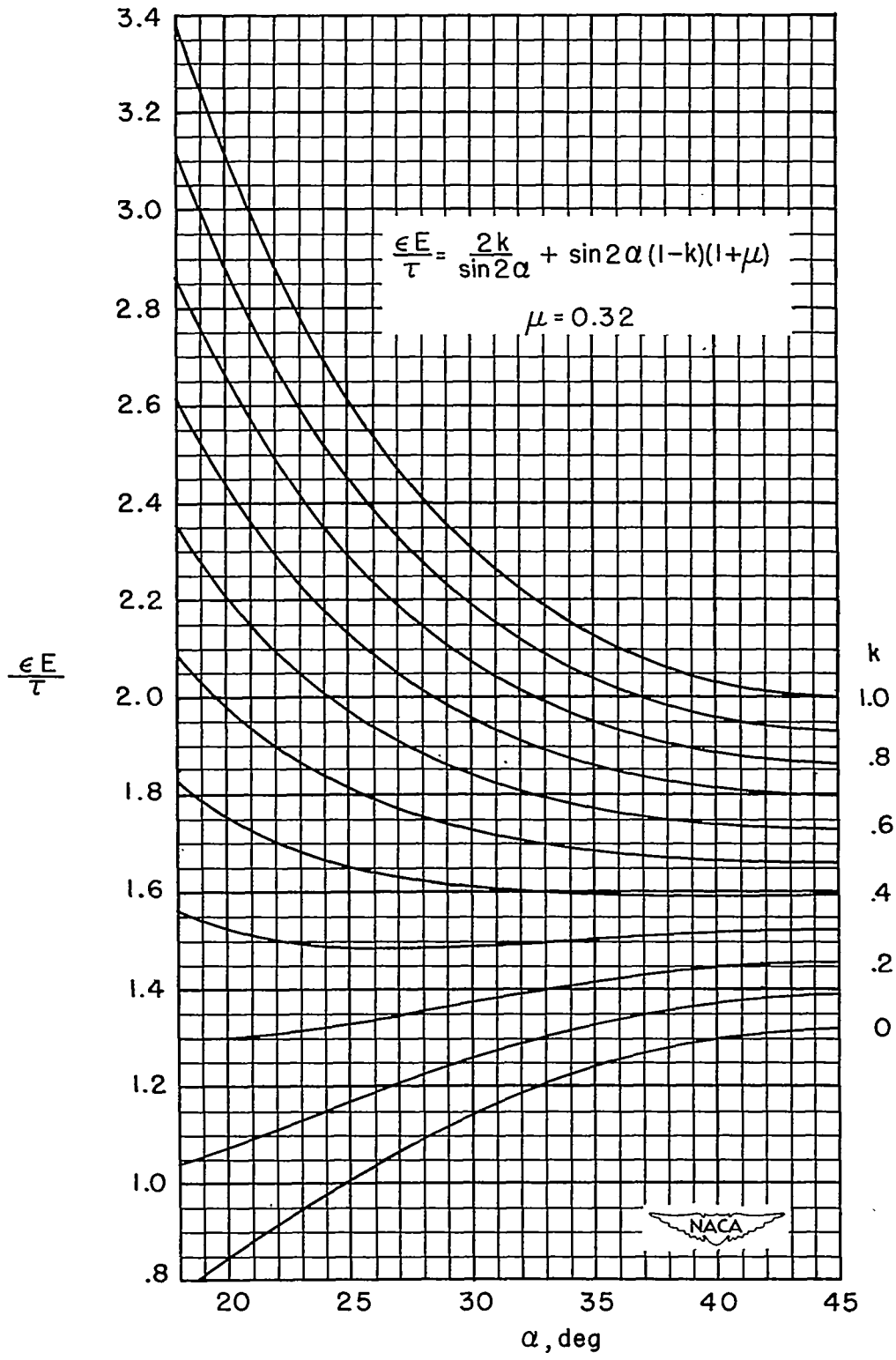

Figure 31.—Graph for calculating web strain.

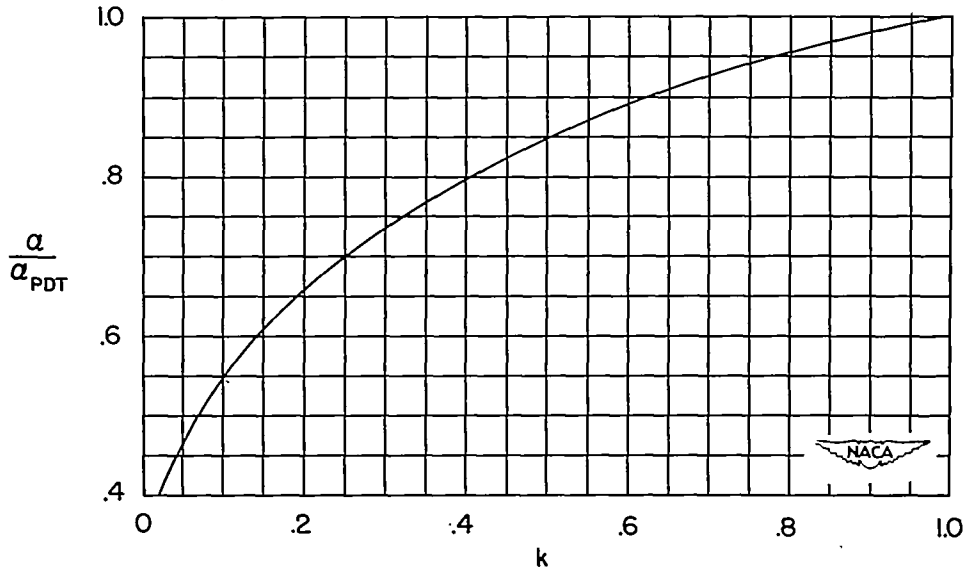

Figure 32.– Correction factor for angle of diagonal tension. $\left(\frac{A_{ST}}{ht}=1.00=\frac{A_{RG}}{dt}\right)$

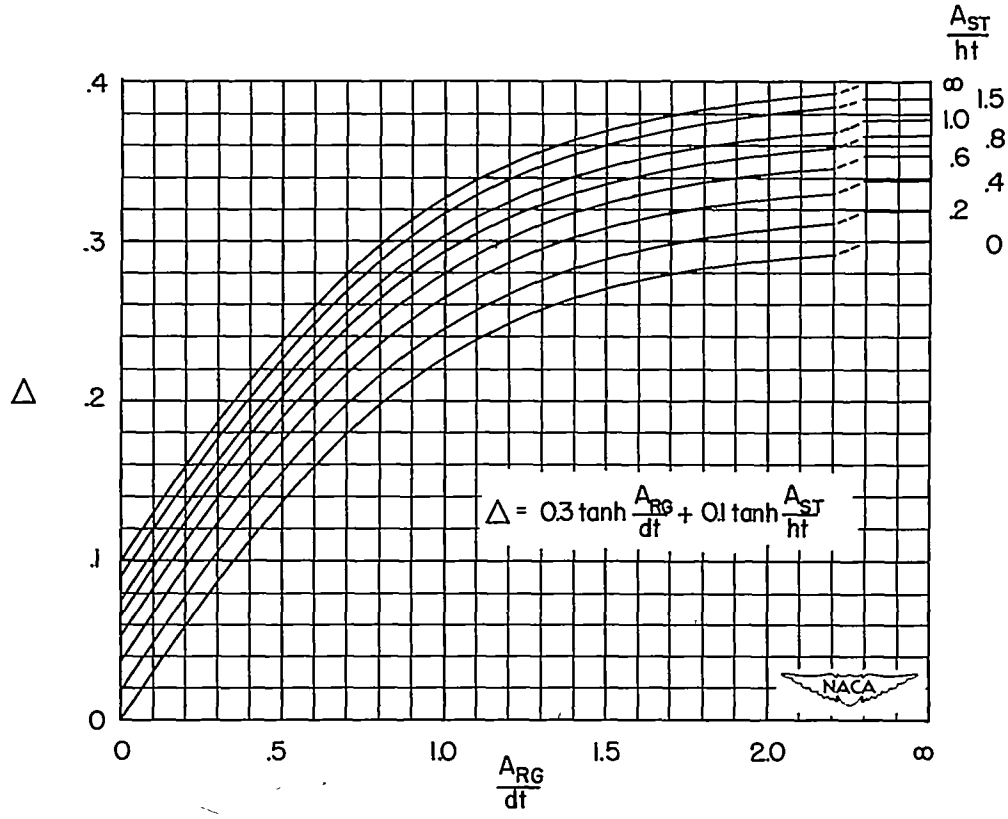

Figure 33.– Correction for allowable ultimate shear stress in curved webs.

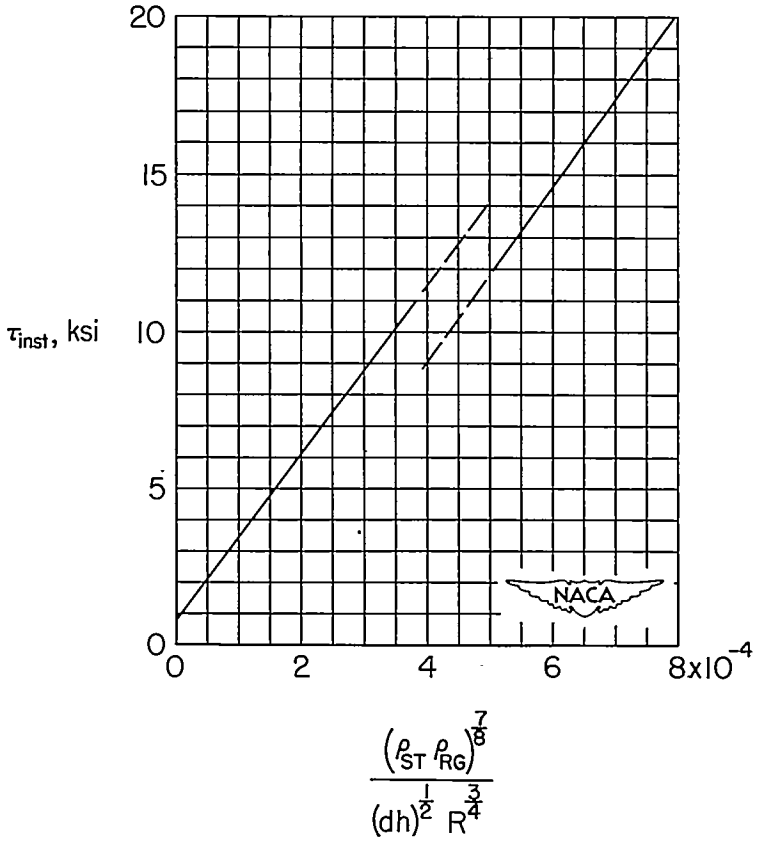

Figure 34.- Empirical criterion for general instability failures of stiffened 24S-T3 aluminum alloy cylinders subjected to torsion. (From reference 28.)

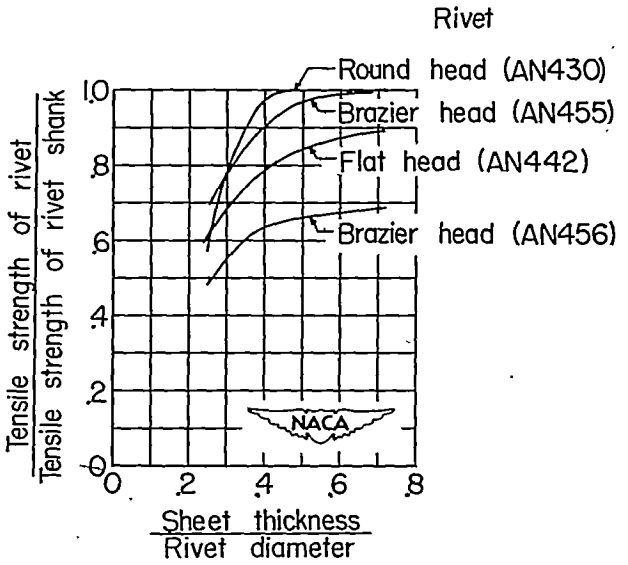

Figure 35.- Tensile strength of four types of A17S-T3 aluminum-alloy rivet in 24S-T3 aluminum-alloy sheet.

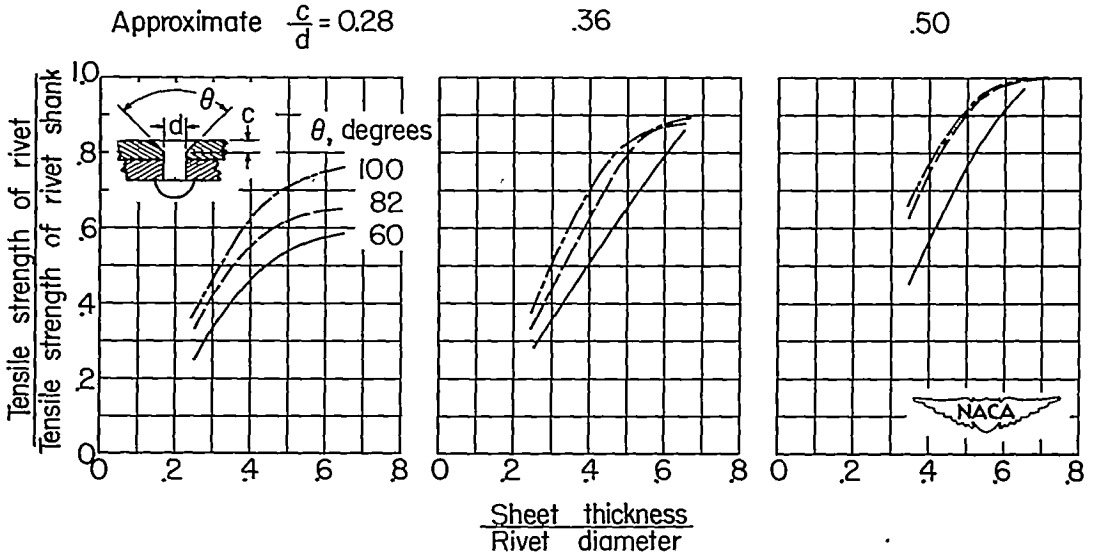

Figure 36.-Tensile strength of NACA machine-countersunk flush rivets of A17S-T3 aluminum-alloy in 24S-T3 aluminum alloy sheet.

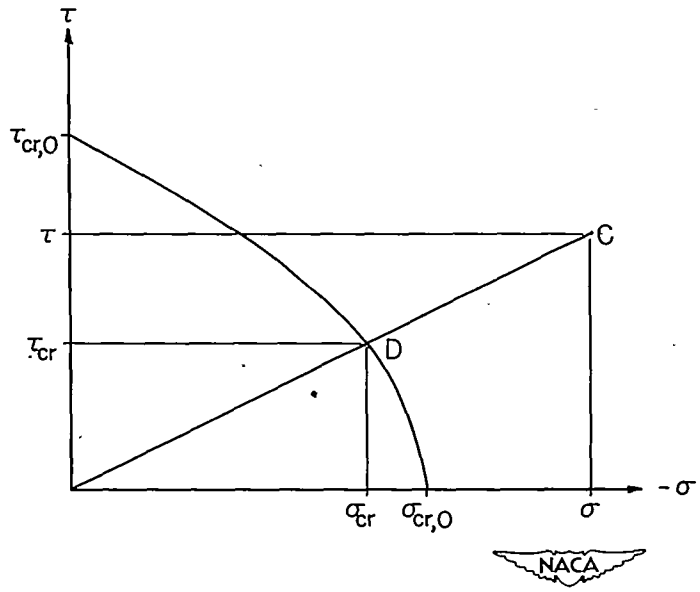

Figure 37.- Interaction diagram for stiffened cylinders subjected to torsion and compression.

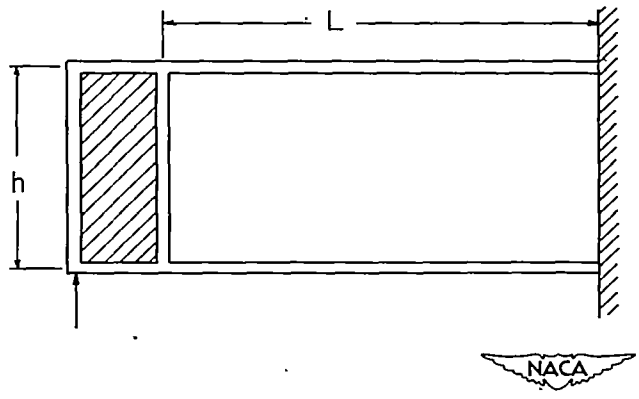

Figure 38.- Portal frame.